EXPERIMENTAL AND THEORETICAL STUDY OF ALKALI RESISTANT CEMENT COMPOSITES FOR RETROFITTING MASONRY STRUCTURES

by

Nora Singla

A Thesis Presented in Partial Fulfillment
of the Requirements for the Degree
Master of Science

ARIZONA STATE UNIVERSITY

December 2004

EXPERIMENTAL AND THEORETICAL STUDY OF FABRIC CEMENT

COMPOSITES FOR RETROFITTING MASONRY STRUCTURES

by

Nora Singla

has been approved

August 2004

APPROVED:

_____, Chair

_____

_____

Supervisory Committee

ACCEPTED:

_____

Department Chair

_____

Dean, Division of Graduate Studies

ABSTRACT

Fiber-reinforced polymer composites are becoming increasingly popular in construction and infrastructure applications where harsh conditions exist and durability is an important consideration. The growing need to take care of deteriorating infrastructure has motivated civil engineers to consider alternatives for conventional materials. Fiber-reinforced composites are being considered for their superior resistance to fatigue, their superior resistance to environmental effects as opposed to metals, their higher strength to weight ratio and their ease of installation. Masonry structures constitute a large part of deteriorating infrastructure all over the world. These structures were designed to resist gravitational and wind loads with little consideration to seismic loads. Fabric reinforcement can improve mechanical properties of existing and already damaged structures. The object of the research is to develop the basic material property data in tension, flexure and bond for high performance thin-sheet fabric-reinforced cement composites to be used for retrofitting projects involving un-reinforced masonry walls to enable proper design and engineering of the retrofit systems.

Tensile, Flexural and Bond testing was done on several batches. Specimens were studied for improvement in tensile and flexural properties using different manufacturing method, fabric orientation, number of fabric layers and fabric direction. Both three-point and four-point bending tests were conducted on the specimens with two layers of fabric. Specimens were cast with a bond between the masonry and the composite to study the tensile properties in unison to get a better idea of tensile strength imparted by the fabric to the masonry block.

Specimens were also subjected to aging at 80ºC for 14 days and 28 days to study their long term durability. Aging at elevated temperatures decreases the ductility of the composite and makes it increasingly brittle. Test results were compared with un-aged tensile and flexural results.

A theoretical model was developed that simulated tensile response of the specimens. This model provides specimen dependent properties of fracture energy, strain and tensile strength. Another model was developed to simulate flexural response which uses the above tensile properties as an input and provides a load-deflection. Both models predict responses very much in accordance with experimental responses.

ACKNOWLEDGEMENTS

I am pleased to express my deep gratitude to my advisor and committee chair, Dr. Barzin Mobasher for his whole hearted co-operation, sincere guidance and liberal help throughout my research period. I would also like to extend sincere gratitude to my committee members Dr. Subramaniam D. Rajan and Dr. Alva Peled for their timely co-operation and for serving on my committee. I am also deeply indebted towards Dr. Dallas Kingsbury and Peter Goguen for their valuable help with the experimental setups. I would also like to express my gratitude towards Dr.Robert Hinks for his generous guidance and inspiration. I am also thankful to Dr.Kamil Kaloush for his help time and again. I would also like to thank Saint Gobain Technical Fabrics for funding this project. I would also like to thank my laboratory mate, Sachiko Sueki for her co-operation and help. I would also like to acknowledge my best friend, Jitendra Pahilajani for his support through every thick and thin, unique encouragement and help throughout the course of the study. I would also like to thank my friends Dnyanesh Naik, Nikhil Malik and Vandana Kaushal for their moral support and help. Last but not the least; nothing would have been possible without the encouragement, understanding, love and blessings of my beloved family and my dear husband, Anshu K. Jain.

….To My Beloved Mother

TABLE OF CONTENTS

CHAPTER Page

LIST OF TABLES

LIST OF FIGURES

CHAPTER 1

INTRODUCTION

1.1 Introduction

A major portion of every country's infrastructure is an immense network of roads, buildings and bridges that are required to meet basic human, social and economic needs. The inability of these resources to meet the demands placed upon them poses tremendous problems for the people who use them everyday. However, in many instances, infrastructure is deteriorating to the point where failure is imminent, solutions are lacking, and price tags are high.

In order to combat the problem of a dilapidating infrastructure, structures must either be rebuilt or repaired. Rebuilding generally costs much more than repairing. Therefore, considering the limited resources available to revive the ageing infrastructure, it is prudent to examine new materials and techniques to effectively and economically retrofit the deteriorating infrastructure. The past decade has seen an increased development of new technologies to address the repair and retrofit of our ageing infrastructure.

Un-reinforced masonry buildings constitute a large portion of the world's building inventory. Forming part of this stock are the most appreciated historical monuments. As an example, more than 20,000 un-reinforced masonry buildings exist in California alone. Masonry construction has a number of advantages. The first of which is the fact that a single element can fulfill several functions including infrastructure, fire protection, thermal and sound insulation, weather protection and sub-division of space. Masonry

materials are available with properties capable of meeting these functions, requiring only to be supplemented in some cases by other materials for thermal insulation, damp-proof courses and the like. The second major advantage relates to the durability of the materials, which, with appropriate selection, may be expected to remain serviceable for many decades, if not centuries, with relatively little maintenance. From architectural point of view, masonry offers advantages in terms of great flexibility of plan form, spatial composition and appearance of external walls for which materials are available in a wide variety of colors and textures. Complex wall arrangements, including curved walls, are readily built without the need for expensive and wasteful formwork. The nature of masonry is such that its construction can be achieved without very heavy and expensive plant.

There are large numbers of existing buildings in North America and around the world that have been constructed with un-reinforced masonry. The masonry elements in these buildings were designed to resist primarily gravity and wind loads with little to no consideration of the forces generated by a seismic event. An earthquake introduces severe in-plane and out-of-plane forces to un-reinforced masonry walls. Typical damage suffered by these buildings during an earthquake ranges from minor cracking to catastrophic collapse. Amongst several conventional rehabilitation and strengthening methods like injection grouting, insertion of reinforcing steel, pre-stressing, jacketing and various surface treatments are the most common. Each of these methods involves the use of skilled labor and disrupts the normal function of the building. For example,

jacketing and surface treatments such as shotcrete, ferrocement, and reinforced plastic can add anywhere between 30 and 100 mm of thickness to the existing wall.

The low tensile strength of masonry is a limiting factor in situations where considerable lateral forces have to be resisted. Reinforced masonry can be used to overcome this limitation in buildings in seismic areas and generally where non load-bearing walls are subjected to substantial wind loads. Various new elements are developed for repair and strengthening of un-reinforced masonry walls (UMW), beams, columns, and other structural elements. Use of reinforcement in these elements is essential in order to improve the tensile and flexural performance. The reinforcements can be either as fiber reinforced plastics (FRP) or cement-based continuous fabric reinforcements. A wide range of fiber types can be used for reinforcement in cement-based materials, resulting in various products with different properties.

Fibers are mainly used because of their high strength and/or stiffness. The presence of fibers minimizes the presence of significant flaws in a brittle material such as glass, and allows the fiber strength to approach the material's theoretical strength. Fibers impart a lot of strength to the composite in the fabric direction. Fibers are not directly usable alone (except in rope or cable) and must be combined with a matrix material. The matrix binds the fibers together, transfers the load to the fibers after cracking and even protects the fibers from damage. The matrix material can be a polymer, a metal, or a ceramic. Matrix used in the given case is cement paste with some percentage of fly ash. Fibers can be continuous – long, continuous fibers, which either run in a single direction in a single sheet of uniform thickness, or are woven into a fabric. Fibers can also be

discontinuous – random or oriented, as in molded plastics. A single layer of unidirectional composite is generally not useful because of very low strength transverse to the fibers. Therefore, laminae (layers or plies) are combined with their fibers oriented in more than one direction to form a laminate. The wide variety of fibers and matrix materials available today has resulted to a large extent from their application in aerospace structures, where the value of saved weight is high. As application of fiber composites has grown, the cost of the raw materials has decreased, and new manufacturing processes have been developed.

There are several methods to produce fabrics: weaving, knitting, breading, and non-woven. The wide variety of production methods allows great flexibility in fabric design. This flexibility enables controlling of fabric geometry, yarn geometry, and orientation of yarns in the fabric in various directions. It is even possible to produce three-dimensional fabrics, providing reinforcement in the plane normal to the panel. This diversity provides important additional advantages in the development of cement composites and allows engineering the performance of the final products for the desired requirements.

The main advantage of fabrics as reinforcements in cement-based composites is in the enhancement of mechanical behavior. There is an improvement in the tensile and flexural performance. Fabric in hardened cement paste, mortar or concrete exhibits three important effects. It tends to increase the stress at which the matrix starts to crack. It improves the strain capacity or ductility of the inherently brittle cementitious matrix, thus increasing its energy absorption capability or toughness characterized in general by the

area under a stress-strain or load-deformation curve or some defined portion of it. A third important effect of fabric is its tendency to inhibit or modify crack development in terms of reducing crack width and average crack spacing. The degree of improvements depends on the mode of loading and the type and amount of fabric. To see the above effects effectively the fabric must have higher tensile strength, ductility (or elongation), elastic modulus, elasticity and Poisson's ratio than that of matrix. Practical use of fabric cement composites is a potentially cost effective retrofit technique.

1.2 Review of Related Literature

Several researchers have recognized the potential for use of fabric reinforcement in cement composites. Various manufacturing techniques have been studied to understand the behavior of fabric reinforced composites. An immediate use of these composites is in retrofitting of earthquake stricken masonry structures. Galano and Gusella (1998) studied the use of steel bracings in reinforcing masonry walls subjected to seismic loading. Fabrics gained more demand because of ease in manufacturing and corrosion resistance. Saadatmanesh (1997) studied the use of fabrics to extend the service life of concrete and masonry structures. These fabrics provide benefits such as excellent bond and anchorage. This anchoring is provided by the non linear geometry of individual yarns within the fabric, induced by the fabric structure; Bentur (1997) and Peled (1998). Pleiman (1987) studied the tensile and bond pull-out of deformed fiber-glass rods. The fabrics can sustain high tensile loads under adverse conditions. Mayrhofer (2001) studied the fabric usage in sustaining blast loads. Jai, Springer, Kollar and Krawinkler (2000)

studied experimental and theoretical properties related to reinforcing masonry walls with fabrics. Albert, Elwi, Cheng (2001) studied about strengthening of un-reinforced masonry walls using FRPs. Studied by Mobasher, Pivacek and Haupt (1997) showed that use of unidirectional AR Glass fabric achieved a tensile strength on 50MPa compared to the average tensile strength of about 10MPa achieved with the use of glass fibers.

1.3 Objective of the Thesis

The main aim is to develop the basic material property data in tension, flexure and bond for high performance thin-sheet fabric-reinforced cement composites used for retrofit projects involving un-reinforced masonry walls to enable proper design and engineering of the retrofit systems. A seismic reinforcing grid made of AR Glass fabric was manufactured by Saint Gobain Techinal fabrics and was used to cast all the specimens cast either in ASU or by the company. The objective can be divided into five parts namely Tension testing, Flexure testing, Masonry-Fabric Composite Bond testing, Ageing effect on tension and flexural properties and Theoretical modeling of tensile results and predicting the flexural response from the tensile response.

1. Tension Test

The purpose of the tension tests is to develop fundamental materials property data that can be used in the design and analysis of these systems. The specimens were cast in ASU and were studied for effect of Specimen Thickness, Number of fabric layers, manufacturing using freely laid fabric and aligned fabric and Orientation. Based on these results specimens were cast by Saint Gobain Technical Fabrics utilizing all the properties that improve the tensile strength. The specimens were cast with lesser thickness, aligned

and stretched fabric. Specimens were cast in both the machine and cross machine direction. The specimens were tested under tension using a closed loop servo-hydraulic testing frame operated under stroke control and the stress and elongation of the specimen was recorded throughout the test.

2. Flexure Tests

The purpose of these tests is to provide a correlation between the tensile properties which are the primary material properties and the flexural data which provides for a simple measure of tensile properties. These tests can also be used as a quality control test for routine measurements during installation and various retrofit projects. The specimens were cast in ASU with fabric held and aligned and were studied for the effect of orientation. The specimens were cast in ASU in both machine and cross machine direction. The flexure tests were conducted using a closed loop servo-hydraulic testing frame operated under stroke control. The load and deflection of the specimen was recorded throughout the test.

3. Masonry – Fabric Composite Bond Testing

Bond tests were conducted to evaluate the strength of the fabrics to the masonry unites. It is expected that the shear strength of these samples is quite important in the ability of the laminate to carry the forces transferred to it through a CMU units. No matter how strong the laminates, or how many layers if fabric are used, the inherent strength of the bond between the fabric and the masonry units will determine the ability of the assembly of the CMU unit and the laminates as a system. The test will be conducted as a tension test.

4. Ageing Effect

In addition to testing samples in the un-aged condition as explained above, additional samples were subject to ageing at 80ºC for 14 days and 28 days. The specimens were cast by Saint Gobain Technical Fabrics in both machine and cross machine directions. The aged specimens were tested under tension as well as flexure. The results of this test will allow study of the long-term durability of the samples subjected to ageing in hot climates. The elevated temperature and moisture content accelerate the formation of the products of hydration of the cement in the matrix, particularly calcium hydroxide. Interaction of calcium hydroxide with fibers has a long term effect on the properties of the composite. The principal mechanism is the formation of calcium hydroxide within the bundles of filaments that form the glass fiber strand. This gradually bonds the filaments together, which reduces filament pull-out. This leads to a reduction in the strain capacity of the composite, thereby reducing the strength of the composite. This decreases the ductility of the composite and makes it increasingly brittle material. Accelerating the formation of the hydration products accelerates their interaction with the fibers, hence accelerating the ageing of the composite.

5. Theoretical Modeling

Theoretical modeling was done to predict the Stress - Strain response of specimens using MATLAB program. The program predicts the Stress - strain response which is approximately same as experimental response till the maximum stress. The program gives the fracture energy, tensile strength of the composite and strain values.

These values were used as an input for the flexure model and it predicts the flexural response very similar to experimental flexure response till the maximum load.

CHAPTER 2

ANALYSIS AND RESULTS OF TENSILE TESTING

2.1 Specimen Preparation

Specimens were prepared using a standard mix design and a standard mixing procedure. Specimens prepared with the Mix design and mixing procedure as described below have been used for tension, flexure as well as bond testing.

2.1.1 Mix Design

The following mix design was used for preparing the samples:

a) W/C Ratio : 0.4

b) % fly ash : 25

c) Portland Cement type I/II produced by Phoenix Cement Company

d) Fine aggregate: river sand at a ratio of 1:1.5 (cement to fine aggregate)

e) Fabric: AR glass fabric with 25 mm opening

2.1.2 Mixing Procedure

Fine aggregate was mixed for 1 minute and then 50% water + super plasticizer was added. After 1 minute 50% of cement plus fly ash was added and mixed for 2 minutes. Then remaining 50% water was added and mixed for 2 minutes with all the contents added previously. After this remaining 50% of cement plus fly ash was added and mixed for 2 more minutes. Then the mixer was stopped and edges were cleaned. Finally mixing was done for 3 minutes prior to use.

The specimens were cast manually. Specimens were water cured at a temperature of 23±1C in a curing chamber containing 5 – 10 grams of Saturated Calcium Hydroxide. All specimens were subjected to minimum 7 days of curing, followed by three days of storage in laboratory environment. For the results presented in this document the samples have been cured for 7 days and were tested on 10th day. Specimens of size 356mmx70mmx10mm (14”x2.75”x0.40”) were prepared by cutting specimens using a water cooled diamond edge blade saw.

2.1.3 Fabric Used

The fabric used was provided by Saint Gobain Technical Fabrics and this fabric was used for casting Tension, Flexure and Masonry-Composite Bond testing specimens. The fabric has 2 rovings per linear inch width or 78.74 rovings per linear meter. There are approximately 1579 filaments per roving where average diameter of a filament is 19 microns. The young's modulus of AR glass is given to be around 10.5 e6 Psi or 72 GPa. The machine direction strands go over the cross machine direction strands. Therefore, cross machine direction strands are straight and machine direction strands have a slight curvature.

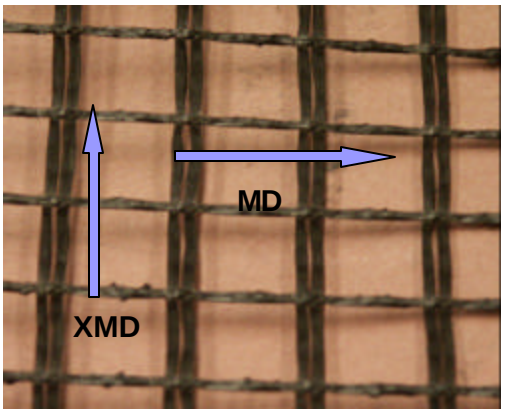

Figure 2.1 Fabric used

2.2 Tension Specimen Preparation

One of the requirements of the tension specimen is the flatness of the finished specimen prior to testing; otherwise, it might fail in the hydraulic grips due to localized grip pressure due to uneven thickness. Figure 2.2a through b shows the process used for preparing the perfectly flat surface at the grip points. A flat surface was selected for the preparation of the sample. Four thin aluminum end tabs were fixed to the work surface and a solid aluminum bar using double sided adhesive tape. Fast setting epoxy was applied to the surface of end tabs, and the specimen was sandwiched between the solid bar and the work surface. Two end blocks of the same dimension which were used at either side of the specimen made sure that the surfaces remained parallel. This procedure has been used for all the tensile specimens before testing.

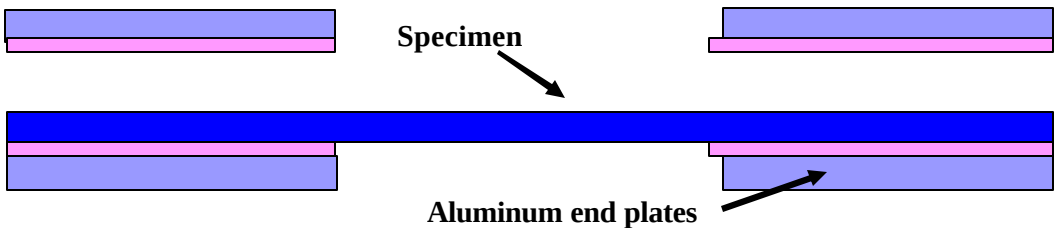

Figure 2.2a Tension specimen

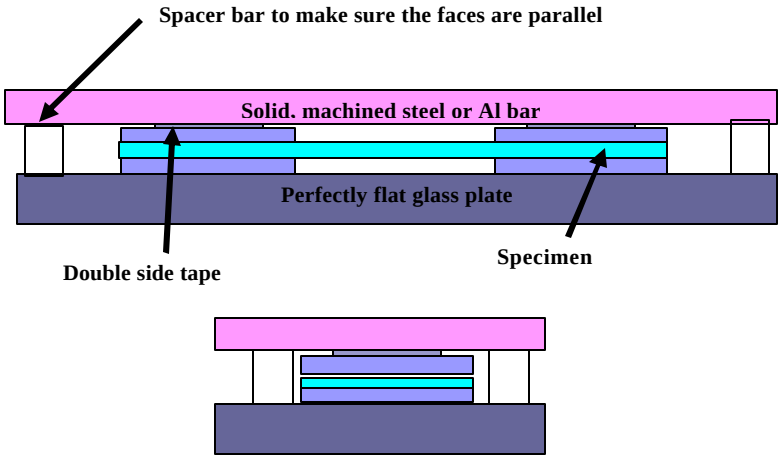

Figure 2.2b Details of the end piece connection for a perfectly flat tension specimen

2.3 Tension test set up

Figure 2.3 shows the tensile specimen gripped in the Hydraulic Grips. The tension test was conducted using a closed loop servo-hydraulic testing frame operated under stroke control, and the load and displacement of the specimen was recorded throughout the test. The analysis was done using MATLAB programs. The width and thickness for stress values are calculated using average of these values at 3 different points on the specimen.

Figure 2.3 Tensile Testing setup

2.4 Study of specimens cast using Freely Laid fabric

Initially, a wooden mold 533.4x419.1x11.43mm (21”x16.5”x0.45”) was used to prepare specimens. The matrix was prepared as described above. The mix was poured up to approximately 2.54mm in thickness, followed by layer of fabric for specimens with 2 layers of fabric. Specimens were also made with 1 layer and 3 layers of fabric to understand the effect of fabric on tensile strength. Specimens with 2 fabric layers were also cast using lesser thickness to study the effect of thickness on tensile properties by pouring the matrix up to approximately 1.9mm and followed by a layer of fabric.

2.4.1 Effect of Specimen Thickness

The fabric was freely laid while casting the specimens and the thickness was varied. The effect of specimen thickness using same number of fabric layers is shown in Figure 2.4. Reducing the thickness of composite increases the ability of the fabric to distribute the cracks throughout, thus improving the ductility of the system. The specimen with a thinner cross section has a higher volume fraction for the same number of fabric layers. This results in higher strength due to multiple cracking behavior. Type A-ST has average maximum tensile stress 5.47MPa whereas; Type A has average maximum stress 2.33MPa. Reducing the thickness by 28.6% can increase Tensile strength by 57.4%.

Table 2.1

Comparison between specimens with different thickness

Specimen Group	No. of Layers	Thickness, mm	Ave. Young's Modulus, E, MPa	Ave. Maximum Stress, MPa	Ave load, N/mm
Type A-ST	2	8.01	4345.21	5.47	21.82
Type A	2	11.43	4910.78	2.33	13.31

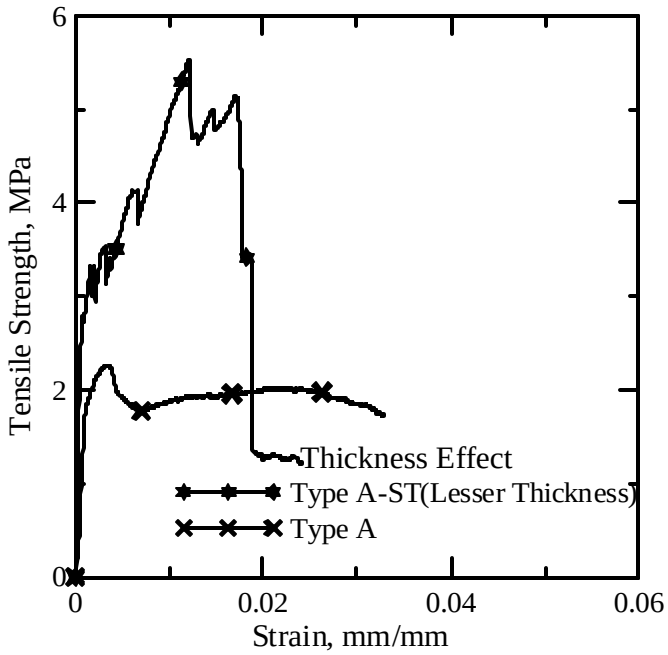

Figure 2.4 Effect of specimen thickness with the same number of fabric layers

2.4.2 Effect of Number of Fabric Layers

Un-reinforced concrete is weak in tension. Adding the fabric improves the tensile strength of concrete. After cracking of the matrix, major portion of the tensile load is carried by the fabric. This effect is very clearly described by the improvement in tensile strength with increase in number of fabric layers as shown in Figure 2.5. Specimen with 3 fabric layers (Type A-3L) has average maximum tensile stress 3.88MPa, specimen with 2 layers (Type A) has average maximum tensile stress 2.33MPa and specimen with only 1 fabric layer (Type A-1L) has average maximum tensile stress 1.50MPa. The fabric was freely laid while casting these specimens.

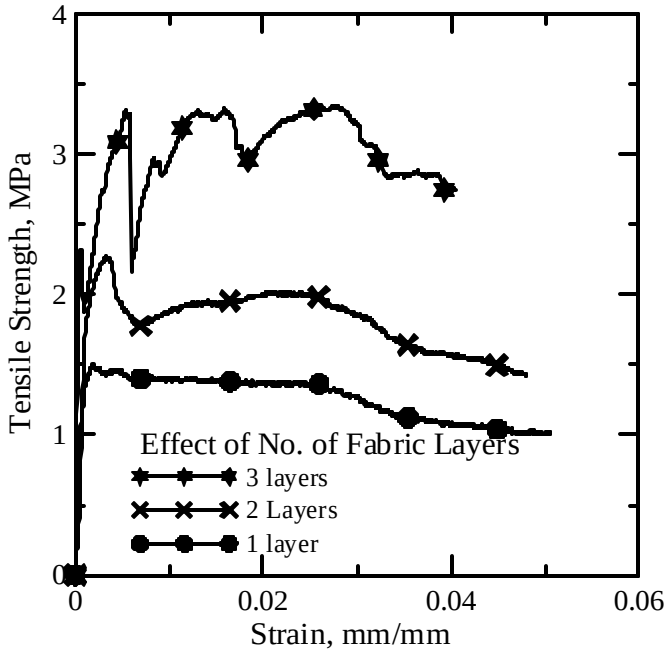

Figure 2.5 Effect of Number of Fabric Layers with same specimen thickness

Table 2.2

Comparison between Specimens with different Number of Fabric layers

Specimen Group	No. of Layers	Thickness, mm	Ave. Young's Modulus, E, MPa	Ave. Maximum Stress, MPa	Ave load, N/mm
Type A-1L	1	11.43	2891.43	1.51	8.61
Type A	2	11.35	4910.78	2.33	13.31
Type A-3L	3	11.32	7580.19	3.88	21.95

2.5 Study of Specimens cast using Aligned fabric

The problem with the mold used above was that the thickness of the layers could not be properly controlled and the fabric could not be properly aligned and stretched. Therefore, a new set up was developed to make sure that the fabric alignment and specimen thickness during the specimen fabrication could be properly maintained. The

setup is shown in Figure 2.6a through d. The specimen was fabricated on a base plate. Several metal strips were used as the edges which build up the specimen. The specimen was fabricated in layers, and multiple layers of paste and fabric were placed sequentially. With each fabric layer, an edge piece with alignment pins and holes was installed to ensure the alignment of the specimen. Four perforated side strips of 3.175mm thickness each was placed on the base first, followed by the matrix that was poured in and leveled to thickness. A fabric layer was laid on top and the process repeated. The resulting plate was cut into 6 samples of 355.6mmx69.85mmx10.16mm (14”x2.75”x0.4-0.5”) in dimensions using a water cooled diamond edge blade saw. The proposed set up could also be used to study the effect of fabric alignment by making samples with fabric placed with a specific orientation. Specimens with two different fabric orientations were also cast. In this method metal strips govern the thickness of matrix layer, and ensure a better bond and a uniform matrix thickness between layers. It is clear that this method contributes to better tensile properties. Figure 2.5a through d shows the specimen preparation. Figure2.5a shows the mold, while figure 2.5b shows the matrix poured in first border and first layer laid on top of it. The batch shown has been cast with 25.4mm orientation of layers resulting in a slope of (1:14). Figure 2.5c shows the final phase of specimen preparation, and Figure 2.5d shows the prepared batch with fabric layers laid at an orientation of 50.8mm (1:7).

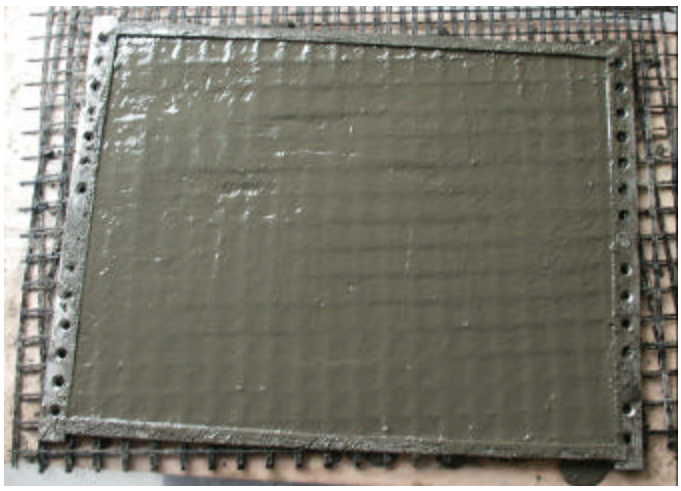

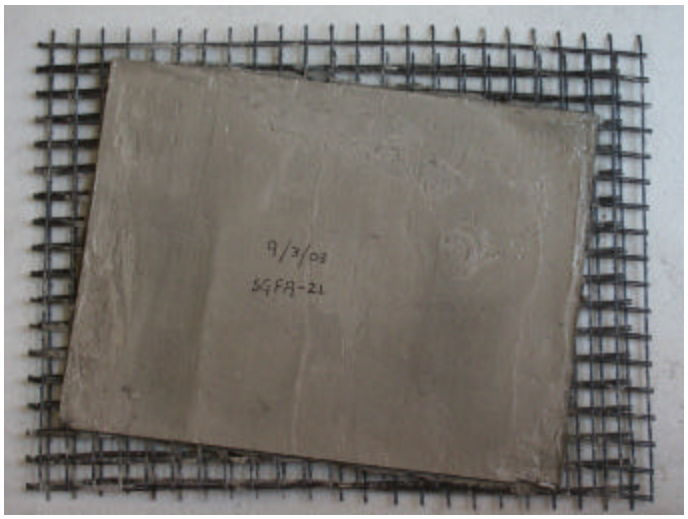

Figure 2.6a) Base plate with 4 strips forming the border, b) Initial layer of an off-axis sample, c) cast of a sample with 2 layers of fabric and a 2 inch offset orientation, d) The de-molded sample.

2.5.1 Effect of Manufacturing

Figure 2.7 shows comparison of Stress-Strain response of specimens cast in a different manner and 2 fabric layers. Type A represents specimen with lesser tensile strength that has been cast with the fabric freely laid and inexact matrix thickness between 2 layers of fabric. Type B represents specimen cast with fabric aligned fabric and held at all sides by the metal strips held in place by metal pins. The fabric was properly aligned and the matrix thickness was exact between the 2 layers of fabric. This led to a better bond between the matrix and the fabric and hence higher tensile strength. Specimen with freely laid fabric has average maximum tensile stress 2.33MPa whereas the specimen with fabric held and aligned has average maximum tensile stress 4.56MPa. The method of manufacturing can increase the tensile strength by 48.9% with both specimens having 2 fabric layers and same dimensions.

Table 2.3

Comparison between specimens cast differently and same number of fabric layers

Specimen Group	No. of Layers	Fabric Arrangement	Ave. Young's Modulus, E, MPa	Ave. Maximum Stress, MPa	Ave load, N/mm
Type A	2	Freely laid	4910.78	2.33	13.31
Type B	2	Aligned & Stretched	6281.89	4.56	26.05

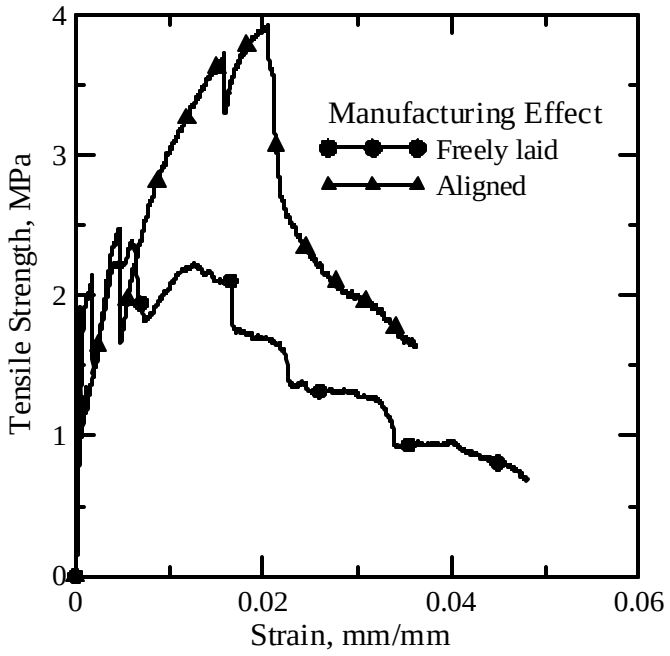

Figure 2.7 Effect of different manufacturing with same number of fabric layers

2.5.2 Effect of Fabric Orientation

The specimens were made with fabric properly held and aligned and were oriented at 25.4 mm and 50.8mm to study the orientation effects. Figure 2.8a, shows the

details of the fabric orientation and how the loading was applied. Table 2.4 shows comparison between tensile properties of these specimens.

Table 2.4

Comparison between specimens with different fabric orientation

Specimen Group	No. of Layers	Degree of Orientation	Ave. Young's Modulus, E, MPa	Ave. Maximum Stress, MPa	Ave load, N/mm
Type B-1"	2	6.009	3989.12	4.89	27.92
Type B	2	0	6281.89	4.56	26.05
Type B-2"	2	12.018	2760.41	2.69	15.35

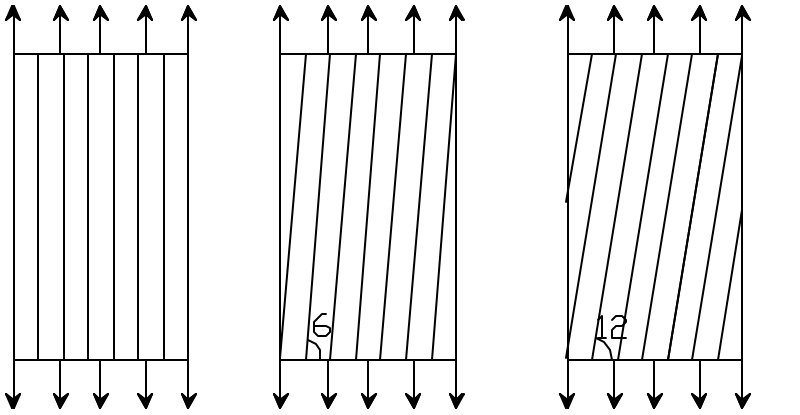

Figure 2.8a Different Orientations of the fabric

In Figure 2.8b, it can be seen that the Type B-1” representing 1” orientation (25.4 mm) sample shows higher tensile load carrying capacity. This can be attributed to the smaller orientation of the sample that increases the anchorage of its fibers in the matrix thus resulting in a relative increase in its load carrying capacity. Type B-2” representing 2” orientation (50.8 mm) sample shows a very low tensile load carrying capacity because

the orientation in this case is so high that the stronger direction of the fiber does not totally take the total tensile load. Finally, for Type B representing no orientation sample the tensile capacity is in between the 1” and 2” orientations. This is because in this case the fiber is oriented exactly parallel to the loading but the anchorage in this case is not very high and the matrix does not play an important role.

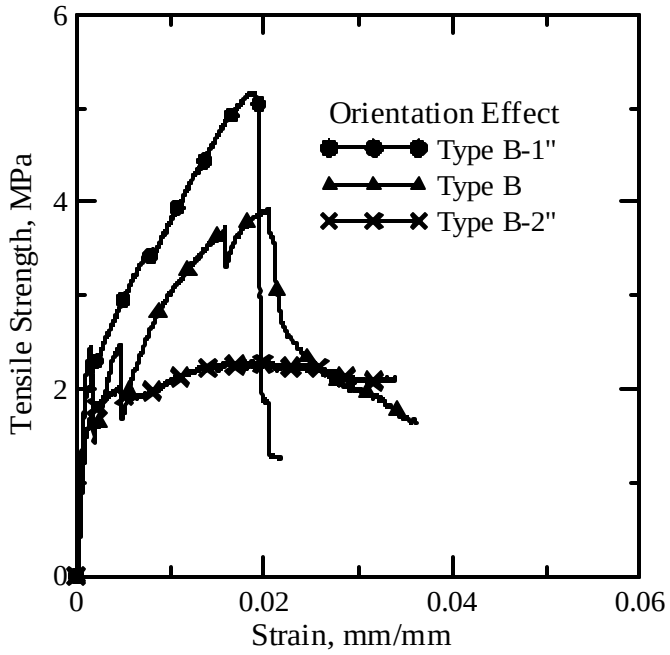

Figure 2.8b Effect of fabric orientation with all specimens having 2 fabric layers

2.6 Study of Specimens cast by Saint Gobain Technical Fabrics

Specimens were cast with 2 different fabric coatings for the same fabric as used for specimen preparation at ASU. Type C-M and XM specimens indicate material 5197(as designated by the company) and machine and cross machine direction of the fabric. Type D-M and XM specimens indicate material 5325(as designated by the

company) and machine and cross machine direction of the fabric. The specimens were prepared to ensure a flat surface inside the grips as described in section 2.2. The specimens were tested using the set up shown in section 2.3. Figure 2.9 through 2.12 shows a comparison using Bar chart of First crack stress, first crack strain, maximum stress and ultimate strain of both Type C and D specimens. The line graph shows the total data range and the average value for all the samples. The average values hence coincide for both the graphs. Table 2.5 shows a comparison of basic properties of these specimens.

Table 2.5

Comparison of specimens with different fabric coating and M, XM fabric direction

Specimen Group	No. of Layers	Fabric Arrangement	Avg. Young's Modulus, E, MPa	Ave. Maximum Stress, MPa	Ave load, N/mm
Type C-M	2	Machine Direction	5537.98	4.94	24.44
Type C-XM	2	Cross Machine Direction	6022.04	6.01	27.96
Type D-M	2	Machine Direction	4344.89	5.13	24.60
Type D-XM	2	Cross Machine Direction	5760.25	4.92	24.7

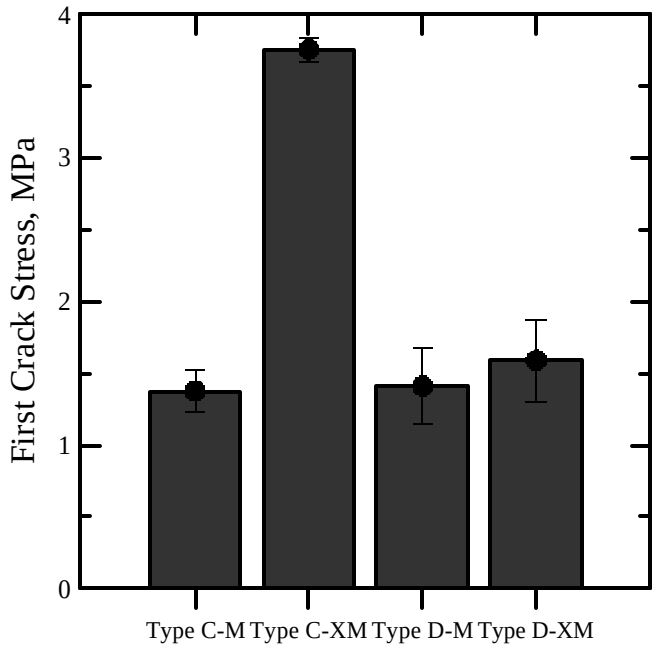

Figure 2.9 First Crack Stress for Type C and D specimens

First crack stress is much higher for Type C-XM specimens as compared to all other specimens. Whereas, the first crack strain is much higher for Type C-M specimens. Therefore, machine direction shows higher ductility till the first crack and cross machine direction shows more strength for fabric coating.

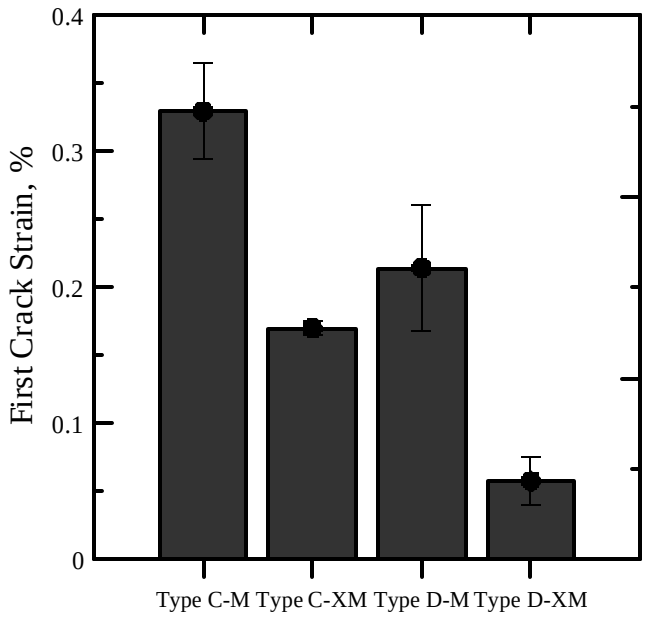

Figure 2.10 First Crack strain for Type C and D specimens

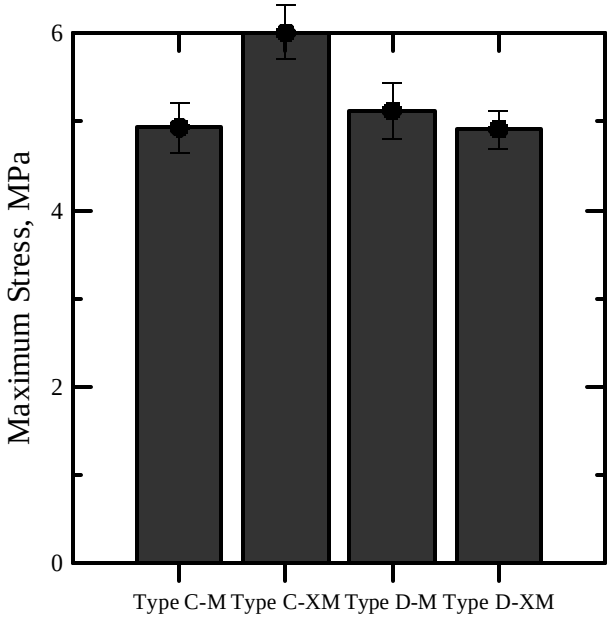

Figure 2.11 Maximum Tensile stress for Type C and D specimens

Maximum Tensile stress as well as Ultimate strain is highest for Type C-XM specimens.

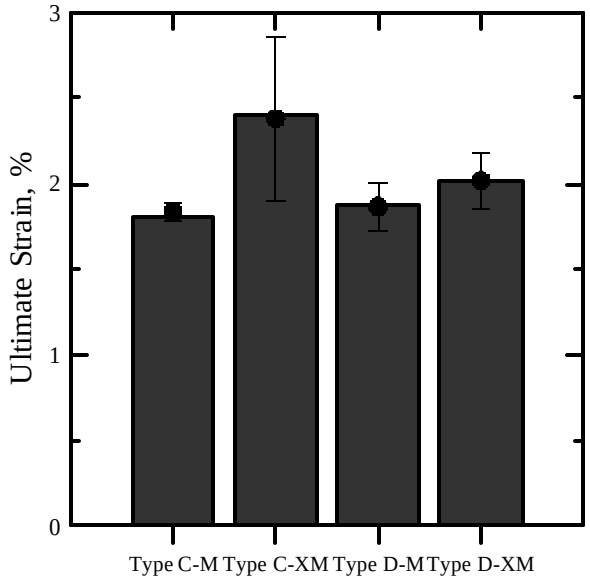

Figure 2.12 Ultimate strain for Type C and D specimens

For Type C, machine direction specimens have average maximum Tensile strength of 4.94MPa and ultimate strain 1.8%. The average first crack stress is 1.38MPa at an average strain of 0.33%. For Type C, cross machine direction samples the average tensile strength 6.01MPa. Average Strain at ultimate load is 2.4%. The average first crack stress is 3.76MPa at an average strain of 0.17%. For Type D, machine direction specimens have average tensile strength of 5.13MPa. Average Strain at ultimate load is 1.87%. The average first crack stress is 1.41MPa at an average strain of 0.21%. For Type D, cross machine direction specimens have average tensile strength of 4.92MPa. Average Strain at ultimate load is 2.02%. The average first crack stress is 1.59MPa at an average strain of 0.06%. These properties differ due to different fabric coatings and orientation of

fabric, which affects the bond and anchorage between the matrix and the fabric. As per the overall average values, Type C – XM has highest tensile strength as well as first crack stress values. The first crack strength is very well defined in cross machine direction and has a higher value of post crack strength. This maybe attributed to the better bond and anchorage of fabric with the matrix in the Cross machine direction as compared to the machine direction. Type C - M direction shows higher ductility and has more strain value at the development of first crack. For Type D, machine direction specimens are stronger and ductile as compared to cross machine direction. This can be attributed to different fabric coating and hence, different bond anchorage.

Figure 2.13 and 2.14 compare the Stress – Strain response of the samples with same fabric coating and different orientation of fabric layers. Figure 2.15 and 2.16 compare the Stress – Strain response of the samples with same orientation of fabric layers but different fabric coating. Figure 2.17 and 2.18 provide a bar chart for Maximum stress and Ultimate strain for Type C and D specimens comparing M and XM specimens.

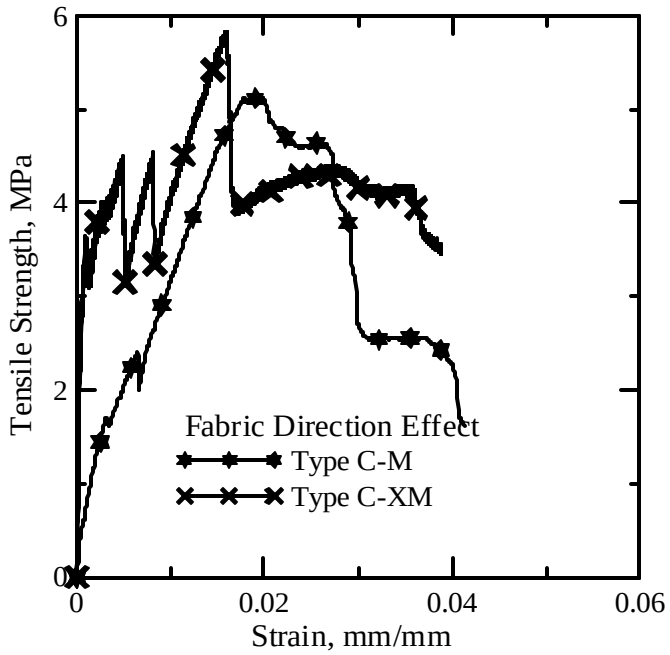

Figure 2.13 Effect of machine vs. cross machine direction for same fabric coating

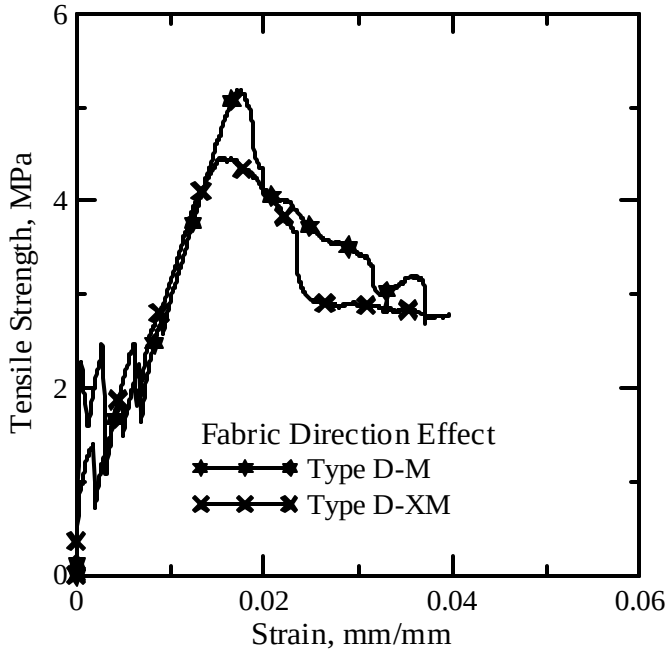

Figure 2.14 Effect of machine vs. cross machine direction for same fabric coating

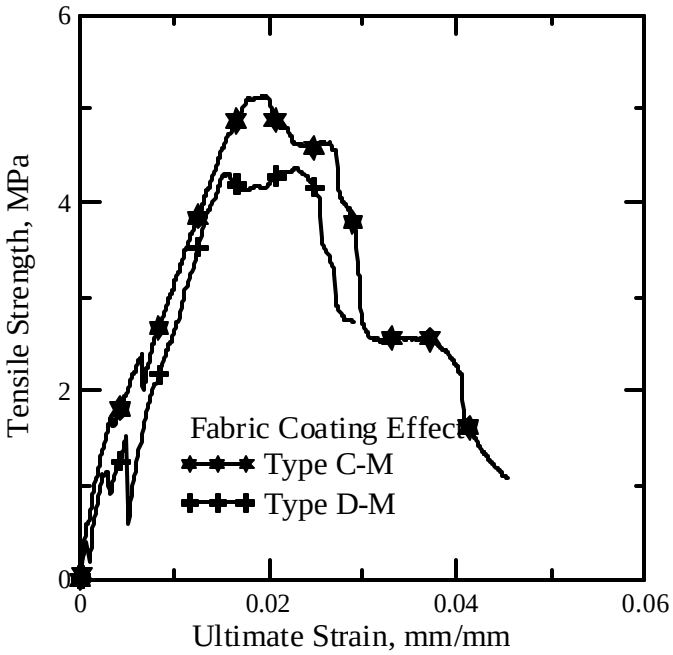

Figure 2.15 Effect of fabric coating for same fabric direction for Type C specimens

Figure 2.15 and 2.16 clearly show Type C specimens are stronger than Type D specimens for a given fabric direction. This may be attributed to the fabric coating of Type C specimens such that it gives a better bond and anchorage between the fabric and the matrix.

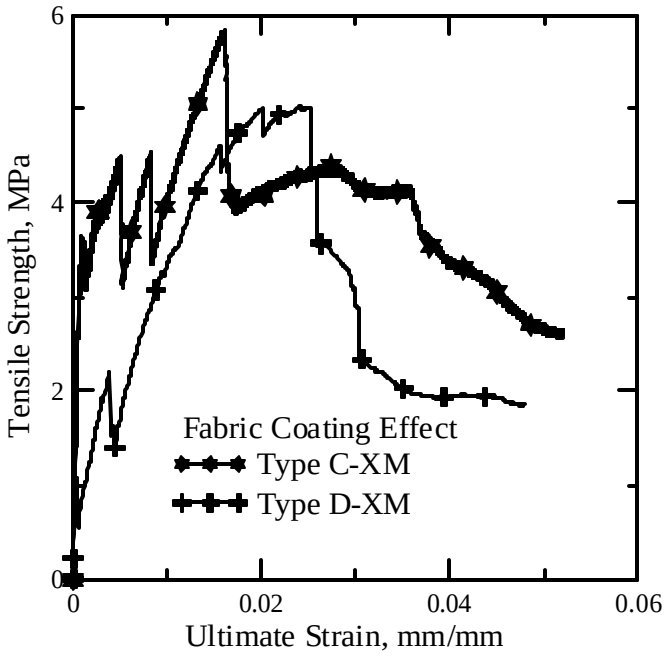

Figure 2.16 Effect of Fabric coating for same fabric direction for Type C and D specimens

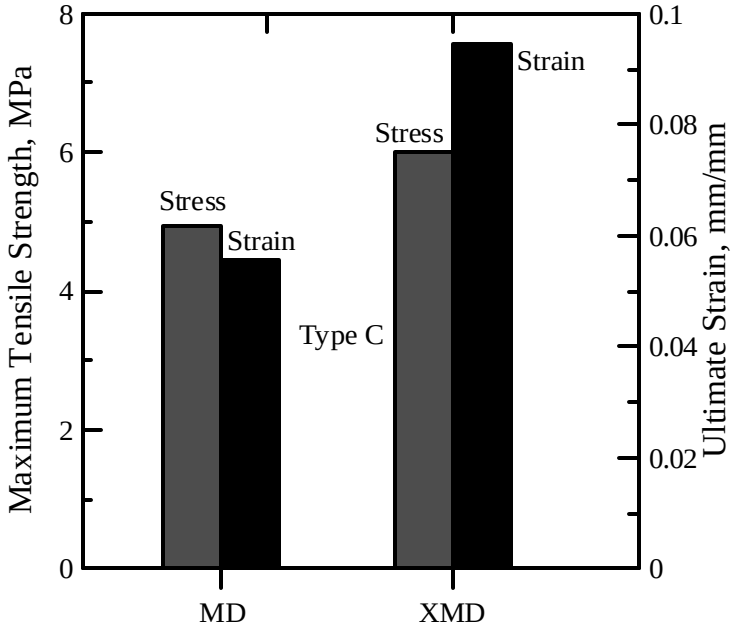

Figure 2.17 Bar chart to show Stress-Strain values for both Type C-M & XM

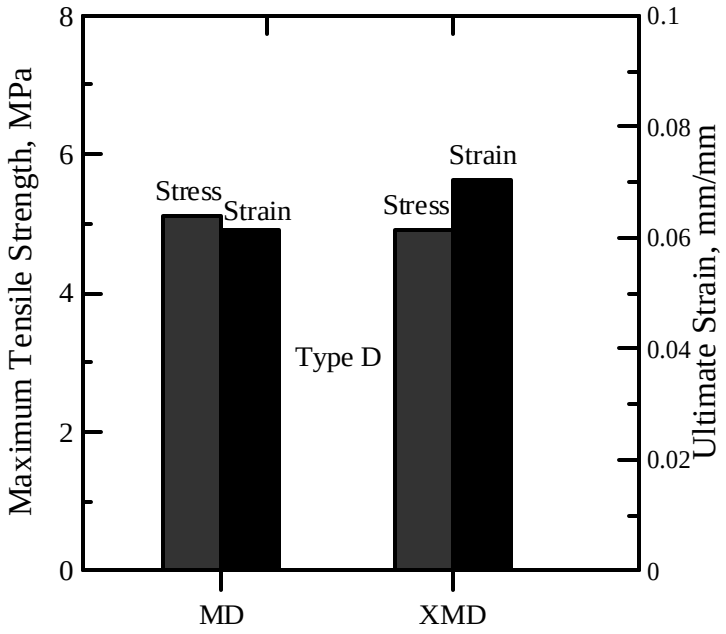

Figure 2.18 Bar chart to show Stress-Strain values for both Type D-M & XM

Out of all 4 types, 5197 XM samples show best combination of high tensile strength (6.01MPa) and Ultimate strain value (2.4%). In general, XM direction samples have higher Ultimate strain value (2.4% and 2.02%) than M direction samples (1.8% and 1.87%).

CHAPTER 3

ANALYSIS AND RESULTS OF FLEXURE TESTING

3.1 Test Set up

Flexure loading setup was developed that can be used for conducting both three point and four point flexure tests. The setup allows for rotation of the supports and loading head in order to ensure the loads are applied as line loads along the width of the specimen. This is particularly important in the response of the fabric cement specimens since a significant amount of deflection is expected in these specimens. The width of the supports is adjustable and can accommodate specimens up to 76.2mm (3") wide, while providing for rotation along two orientations. The base plate can be adjusted to be used for different sample lengths up to (457mm) 18". The samples have been tested for 254 mm (10") as well as 304.8mm (12") effective length. An LVDT (linear variable differential transformer) that is mounted on a deflection jig is used to measure the deflection of the sample during the test. Two clamps were fixed on the sample at the support locations and a rod connected these points. The rod was used to hold a LVDT so that the deflection at the center could be measured. The deflection was measured by the LVDT at the center point of the specimen. The range of the LVDT was 6.35mm ($\pm$0.125"), and once the specimen was loaded to this deflection, the LVDT was removed from the specimen and the test was further continued. Thereafter, actuator movement was used to measure the specimen deflection. The stroke response can be used to measure a total displacement of 76.2 mm (3"). After 6.35mm (0.25") of deflection, the

LVDT was removed. The tests can be conducted under stroke control or LVDT control. As the actuator moves down during the test, the specimen is loaded and the load, actuator, and LVDT displacements were recorded. The actuator measured the overall deflection of the specimen. The LVDT response has been used for the measurement of Young's Modulus because LVDT provides a better load and deflection response. The flexure test results for all the specimens were analyzed using Matlab and were plotted in Grapher.

Figure 3.1 shows the sample set up on the flexure testing machine with the LVDT mounted on it for a 3 point bending test. Figure 3.2a through c show the various stages of a flexure test in progress. After 6.35mm of deflection, the LVDT was removed. Figure 3.2b shows the test in progress almost at the time of completion. The test was stopped after this point since the bearings could eventually touch the specimen at the sides, making the results invalid. Due to these geometrical effects, the test was stopped before complete failure of the specimens. Figure 3.2c shows the sample after the test has been stopped.

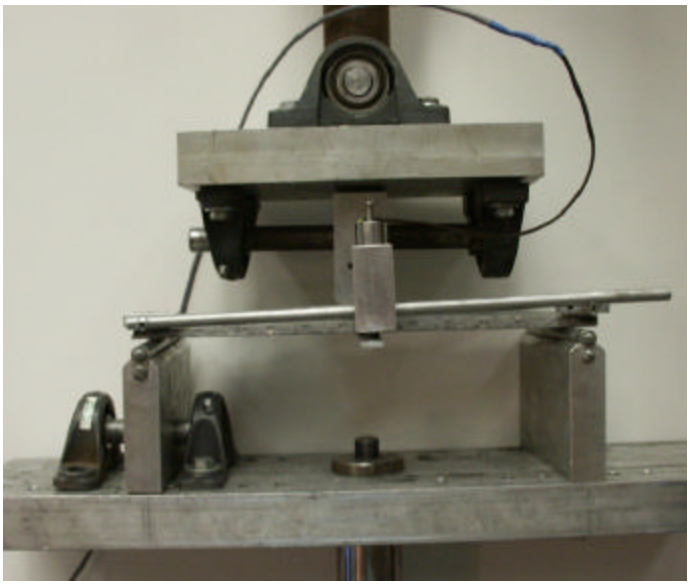

Figure 3.1 Sample with LVDT mounted for deflection measurements in 3 point bend test

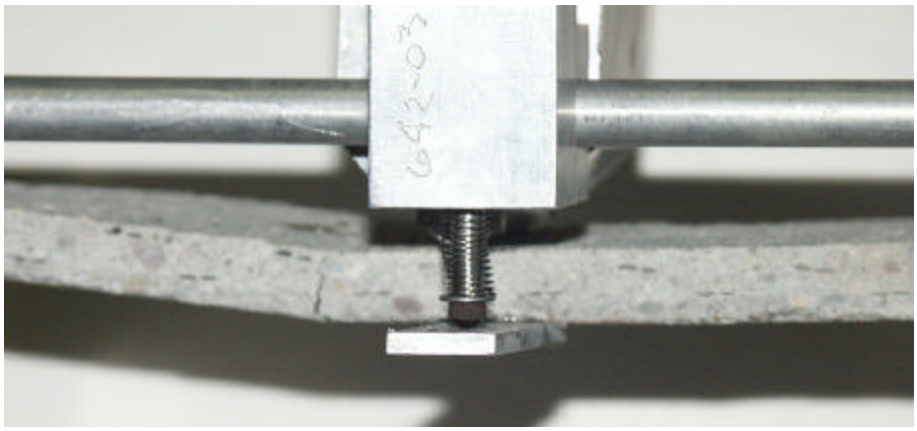

Figure 3.2a Specimen being loaded and deflection less than 6.35mm

Figure 3.2b Test very near to completion, LVDT has been removed

Figure 3.2c Test completed, Load cell is going back

Figure 3.2a through c: Various Stages in Flexural loading of a 3 point bend test

Figure 3.3 shows a sample setup for a 4 point bending test. Figure 3.4a through b shows various stages of 4 point bend test in progress.

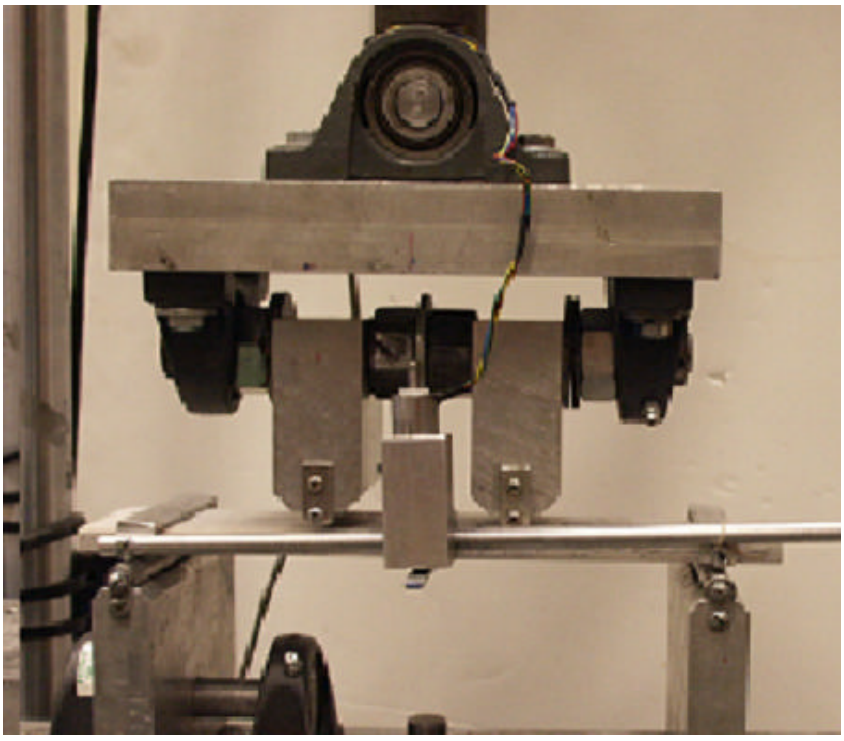

Figure 3.3 Sample with LVDT mounted for deflection measurements in 4 point bend test

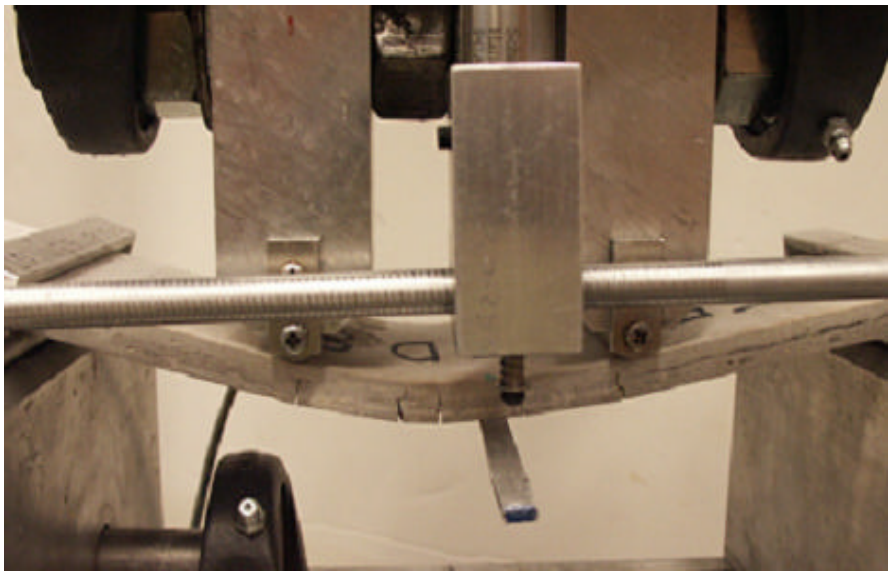

Figure 3.4a Deflection is more than 6.35mm and LVDT will be removed at this point

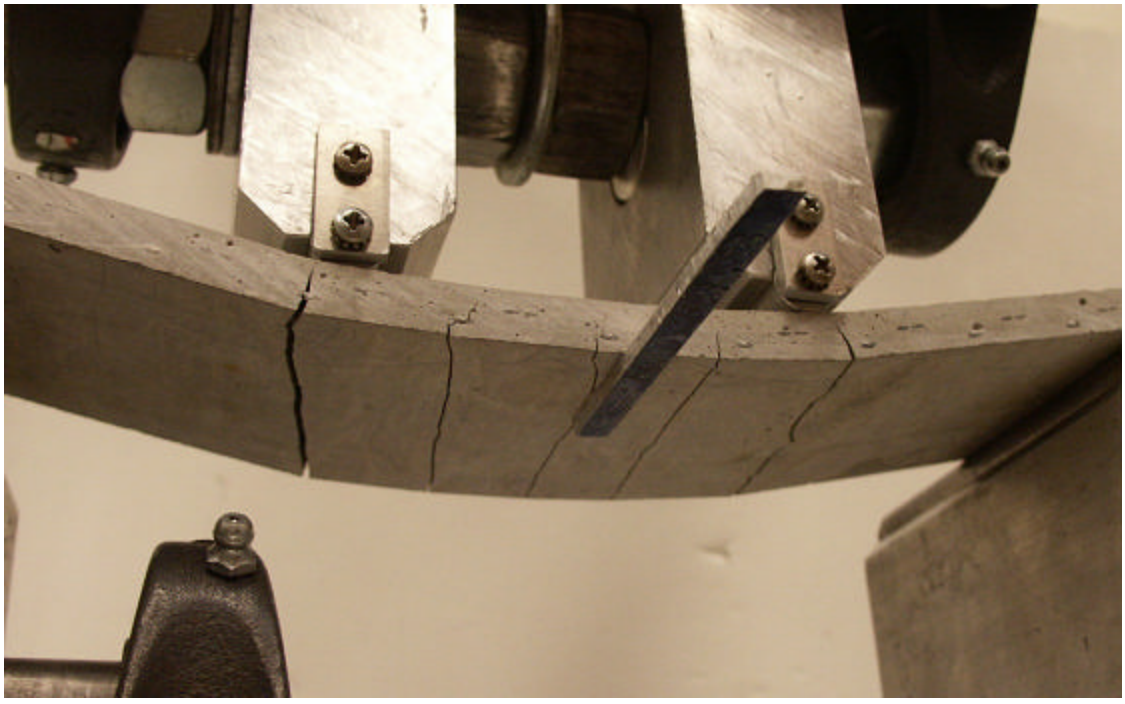

Figure 3.4b LVDT has been removed, test under progress

Figure 3.4b shows the formation of crack during the flexure test. The crack propagates through the matrix and as it strikes the fabric it moves along the fabric direction. Otherwise, it would have gone through the matrix and cracked it. This explains the high flexure strength due to presence of fabric layers.

3.2 Study of Specimens cast using Aligned fabric

The specimens were cast using the Mix design and mixing procedure given in Chapter 2. The specimens were cast using the mold mentioned in section 2.5. The specimens were cast with 2 fabric orientations of 25.4mm and 50.8mm. The tests were conducted as 3 point bending tests. Figure 3.5 shows a comparison of the representative specimens of these batches. Type B-1” specimens have average maximum Load of 455.26N and average maximum deflection of 7.09 mm. Type B-2” specimens have average maximum Load of 411.68N and average maximum deflection of 4.68 mm. Type B-1” specimens have a higher first crack load as compared to Type B-2”. This may be due to the fact that 25.4mm orientation leads to better bond and anchorage of the fabric with the matrix and the stronger fabric direction can still take the load till its maximum capacity. On the other hand, orientation of 50.8mm does not allow the stronger direction of the fabric to take the load properly. Therefore, Type B-1” specimens show higher first crack load as well as maximum load values. Table 3.1 compares the basic properties of Type B-1” and 2” specimens.

Table 3.1

Comparison of specimens with fabric oriented at 25.4mm and 50.8mm

Specimen Group	No. of Layers	Degree of Orientation	Young's Modulus, E, MPa	Maximum Load, N	Ave load, N/mm
Type B-1"	2	6.009	13862.53	455.26	33.02
Type B-2"	2	12.018	12609.87	411.68	31.62

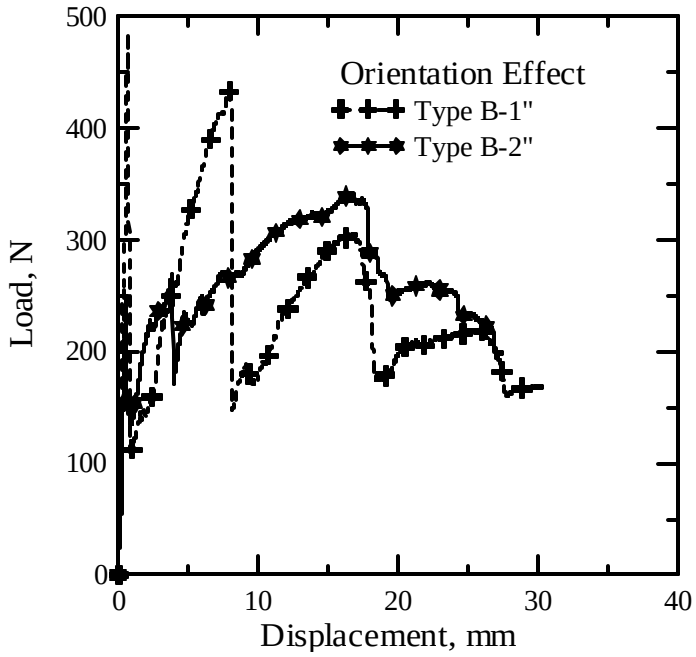

Figure 3.5 Effect of fabric orientation with all specimens having 2 fabric layers

3.3 Study of specimens cast by Saint Gobain Technical Fabrics

Specimens were cast with 2 different fabric coatings for the same fabric as used for specimen preparation at ASU. Type C-M and XM specimens indicate material 5197(as designated by the company) and machine and cross machine direction of the fabric. Type D-M and XM specimens indicate material 5325(as designated by the

company) and machine and cross machine direction of the fabric. The tests were conducted as 4 point bending tests. Figure 3.6 shows a load displacement plot with both displacements of actuator as well as LVDT for a Type C-M specimen. It is clear from the graph that the LVDT predicts a more accurate response than the actuator. LVDT eliminates extraneous deformations such as support settlement and specimen rotations. Therefore, Young's Modulus, first crack load and first crack deflection were calculated using LVDT response for all the specimens.

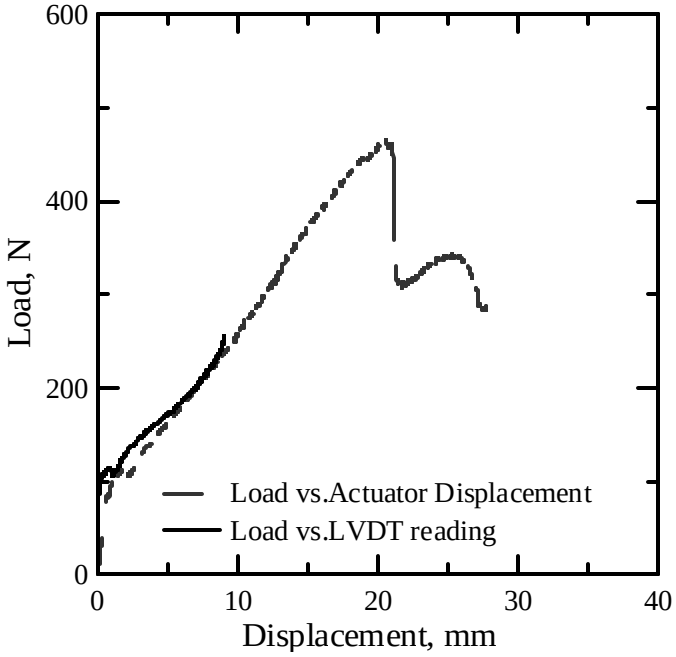

Figure 3.6 Load vs. Displacement plot for a Type C-M specimen

Figure 3.7 through 3.10 show bar charts for Type C and D specimens for both machine and cross machine direction of the fabric. The bar charts show first crack stress, first crack displacement, maximum stress and deflection at maximum load. Studying these specimens helps to understand the effect of direction of fabric and effect of fabric

coating with same direction of fabric. Table 3.2 compares the basic properties of these specimens.

Table 3.2

Comparison of Type C and D specimens

Specimen Group	No. of Layers	Fabric Direction	Young's Modulus, E, MPa	Maximum Stress, MPa	Ave load, N/mm
Type C-M	2	Machine	7047.00	15.7	31.6
Type C-XM	2	Cross Machine	10679.00	17.64	32.5
Type D-M	2	Machine	8226.20	16.79	36.30
Type D-XM	2	Cross Machine	10784.00	12.77	27.70

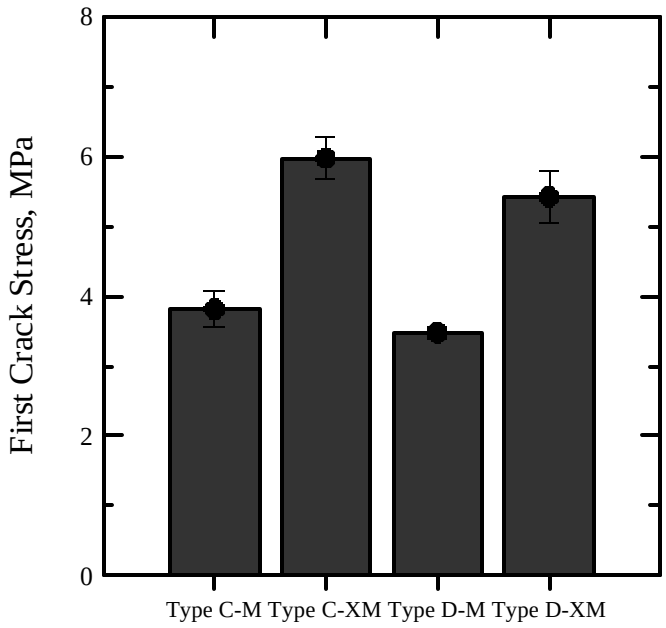

Figure 3.7 Bar chart showing first crack stress values for Type C and D specimens

The above comparisons show that Type C-XM specimens have most defined first crack stress as well as first crack deflection values. The Type D- XM specimens also have first crack stress values higher than machine direction fabric specimens for the same fabric coating. Bar chart shows average values. The standard deviation plot is for all the specimens of a given type and hence coincides with the average value.

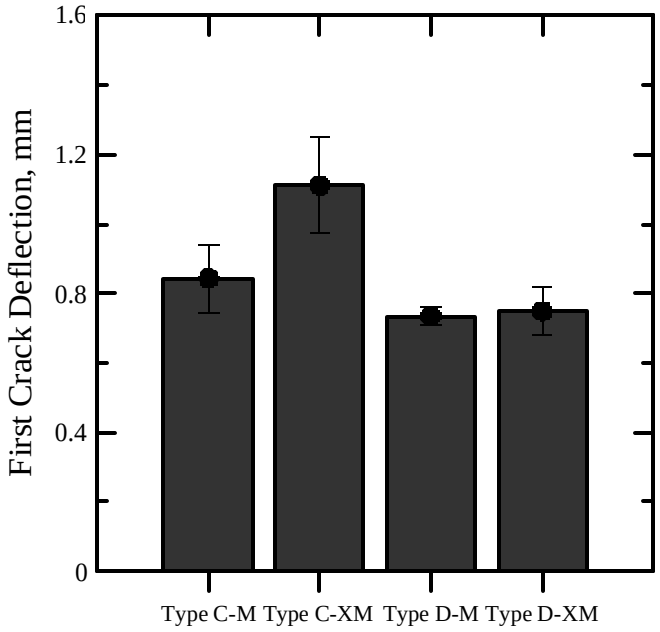

Figure 3.8 Bar chart showing first crack deflection values for Type C and D specimens

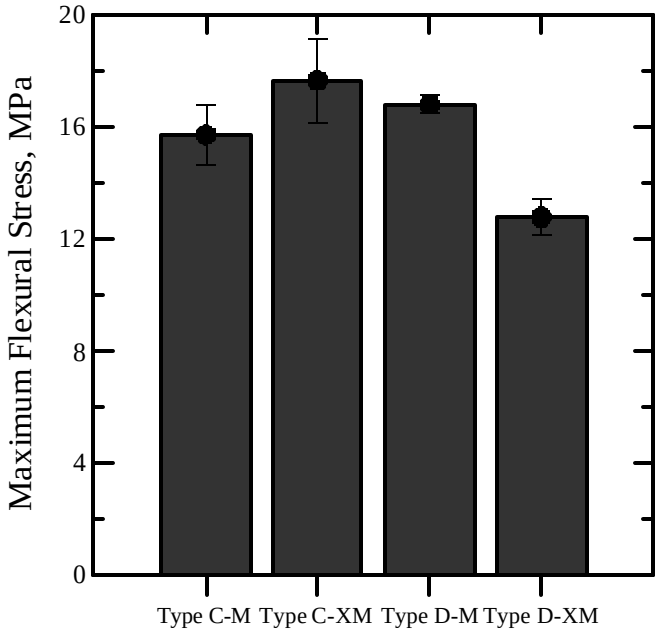

Figure 3.9 Bar chart showing maximum stress values for Type C and D specimens

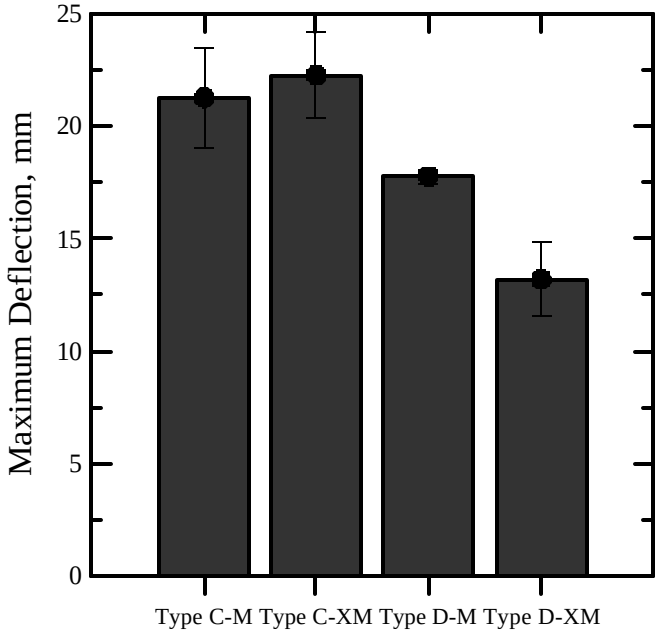

Figure 3.10 Bar chart showing maximum deflection values for Type C and D specimens

The average flexural strength for Type C-M samples is 15.7MPa. The average first crack stress is 3.8MPa at a deflection of 0.8 mm. The deflection at maximum load for these specimens is 21.3mm. The average flexural strength for Type C-XM samples is 17.64MPa. The average first crack stress is 6.0MPa at a deflection of 0.4 mm. The deflection at maximum load is 22.3mm. The average flexural strength for Type D-M specimens is 16.8MPa. The average first crack stress is 3.5MPa at a deflection of 0.7mm. Deflection at maximum load for these specimens is 17.8mm. The average flexural strength for Type D-XM samples is 12.8MPa. The average first crack stress is 5.4MPa at a deflection of 0.7 mm. The deflection at maximum load is 13.2mm. These properties differ due to different fabric coatings and orientation of fabric, which affects the bond and anchorage between the matrix and the fabric.

Figure 3.11 compares the Load deflection response of the Type C specimens with same fabric coating and different orientation of fabric layers. Figure 3.12 shows the magnified view of the initial loading stages as recorded by the LVDT. The specimen with XM direction of fabric has a Flexural strength 17.64MPa, approximately 11% higher from the specimen with M direction of fabric. This maybe attributed to the better anchorage of fabrics in the cross machine direction. The better bond development due to better anchorage enables the specimens to take more flexural load. The first crack stress is approximately 37% higher for cross machine direction specimens as compared to machine direction specimens. The first crack values are more significant for cross machine direction specimens. Therefore, having same fabric coating but varying the fabric direction can affect the strength considerably.

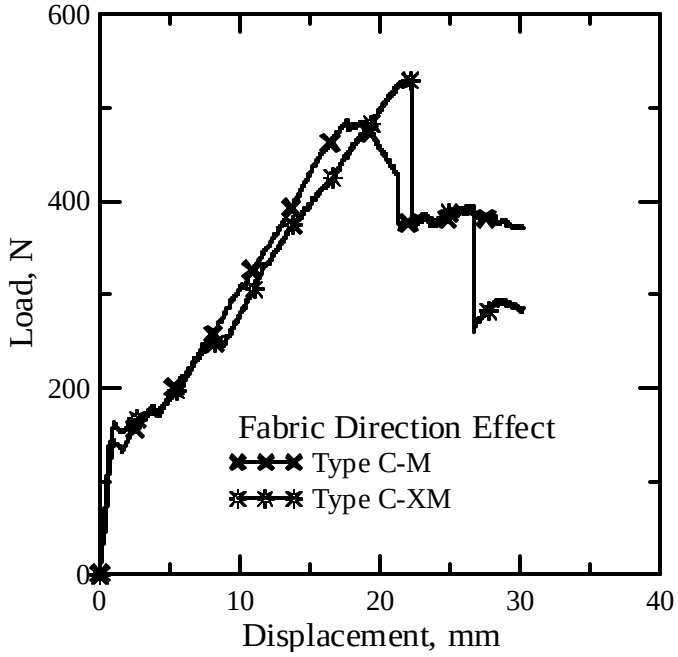

Figure 3.11 Effect of fabric direction on flexural properties with same fabric coating

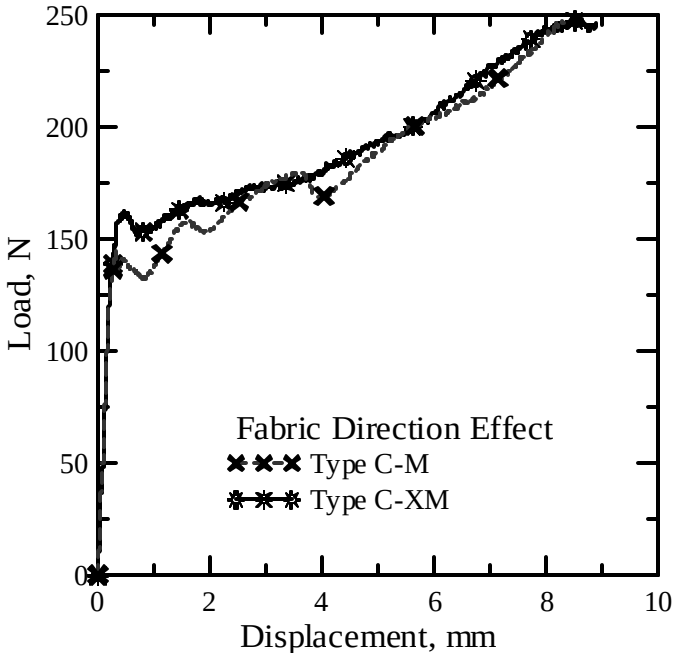

Figure 3.12 LVDT response for Type C specimens

Figures 3.13 and 3.14 show a similar treatment of comparisons for machine vs. cross machine directions for the Type D specimens. The specimen with machine

direction of fabric has a Flexural strength 16.8MPa, approximately 24 % higher from the specimen with cross machine direction of fabric. The first crack stress is 3.5MPa for Type D-M specimens and 5.4MPa for Type D-XM specimens. The first crack deflection is 0.7mm for Type D-M and XM specimens. The first crack strength is very well defined in cross machine direction and has a higher value whereas the post crack strength is lesser in this case. This maybe attributed to the fact that cross machine direction had a better anchorage initially and after the application of load the fabric being in XM direction could not sustain high strength. Whereas, the fabric in M direction could take a higher load as the M direction is a stronger direction.

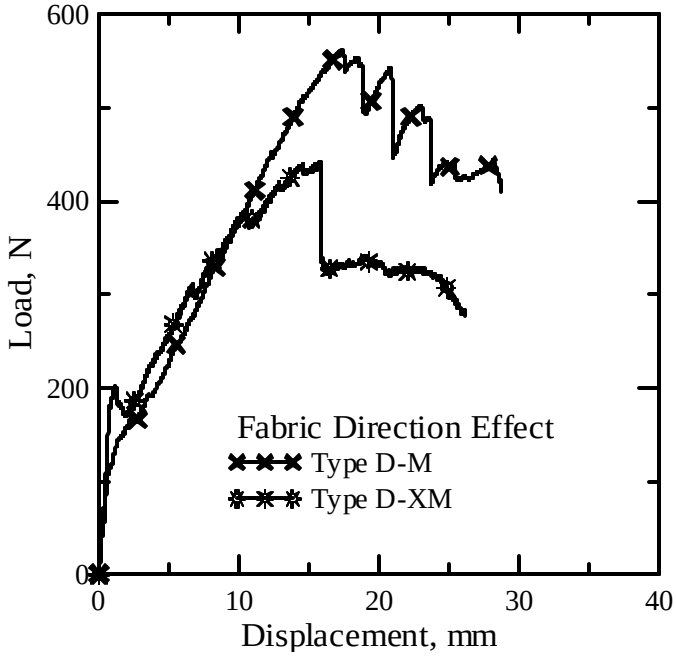

Figure 3.13 Effect of fabric direction on flexural properties with same fabric coating

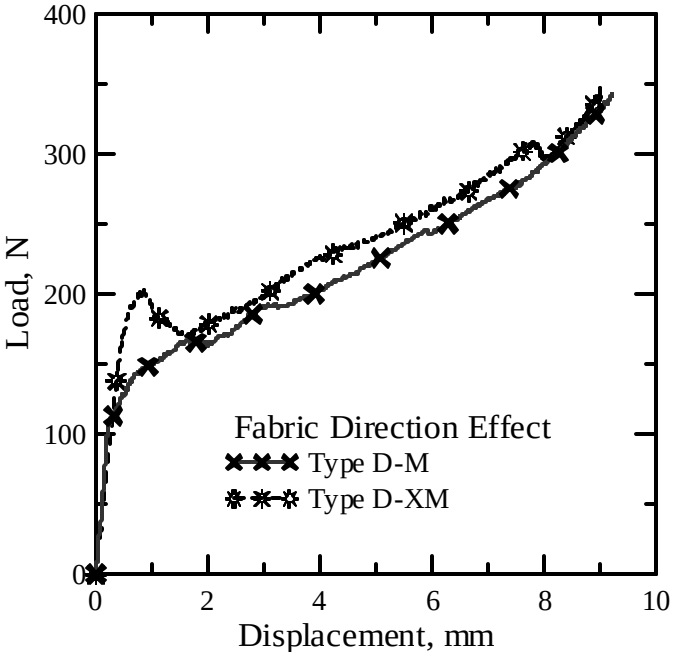

Figure 3.14 LVDT response for Type D specimens

Figure 3.15 compares the Load deflection response of the samples with different fabric coating and same orientation of fabric layers. Specimen from Type C-M has well defined and higher First crack stress of 3.8MPa as compared to 3.5MPa of specimen from Type D-M. First crack deflection is 0.8mm for Type C-M and 0.7mm for Type D-M. Ultimate flexural strength for Type C-M is 15.7MPa and 16.8MPa for Type D-M. These values are statistically insignificant. The differences maybe attributed to Type C having a different fabric coating. After cracking, due to a weaker bond between fabrics and fabric coating, a lower strength is obtained. Whereas, it can be observed that for Type D fabric coating is such that it gives a better bond between fabric and matrix, thus making the specimen behave as a composite which leads to a higher post crack strength.

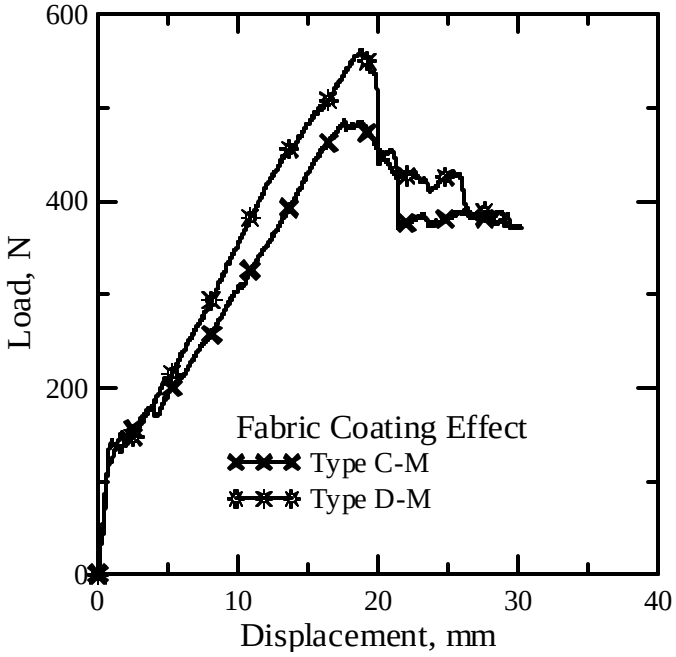

Figure 3.15 Effect of fabric coating on flexural properties with same fabric direction

Figure 3.16 shows the LVDT response for the Type C-M and D-M specimens.

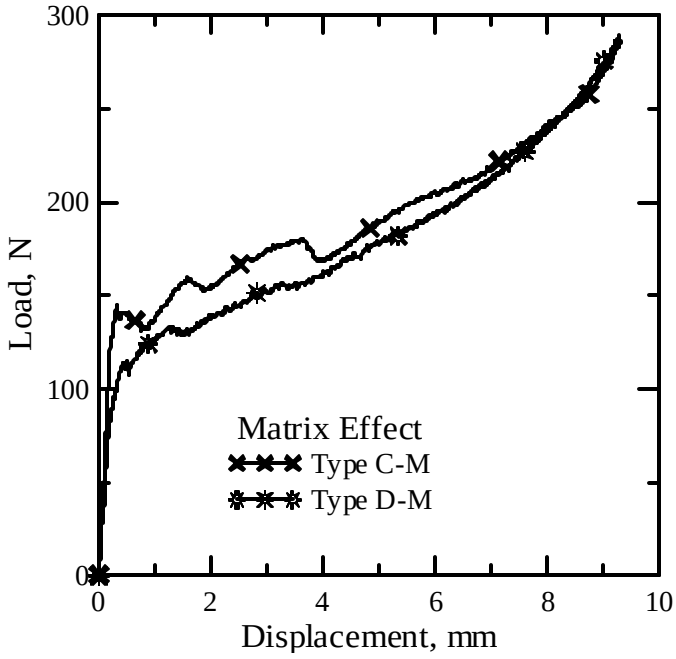

Figure 3.16 LVDT response for Type C-M and D-M specimens

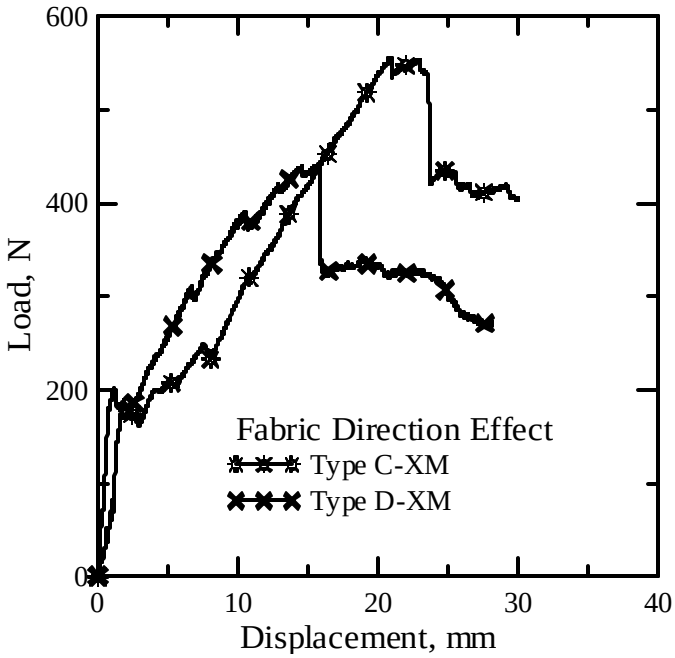

Figure 3.17 Effect of matrix on flexural properties with same fabric direction

Figure 3.17 compares the Load deflection response of the samples with different fabric coating and same orientation of fabric layers. Specimen from Type C has average First crack stress of 6MPa as compared to 5.4MPa of specimen with Type D. First crack deflection is 1.1mm for Type C-XM and 0.7mm for Type D-XM. Ultimate Flexural strength is 17.6MPa for Type C-XM and 12.8MPa for Type D-XM. The above plot clearly shows that keeping the fabric direction same, Type C fabric coating makes the specimens stronger than Type D. Figure 3.18 below shows the LVDT response for the above specimens.

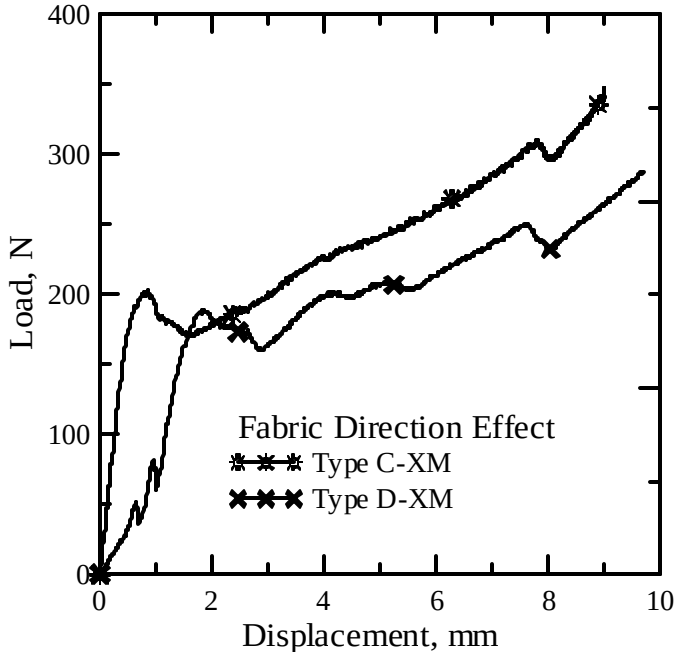

Figure 3.18 LVDT response for Type C-M and D-M specimens

On the basis of above figures, bar charts and discussions it can be concluded that Type C-XM samples show best combination of highest flexural strength (17.64MPa) and deflection under maximum load(22.3mm). For Type C-XM direction samples have higher value of First crack stress (6MPa) than M direction samples (3.8MPa). First crack deflection for XM direction samples is 1.1mm whereas for M direction samples it is 0.8mm. This maybe attributed to the better anchorage of fabrics in the cross machine direction. For Type D, XM direction samples have lower value of Flexural stress (12.8MPa) than M direction samples (16.8MPa). Maximum deflection for XM direction samples is 13.2mm whereas for M direction samples it is 17.8mm. This maybe attributed to the fact that cross machine direction had a better anchorage initially and after the application of load the fabric being in XM direction could not sustain high strength. Whereas, the fabric in M direction could take a higher load as the M direction is a

stronger direction. This behavior is different for Type D specimens which maybe due to the difference in fabric coating.

CHAPTER 4

MASONRY – FABRIC COMPOSITE BOND TESTING

4.1 Bond Specimen preparation

A setup was prepared to measure the bond of a fabric-cement composite sample with a typical masonry block. The sample preparation was based on casting a two layer composite system directly on a masonry block. In this set up the specimen was cast on two masonry blocks, however, one of the blocks was prevented from bonding to the composite using a thin polyethylene film. After the initial curing cycle of 24 hours was completed, the sample was removed from the support masonry. The resulting specimen and the bond sample are shown in Figures 4.1a-d. The schematics of the fixture set up are shown in Figure 4.1e - f represents the specimen placed in the fixture ready to be tested under a tensile loading condition. Figure 4.2a-b show the bond test setup and the sample placed in the fixture mounted over in the setup. The sample is completely placed in Figure 4.2.b and tested after this stage.

Figure 4.1a Casting of bond sample on 2 masonry blocks. The block covered with yellow sheet (bond breaker) will be removed after initial curing of 24 hours.

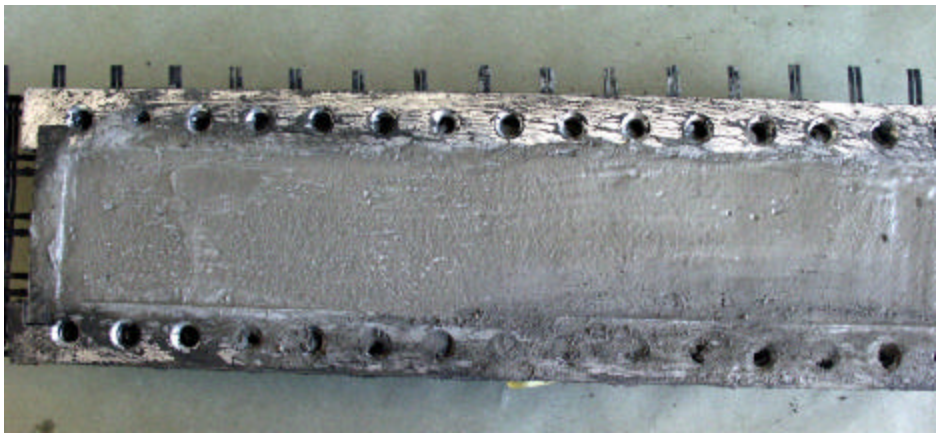

Figure 4.1b Top View of the Bond Sample prior to de-molding

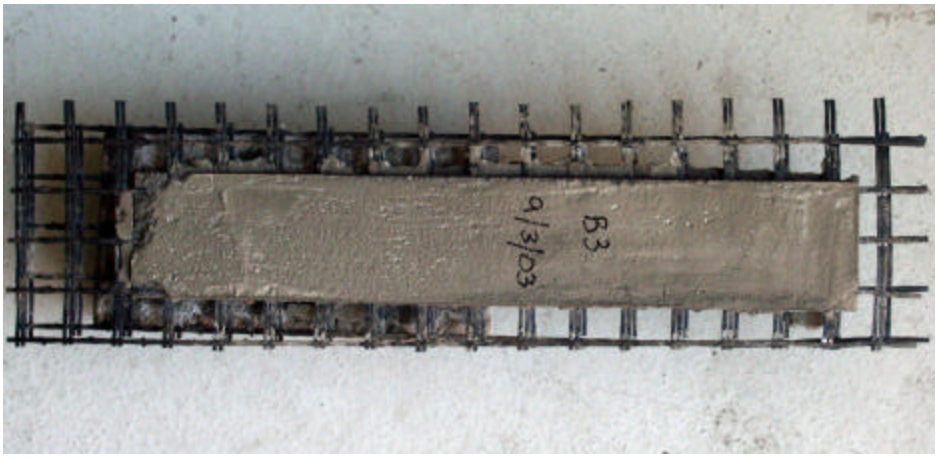

Figure 4.1c Top view of the sample after removing from the mold

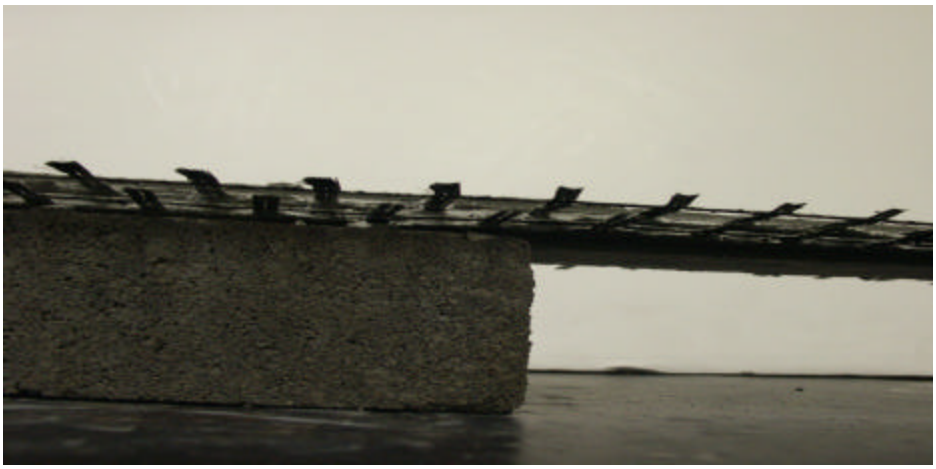

Figure 4.1d Side view of the sample after removing from the mold

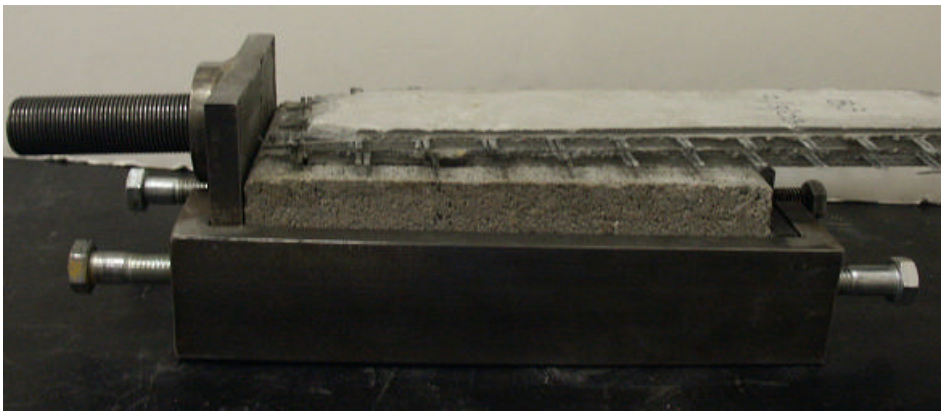

Figure 4.1e Side view of the sample placed in the fixture

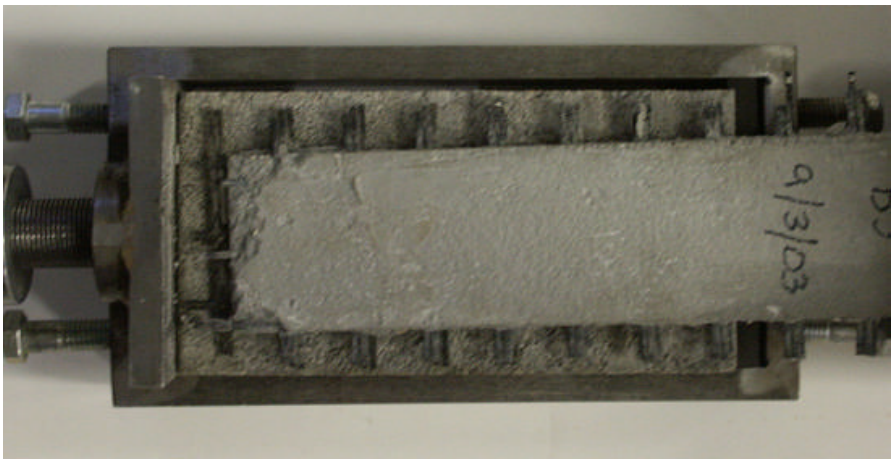

Figure 4.1f Top view of the sample placed in the fixture

The mix design and the mixing procedure for casting the specimen over the masonry block used are the same as mentioned in section 2.1.The fixture was designed in a manner that nut was locked in one of the grips and the other grip held the cast specimen unsupported by the masonry block. Figure 4.2a shows the fixture mounted on the Hydraulic Grips. The test was run as a tension test with the help of shown fixtures. It was conducted using a closed loop servo-hydraulic testing frame operated under stroke control, and the load and elongation of the specimen was recorded

throughout the test. Figure 4.2b shows the specimen placed in the fixtures and ready for testing.

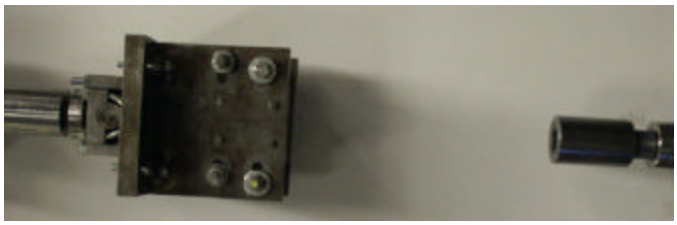

Figure 4.2a Bond Test setup (view rotated)

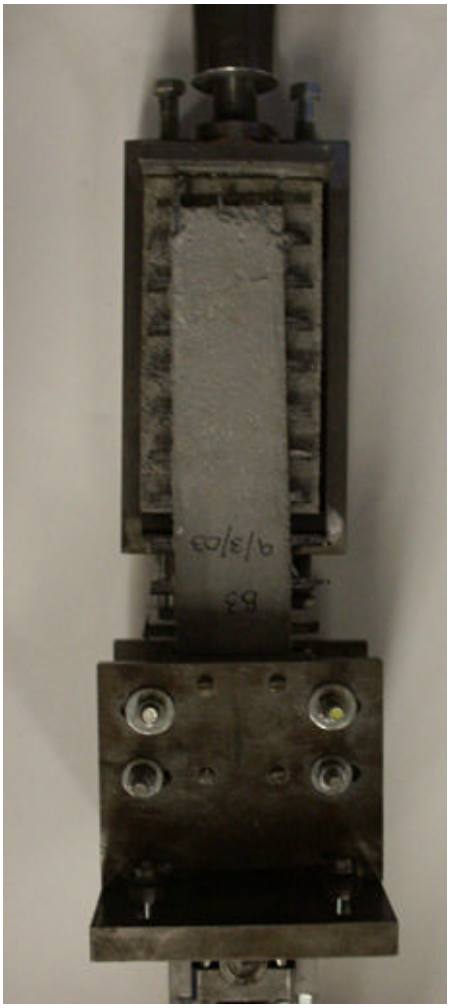

Figure 4.2b Bond test setup with the sample placed in the fixture

4.2 Results

Figure 4.3 shows Load – Deflection response of a Bond sample. Figure 4.4 shows a comparison of Load Deflection response of 5 bond samples. A representative sample has been selected out of the 5 samples which have experimental values very near to average value of Load and Deflection for all the specimens. Figure 4.5 shows a comparison between Load deflection response of a specimen tested under tension and a Bond sample tested under tension.

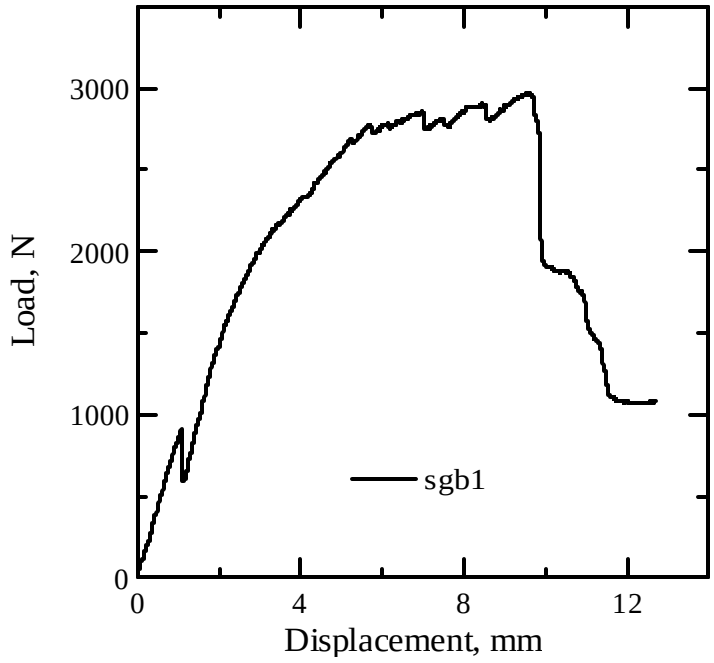

Figure 4.3 Load – Displacement response of sgb1

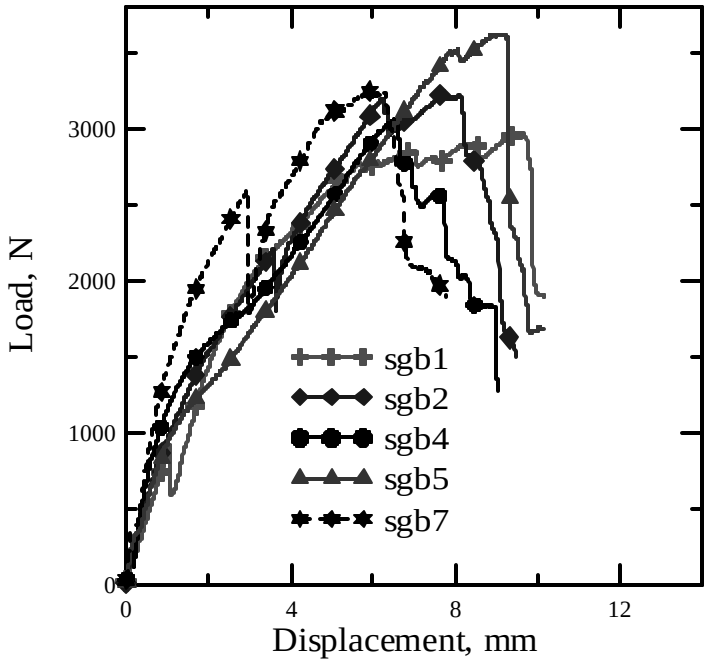

Figure 4.4 Comparison between Load – Displacement response of all samples

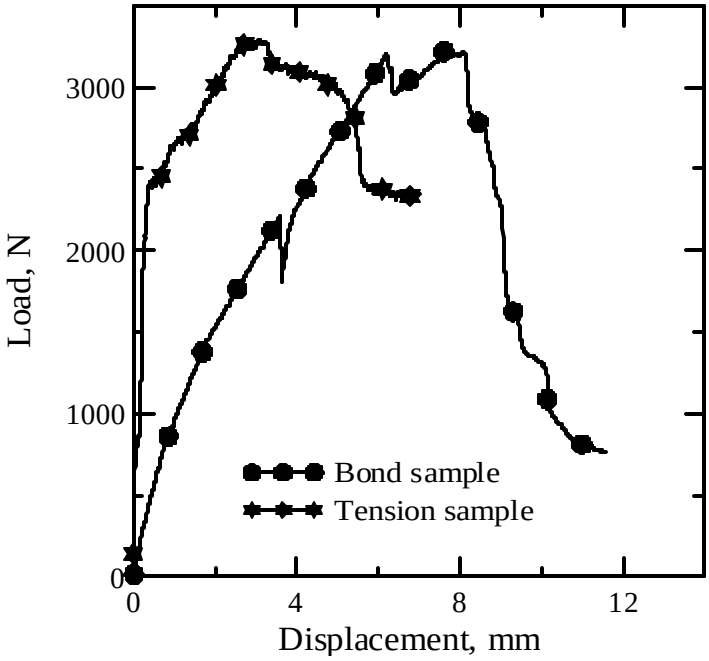

Figure 4.5 Comparison between Load – Displacement plot of a Bond & Tension specimen

The above plot shows a tensile specimen that has been cast and tested as the procedure mentioned in chapter 2. Both tensile and bond specimen have 2 layers of fabric. The fabric has been held and aligned in both cases. A similar mold as mentioned in chapter 2 was developed for bond specimen of the required dimensions. The matrix thickness between the layers of the fabric was maintained. Both specimens have similar maximum load value. The maximum load for tensile specimen is 3280N at a deflection of 3.22mm. The maximum load for bond specimen is 3219N at a deflection of 7.62mm. This shows that if a composite is cast on the masonry wall, the block will have a tensile strength equal to that of the tensile strength of the cast composite. This can be used to reinforce seismic hit masonry walls and improve their tensile strength.

CHAPTER 5

STUDY OF AGEING EFFECT ON TENSILE AND FLEXURAL PROPERTIES

5.1 Introduction

The specimens using 2 layers of seismic reinforcing grid provided by Saint Gobain Technical fabrics were studied for ageing effect on tensile and flexural properties. The specimens were kept at fan elevated temperature of 80^{o}C in water with saturated calcium hydroxide in it. The details of the setup are provided in section 5.2. The basis of these tests is that it will develop data that indicates real life natural weathering performance. The basic principle is that elevated temperature and moisture content is an indicator of the long term behavior of fabric reinforced composites. Elevated temperature and moisture content accelerate the formation of the products of hydration of cement in the matrix particularly calcium hydroxide. The interaction of these products of hydration especially calcium hydroxide with the fabric has a long term effect on the composite properties. The principal mechanism that occurs is that the calcium hydroxide forms within the bundles of filaments that form the glass fiber strand. This gradually bonds the filaments together, which reduces filament pull-out. This causes a reduction in the strain capacity of the composite, thereby reducing the strength of the composite and changing the composite from a ductile material to an increasingly brittle material. Accelerating the formation of the hydration products accelerates their interaction with the fibers, hence accelerating the ageing of the composite.

5.2 Experimental Set up

The Ageing Setup was developed using a constant temperature oven calibrated at 80 degrees Celsius. The samples were stored in a metal container with water and 15 grams of saturated calcium hydroxide. The thermometer was used to monitor the temperature inside the oven at a constant preset level. Temperature was checked every 12 hours to make sure that temperature was constant. A long copper tube was used to connect the inside of the metal container to the outside, allowing for the evaporation and subsequent condensation of the water from the container. The evaporated water condensed in the tube and fell back into the metal container. This maintained moisture level inside the metal container where specimens were kept. Figure 5.1 shows the ageing set up that was used to age the specimens. A set of 60 specimens was cast with same design by Saint Gobain Technical Fabrics using two layers of fabric to study ageing effect on tensile and flexural properties of the specimens. 30 specimens were cast in machine direction and 30 in cross machine direction designated M and XM respectively. Table 5.1 and 5.2 shows the experimental plan followed.

Table 5.1

Experimental plan followed to study the ageing effect in tension

Specimen Type	No. of specimens tested in tension	Un-aged	Age 14 days	Age 28 days
Type E - M	5	X		
Type E - XM	5	X		
Type EM-AGE14	5		X	
Type E XM-AGE14	5		X	
Type EM-AGE28	5			X
Type E XM-AGE28	5			X

Table 5.2

Experimental plan followed to study the ageing effect in flexure

Specimen Type	No. of specimens tested in tension	Un-aged	Age 14 days	Age 28 days
Type E - M	5	X		
Type E - XM	5	X		
Type EM-AGE14	5		X	
Type E XM-AGE14	5		X	
Type EM-AGE28	5			X
Type E XM-AGE28	5			X

Figure 5.1 Ageing Setup (from Inside the oven) showing the container as well thermometer and copper tube

5.3 Study of ageing effect on tensile properties

The specimens were tested un-aged as well as after ageing for 14 days and 28 days and were tested in tension. The specimens were tested using a closed loop servo-hydraulic testing frame operated under stroke control, and the load and displacement of the specimen was recorded throughout the test. The details of tensile specimen preparation to get a flat surface are same as provided in section 2.2. Figure 5.2 below

provides a comparison stress vs. strain plot of specimens that were un-aged in machine and cross machine direction.

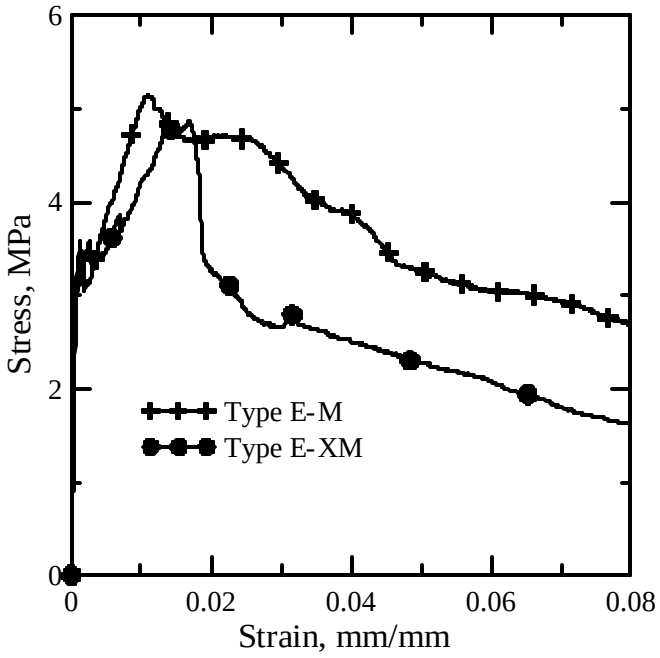

Figure 5.2 Comparison of stress vs. strain plot of un-aged specimens in machine and cross machine direction with each having 2 layers of fabric and same mix design

The specimens in machine direction have an average maximum tensile stress of 5.03MPa at a strain of 1.07%whereas, the specimens in cross machine direction the average maximum tensile stress is 4.65MPa at a strain of 1.62%. This can be attributed to the fact that fabric is stronger in machine direction and therefore can take higher load. It can also be seen that specimens n cross machine direction can go till a higher ultimate strain. This may be due to the fact that cross machine direction can form a better bond and will therefore, stretch more to go till a maximum load. Table 5.3 shows the tensile properties of these specimens.

Table 5.3

Comparison of tensile properties of un-aged specimens

Specimen Group	Fabric direction	Ave. First Crack stress, MPa	Ave. First Crack strain, %	Ave. Maximum Stress, MPa	Ave load, N/mm
Type E-M	Machine	3.41	0.16	5.03	26.45
Type E-XM	Cross machine	3.35	0.12	4.65	23.67

Figure 5.3 and 5.4 show the fabric geometry in machine direction and cross machine direction. The fabric geometry shows that there is a bulge of filaments at the intersection of the machine and cross machine direction in the machine direction of fabric. The cross machine direction strands go straight and machine direction strands go over them and there is a curvature at the point where they go over the cross machine direction strands. When the specimens were tested un-aged this portion will simply stretch and will let the specimen bend thereby utilizing the maximum stress that fabric can take. When the specimens were aged the products of hydration may occupy this space and will make the fabric weak at this point. Therefore, when the specimens were tested in tension the fabric took lesser stress in machine direction as the fabric breaks easily due to these intersection sights. This observation is strengthened by the fact that during the experiments machine direction specimens had more crack formation as compared to cross machine direction specimens.

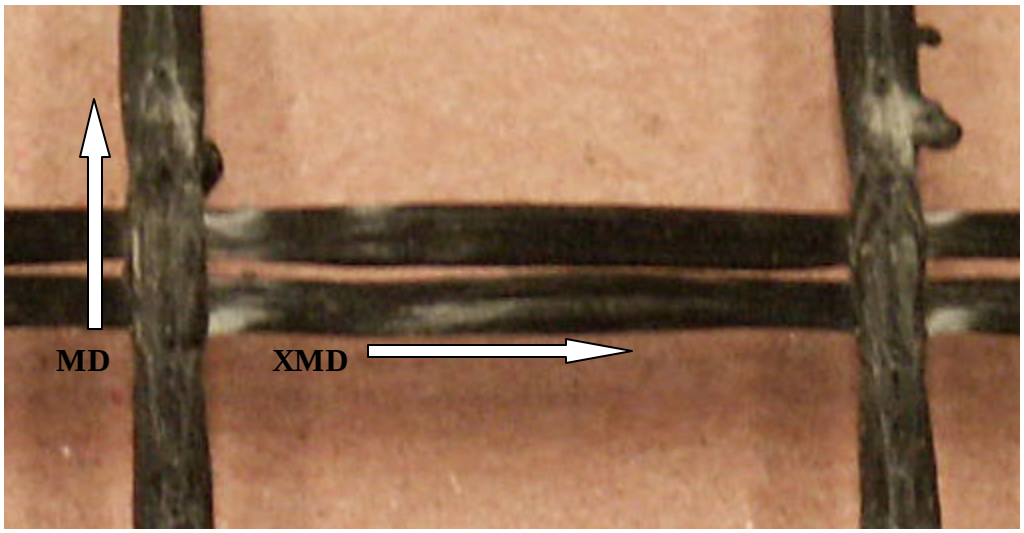

Figure 5.3 Fabric used

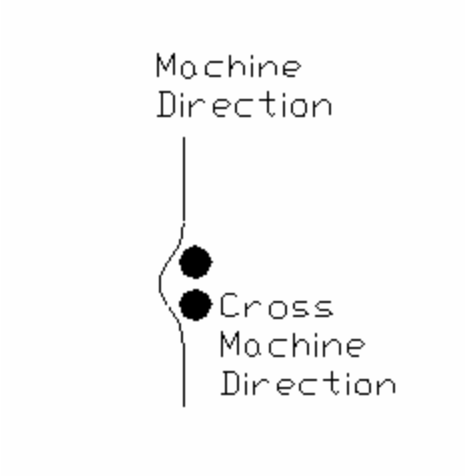

Figure 5.4 Side view of fabric to show the curvature in the machine direction strands

The figure 5.5 compares the stress vs. strain plot of specimens aged for 14 days in machine and cross machine direction. Figure 5.6 provides stress vs. strain plot of specimens aged for 28 days. Table 5.4 gives the tensile properties of specimens aged for 14 days and 28 days.

Table 5.4

Comparison of tensile properties of specimens aged for 14 and 28 days

Specimen Group	Fabric direction	Ave. First Crack stress, MPa	Ave. First Crack strain, %	Ave. Maximum Stress, MPa	Ave load, N/mm
Type EM-AGE14	Machine	2.13	0.12	3.76	17.99
TypeEXM-AGE14	Cross machine	2.99	0.17	4.02	20.16
Type EM-AGE28	Machine	2.57	0.095	3.87	18.95
TypeEXM-AGE28	Cross machine	2.85	0.11	3.85	19.15

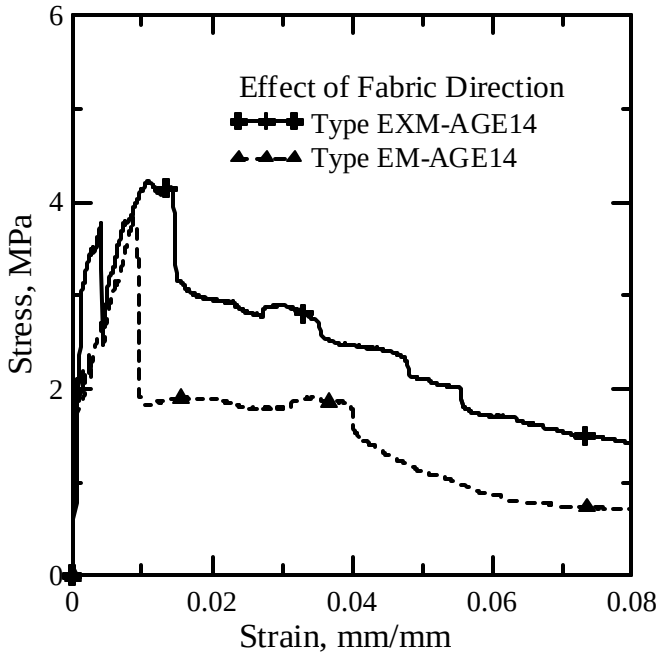

Figure 5.5 Comparison of stress vs. strain of specimens aged for 14 days in machine and cross machine direction

The specimens aged for 14 days in machine direction have an average maximum tensile stress of 3.76MPa at an average ultimate strain of 0.88%, whereas, cross machine

direction specimens have average maximum tensile stress of 4.02MPa at an average ultimate strain of 1.11%. Cross machine direction specimens have 6.5% higher stress than machine direction specimens. But the same specimens when un-aged were 7.55% weaker than machine direction specimens. This may be attributed to the machine direction being able to take lesser stress after ageing as per the above discussion. Similar trend is observed in specimens aged for 28 days. Machine direction specimens aged for 28 days have an average maximum stress of 3.87 MPa at an average ultimate strain of 0.83%. Cross machine direction specimens aged for 28 days have an average maximum stress of 3.85 MPa at an average ultimate strain of 0.71%.

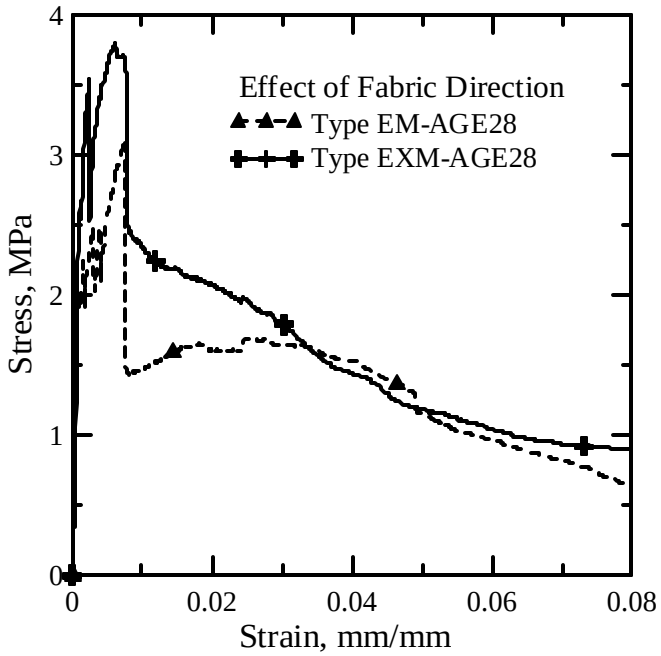

Figure 5.6 Comparison of stress vs. strain of specimens aged for 28 days in machine and cross machine direction

Figure 5.7 and 5.8 show the comparison plots between un-aged and aged specimens. The stress-strain plot has a significant difference in maximum stress values in

machine direction. The difference in cross machine direction is not that significant. Table 5.5 and 5.6 compare the average tensile properties of these specimens.

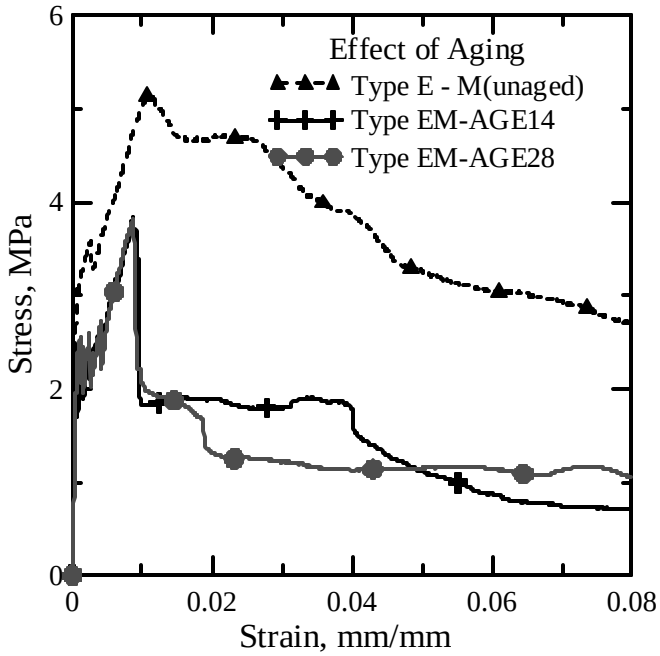

Figure 5.7 Comparison of stress vs. strain of specimens un-aged and aged for 14 days and 28 days in machine direction

The average maximum tensile stress for un-aged specimens in machine direction is 5.03MPa at an average ultimate strain of 1.07% and for aged specimens is 3.76MPa at an average ultimate strain of 0.88%. The 14 days aged specimens take 25.24% lesser tensile stress than the un-aged specimens. The 28 days aged specimens take 23.06% lesser tensile stress than un-aged specimens. The first crack stress for un-aged specimens is 3.41MPa at a strain of 0.16%. The first crack stress for 14 days aged specimens is 2.13MPa at a strain of 0.12%. The first crack stress is 37.53% lesser for these specimens. The first crack stress for 28 days aged specimens is 2.57 MPa at a strain of 0.095%. The first crack stress is 24.6% lesser for these specimens.

Table 5.5

Comparison of tensile properties of un-aged and aged specimens in machine direction

Specimen Group	Ageing status	Ave. Young's Modulus, MPa	Ave. First Crack stress, MPa	Ave. Maximum Stress, MPa	Ave load, N/mm
Type E-M	Un-aged	5515.42	3.41	5.03	26.45
TypeEM-AGE14	Aged-14 days	4482.19	2.13	3.76	17.99
TypeEM-AGE28	Aged-28 days	4783.62	2.57	3.87	18.95

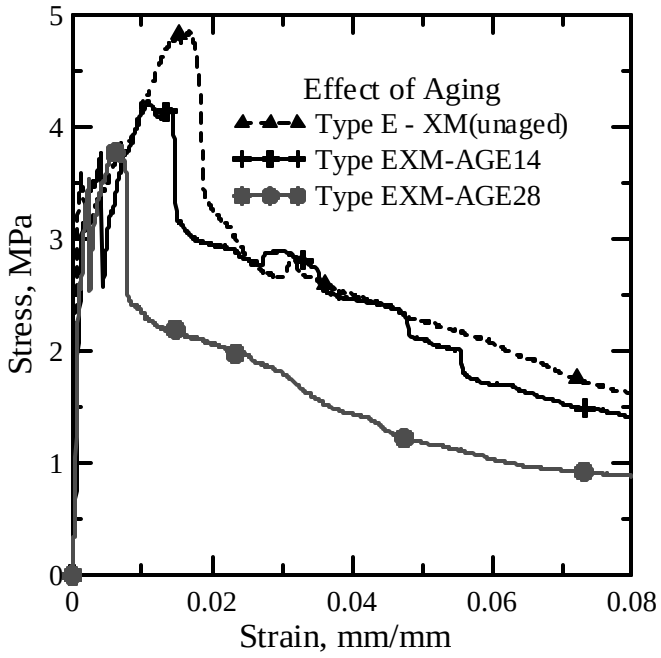

Figure 5.8 Comparison of stress vs. strain of specimens un-aged and aged for 14 days and 28 days in cross machine direction

The average maximum tensile stress for un-aged specimens in cross machine direction is 4.65MPa at an average ultimate strain of 1.62% and for 14 days aged specimens is 4.02MPa at an average ultimate strain of 1.11%. The aged specimens take

13.55% lesser tensile stress than the un-aged specimens. The 28 days aged specimens have an average maximum tensile stress of 3.85 MPa at an average ultimate strain of 0.71%. The 28 days aged specimens take 17.2% lesser tensile stress than un-aged specimens. The first crack stress for un-aged specimens is 3.35 MPa at a strain of 0.12%. The first crack stress for 14 days aged specimens is 2.99 MPa at a strain of 0.17%. The first crack stress for 28 days aged specimens is 2.85 MPa at a strain of 0.11%. The first crack stress is 10.75% lesser for 14 days aged specimens. The first crack stress is 14.9% lesser for 28 days aged specimens.

Table 5.6

Comparison of tensile properties of un-aged and aged specimens in XM direction

Specimen Group	Ageing status	Ave. Young's Modulus, MPa	Ave. First Crack stress, MPa	Ave. Maximum Stress, MPa	Ave load, N/mm
Type E-XM	Un-aged	4615.47	3.35	4.65	23.67
TypeEXM-AGE14	Aged-14 days	3225.62	2.99	4.02	20.16
TypeEXM-AGE28	Aged-28 days	3760.37	2.85	3.85	19.15

Figure 5.9 through 5.12 compares the respective tensile property of the aged and un-aged specimens in both machine and cross machine direction. The bar chart shows average properties of a specimen type and the standard deviation plot is for all the specimens in a given group.

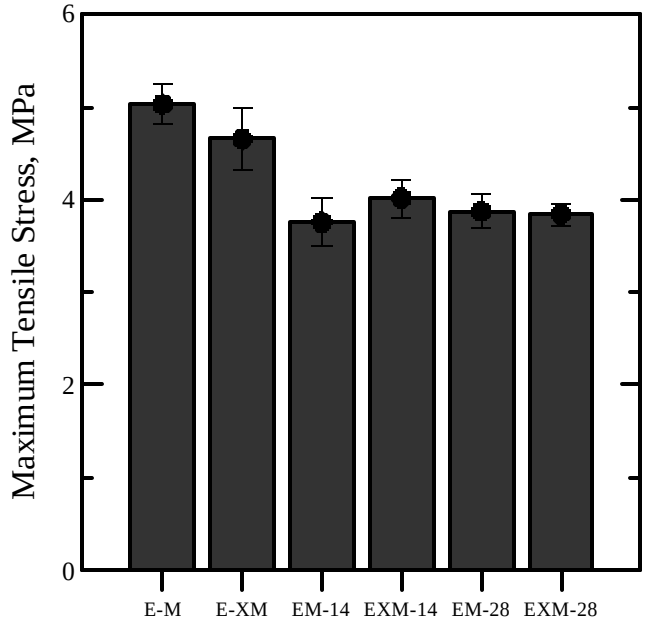

Figure 5.9 Comparison of maximum stress for un-aged and aged specimens

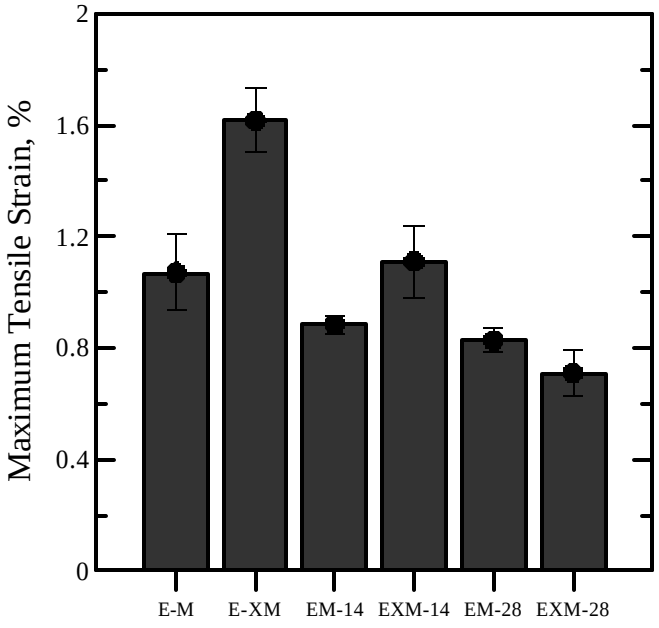

Figure 5.10 Comparison of maximum strain for un-aged and aged specimens

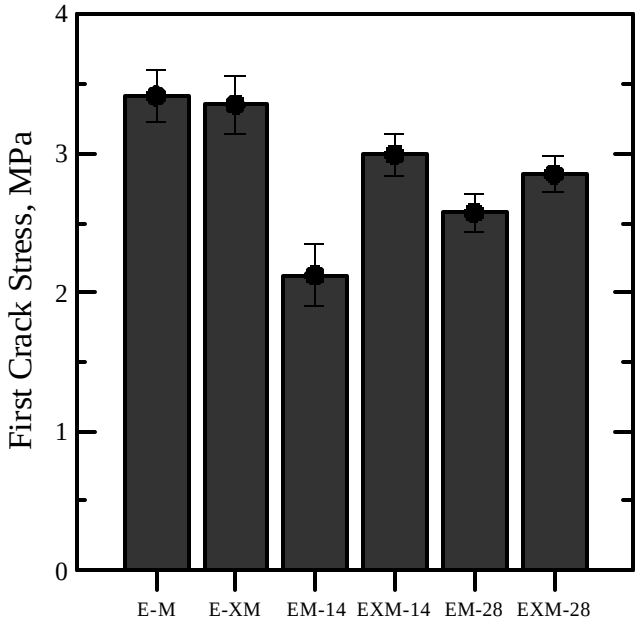

Figure 5.11 Comparison of first crack stress for un-aged and aged specimens

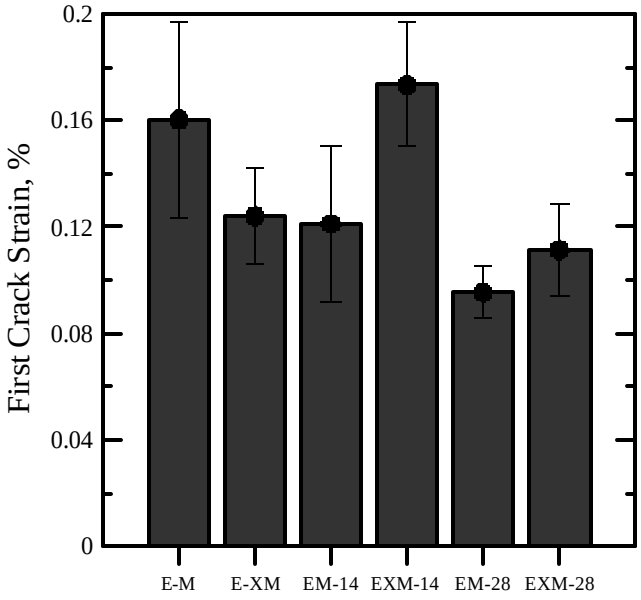

Figure 5.12 Comparison of first crack strain for un-aged and aged specimens

5.4 Study of ageing effect on flexural properties

The specimens were tested un-aged as well as after ageing for 14 days and 28 days and were tested in flexure. The test set up used for testing in flexure is same as explained in chapter 3. Figure 5.13 shows a load vs. displacement plot of un-aged specimens in machine and cross machine direction. Figure 5.14 shows similar plot but the displacement is measured by LVDT.

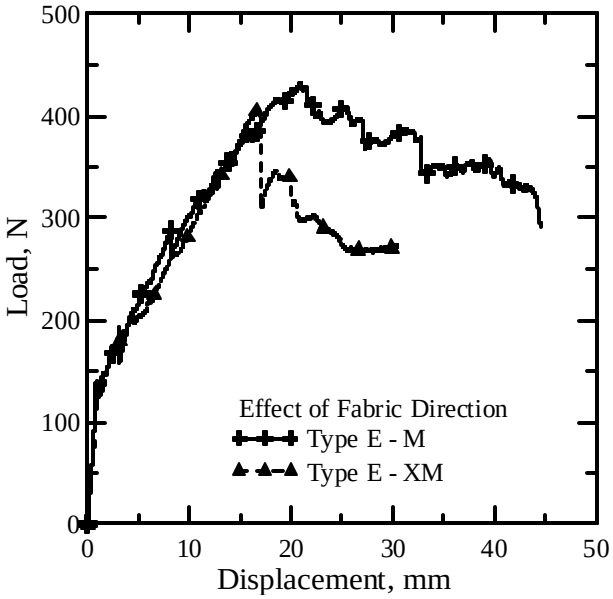

Figure 5.13 Load vs. displacement plot for un-aged specimens

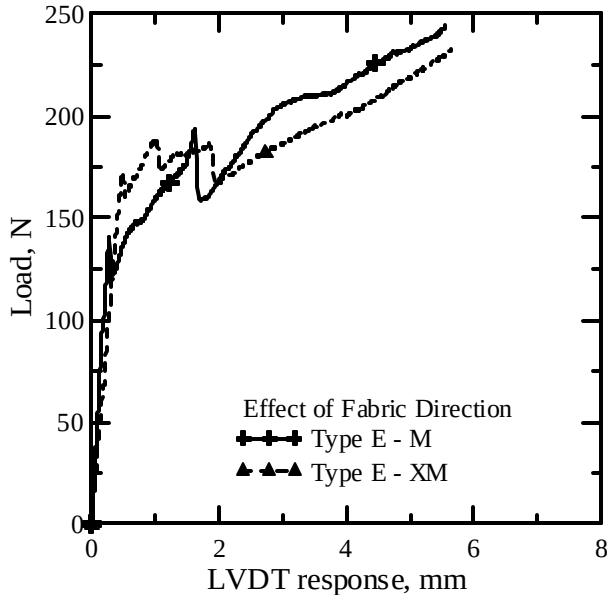

Figure 5.14 Load vs. LVDT response plot for un-aged specimens

Average maximum load is 422.6N for machine direction specimens at a deflection of 18.53mm whereas; it is 395.2N at 16.67mm for cross machine direction specimens. The first crack load is 139.02N at a deflection of 0.28mm for machine direction specimens whereas; it is 150.24N at a deflection of 0.4mm. The specimens in machine direction are stronger than specimens in cross machine direction. This may be attributed to the fact that fabric is stronger in machine direction. Table below compares the average flexural properties of these specimens.

Table 5.7

Comparison of flexural properties of un-aged specimens

Specimen Group	Fabric direction	Ave. Young's Modulus, MPa	Ave. First Crack load, N	Ave. Maximum load, N	Ave load, N/mm
Type E-M	Machine	24378.2	139.02	422.60	29.31
Type E-XM	Cross machine	20314.09	150.24	395.20	27.59

Figure 5.15 and 5.16 show a load vs. displacement and LVDT displacement plots of specimens aged for 14 days in both machine as well as cross machine direction. Figure 5.17 and 5.18 show similar plots of specimens aged for 28 days.

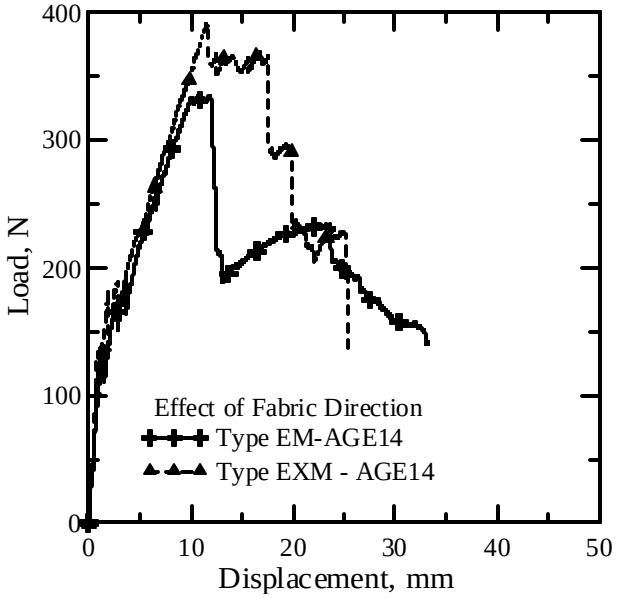

Figure 5.15 Load vs. displacement response for specimens aged for 14 days

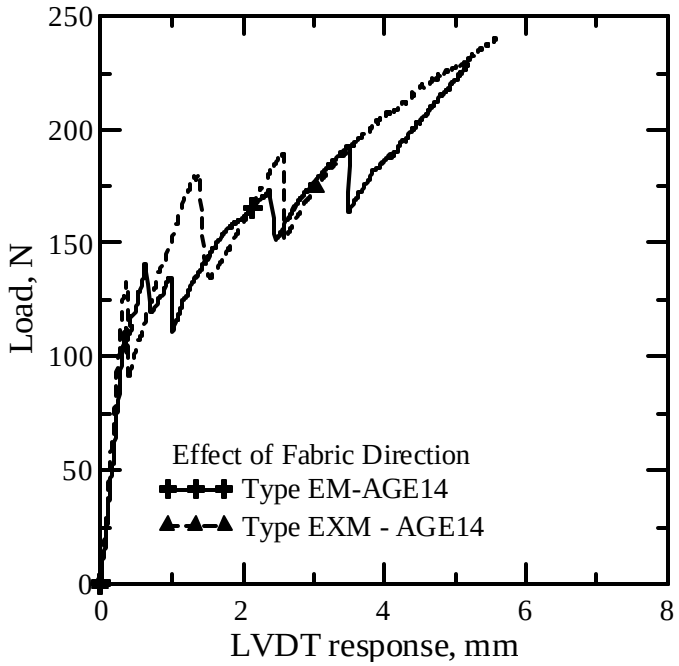

Figure 5.16 Load vs. LVDT response for specimens aged for 14 days

Average maximum load is 330.47N for machine direction specimens at a deflection of 10.74mm whereas; it is 377.56N at 14.74mm for cross machine direction specimens. The first crack load is 114N at a deflection of 0.31mm for machine direction specimens whereas; it is 145.20N at a deflection of 0.34mm. The specimens in machine direction are weaker than specimens in cross machine direction. The machine direction took 6.48% more maximum load than cross machine direction for un-aged specimens whereas; for similar specimens after ageing machine direction takes 12.47% lesser maximum load after ageing for 14 days. Specimens aged for 28 days in machine direction have average maximum load of 304.02N at a deflection of 12.19mm. The cross machine direction specimens have average maximum load of 377.35N at a deflection of 16.46mm. The first crack load is 101.09N at a deflection of 2.41mm for machine direction specimens whereas; it is 118.86N at a deflection of 2.27mm. The machine direction specimens take 19.43% lesser load than cross machine direction specimens. This can be explained using same reasoning as explained in section 5.3 that after ageing machine direction becomes weaker than cross machine direction.

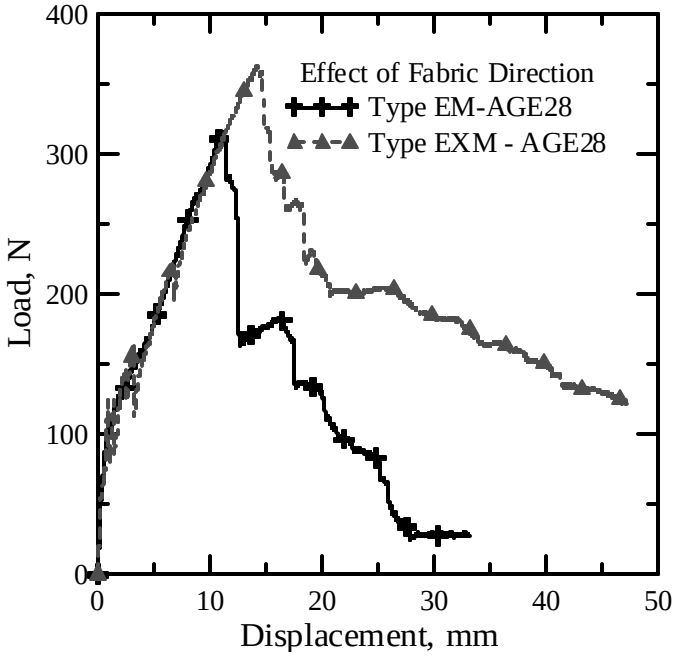

Figure 5.17 Load vs. displacement response for specimens aged for 28 days

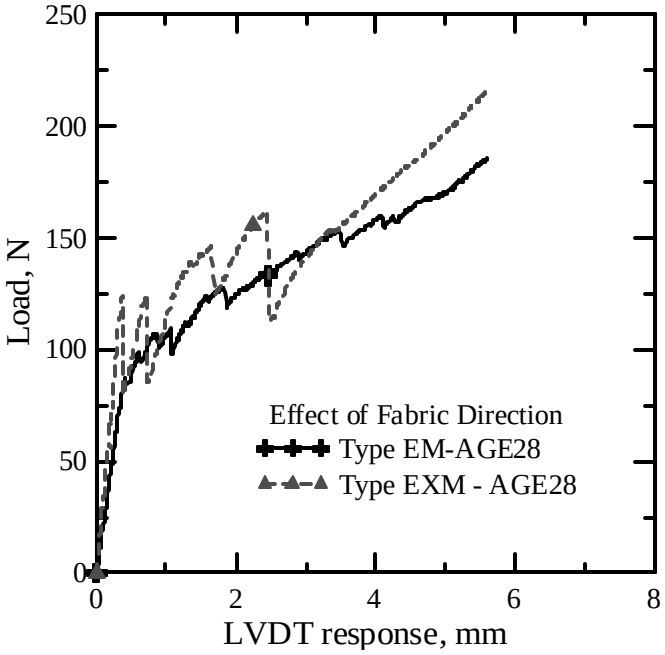

Figure 5.18 Load vs. LVDT response for specimens aged for 14 days

Table 5.8 has been provided below for a better understanding of how the flexural properties compare with each other for 14 days and 28 days aged specimens.

Table 5.8

Comparison of flexural properties of specimens aged for14 days and 28 days

Specimen Group	Fabric direction	Ave. Young's Modulus, MPa	Ave. First Crack load, N	Ave. Maximum load, N	Ave load, N/mm
Type EM-AGE14	Machine	22538.59	114	330.47	23.01
Type EXM-AGE14	Cross machine	23677.8	145.2	377.56	26.23
Type EM-AGE28	Machine	10887.2	101.09	304.02	20.78
Type EXM-AGE28	Cross machine	9463.02	118.86	377.35	25.48

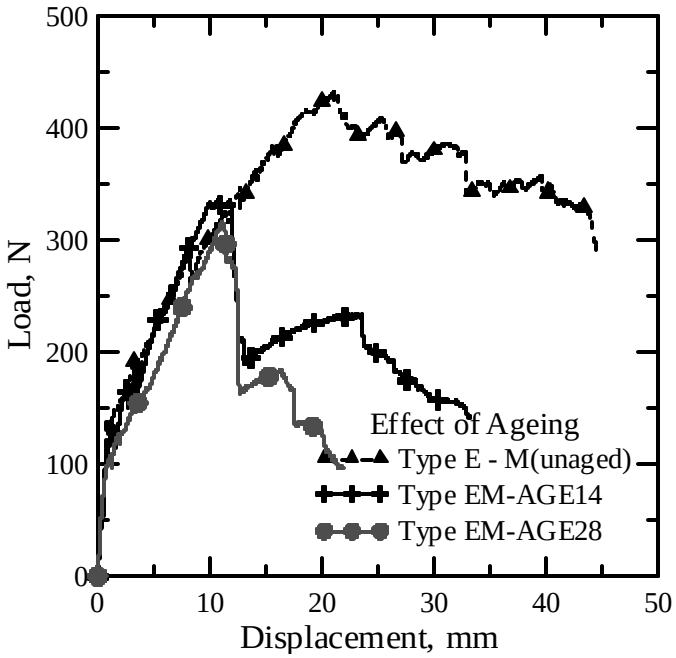

Figure 5.19 Load vs. displacement plot for un-aged and aged specimens with fabric in machine direction

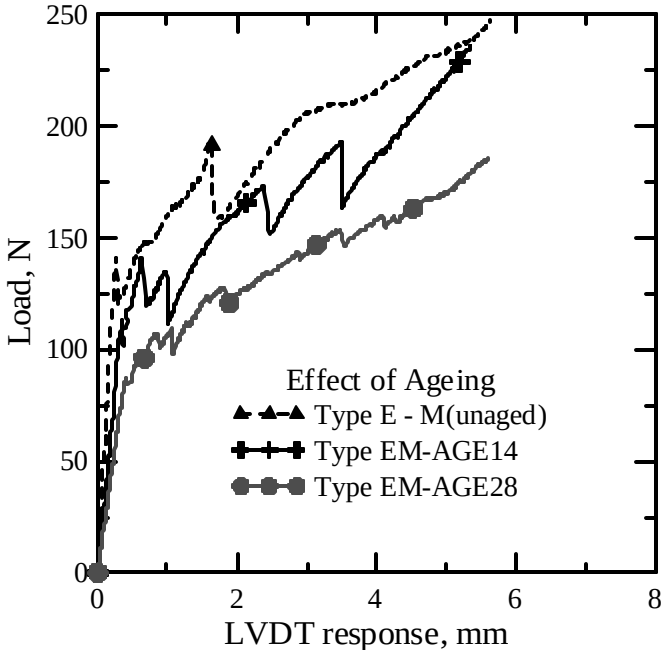

Figure 5.20 Load vs. LVDT response for un-aged and aged specimens with fabric in machine direction

Figure 5.19 shows a load vs. displacement plot for machine direction specimens un-aged and aged for 14 days. Figure 5.20 shows load vs. LVDT response of similar specimens. Aged machine direction specimens are much weaker than un-aged specimens. The average maximum load of un-aged specimens is 422.6N at a displacement of 18.93mm and average maximum load for similar 14 days aged specimens is 330.47N at a displacement of 10.74mm and for 28 days aged specimens is 304.02N at a displacement of 12.19mm. This shows that specimens aged for 14 days can take 21.8% lesser maximum load than un-aged specimens and specimens aged for 28 days can take 28.06% lesser maximum load than un-aged specimens. Table 5.9 compares the flexural properties of these specimens.

Table 5.9

Comparison of flexural properties of specimens with fabric in machine direction

Specimen Group	Ageing status	Ave. Young's Modulus, MPa	Ave. First Crack load, N	Ave. Maximum load, N	Ave load, N/mm
Type EM	Un-aged	24378.2	139.02	422.6	29.31
Type EM-AGE14	aged	22538.59	114	330.47	23.01
Type EM-AGE28	aged	10887.2	101.09	304.02	20.78

Figure 5.21 shows a load vs. displacement plot for cross machine direction specimens un-aged and aged for 14 days. Figure 5.22 shows load vs. LVDT response of similar specimens. Figure 5.23 and 5.24 show similar plots of specimens aged for 28 days. Aged cross machine direction specimens are weaker than un-aged specimens but the difference is not as significant as in machine direction. The average maximum load of un-aged specimens is 395.2N at a displacement of 16.67mm and average maximum load for similar 14 days aged specimens is 377.56N at a displacement of 14.74mm and 28 days aged specimens is 377.35N at a displacement of 16.46mm. This shows that specimens aged for 14 days can take 4.46% lesser maximum load than un-aged specimens. Table 5.10 compares the flexural properties of these specimens.

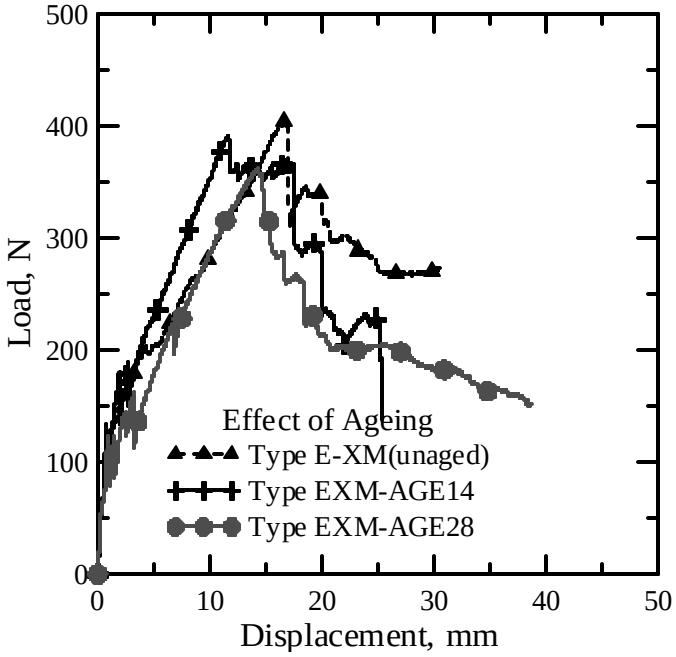

Figure 5.21 Load vs. displacement plot for un-aged and aged specimens with fabric in cross machine direction

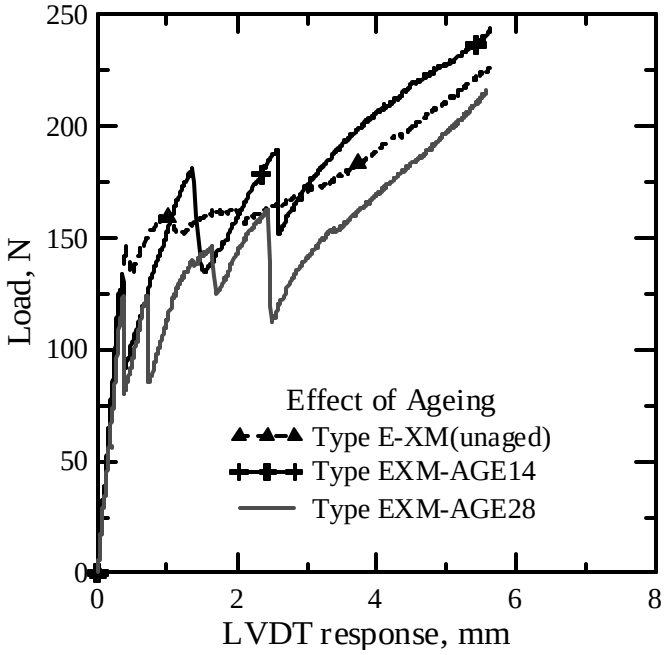

Figure 5.22 Load vs. LVDT response for un-aged and aged specimens with fabric in cross machine direction

Table 5.10

Comparison of flexural properties of specimens with fabric in cross machine direction

Specimen Group	Ageing status	Ave. Young's Modulus, MPa	Ave. First Crack load, N	Ave. Maximum load, N	Ave load, N/mm
Type EXM	Un-aged	20314.09	150.24	395.2	27.59
Type EXM-AGE14	aged	23677.8	145.2	377.56	26.23
Type EXM-AGE28	aged	9463.02	118.86	377.35	16.46

Figure 5.23 through 25 provide comparison plots for respective flexural property for all un-aged and aged specimens in both machine and cross machine direction of fabric. Bar chart shows average value for a given specimen type and standard deviation plot shows value for all the specimens.

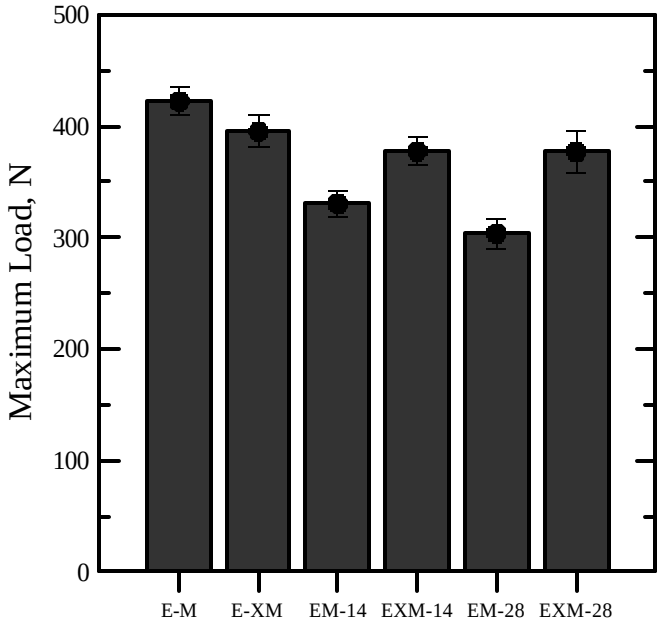

Figure 5.23 Comparison of maximum load for all un-aged and aged specimens

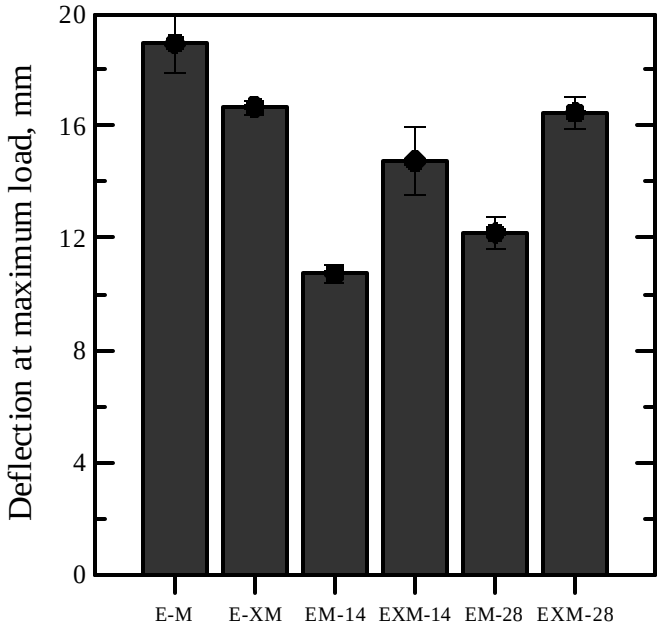

Figure 5.24 Comparison of deflection at maximum load for all un-aged and aged specimens

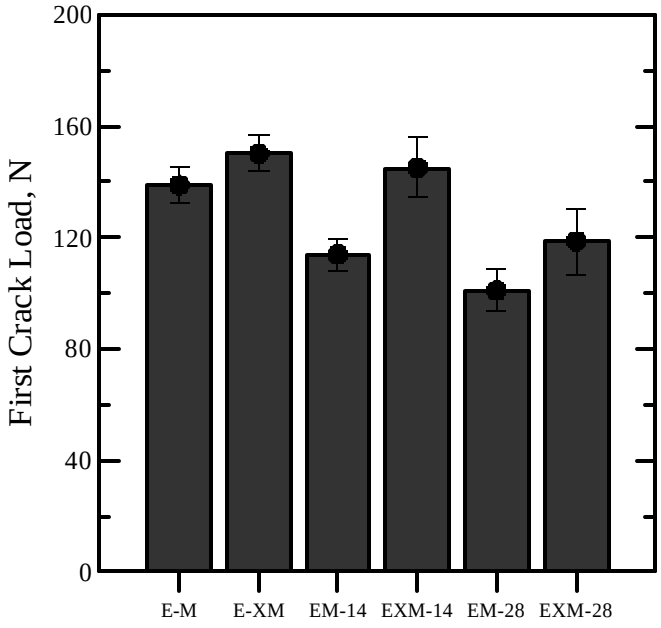

Figure 5.25 Comparison of first crack load for all un-aged and aged specimens

It has been observed from the experimental data that the tensile strength is low as compared to the equivalent flexural strength for similar type of specimens. This can be attributed to the fact that an extensometer was not used while doing the tensile tests. Therefore, the tensile stress values are a little lower than actual values as slippage in the grips was not recorded. To explain this difference average load per unit length was calculated for both tensile and flexure specimens. Average load per unit length in flexure is calculated as Moment/ (Width x Lever arm). It has been assumed for calculations that distance between line of action of tensile and compressive force is 8mm (assuming 1mm cover on each side). Average load per unit length in tension is calculated using Load/Width. The average load is a much better idea of specimen strength and this value has been provided for all the specimens.

CHAPTER 6

THEORETICAL MODELING OF TENSILE AND FLEXURE RESPONSE

6.1 Introduction

A theoretical model was developed to simulate the experimental tensile response. The model can be applied to plain as well as fabric reinforced specimens. The model uses various parameters like ultimate tensile strength (ft), fracture energy (Gf), localization zone for crack development (lgage) and strain values. Using these parameters, the model predicts a stress – strain response which is very similar to the experimental response. Three different strain values are used by the model which is explained by figure1. Strain is applied incrementally and the stress value is calculated for the corresponding strain. The figure below shows the significance of strain values, fracture energy and young's modulus used in the model.

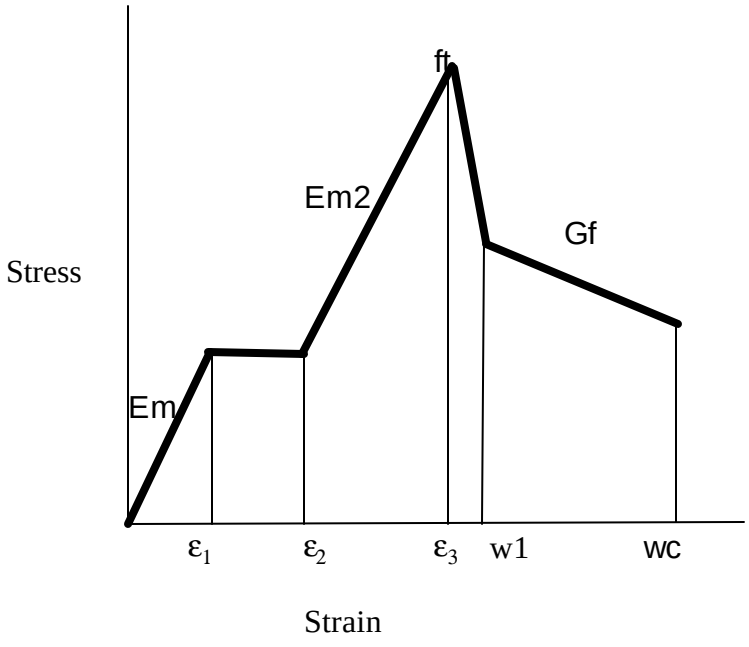

Figure 6.1 Explanation of various parameters used by the model

In figure 6.1, ε_1 is the strain at which matrix cracking starts, ε_2 is the end of matrix cracking zone and $\varepsilon_3$is the ultimate strain. G_f is fracture energy and affects the post cracking response. E_m is young's modulus for uncracked matrix and E_{m2} is cracked young's modulus. ft represents ultimate tensile strength. w1 and wc are functions of fracture energy calculated from the equations below

$w1 = 0.75*G_f/ft$, $wc = 5.*G_f/ft$

Figure 6.2a and 6.2b clearly show the variation of w1 and wc with fracture energy.

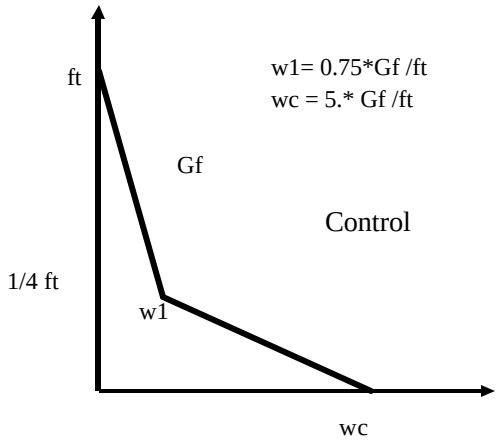

Figure 6.2a Variation of w1 and wc with fracture energy for Matrix

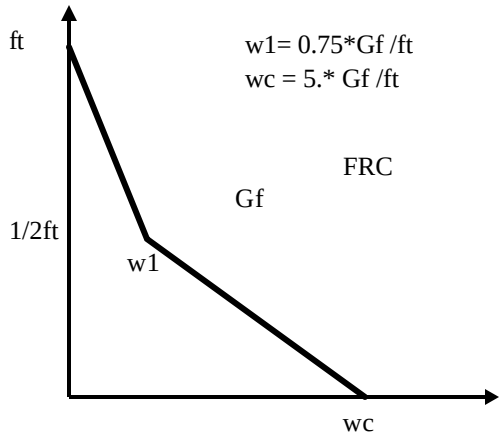

Figure 6.2b Variation of w1 and wc with fracture energy for fabric reinforced specimen

Another theoretical model was developed to simulate flexure response. The incremental curvature is applied for the calculation of stress. Strain is calculated due to applied curvature and stress is calculated from the strain. The model uses the same procedure for stress-strain calculations as the tensile model. It uses all the above parameters fracture energy, ultimate tensile strength, localization zone for crack development and strain values as an input. It calculates the moment from the calculated stress. Then it evaluates the load-deflection response from the moment curvature response. The model predicts the load-deflection response till 6mm deflection. After this much deflection the load is carried mainly by the fabric.

6.2 Explanation of Tensile model

There are 6 parameters used to define the tensile response. Strain is applied incrementally as a linear function of i^{th} iteration. It uses 3 strain values as shown above to calculate the stress- strain response till the maximum stress. For calculating the post peak response another variable w(i) is introduced whose value is calculated at i^{th} iteration and is compared with w1 and wc.

$w(i) = \varepsilon_3(lgage)+(\varepsilon- \varepsilon_3) lgage$

where, lgage represents localization zone.

The localization zone of crack development represents the spacing between the cracks. It represents the length in which the cracks have localized. The crack spacing was approximately 76.2mm for the tensile specimens. This value has been used to model the experimental response.

For a given value of strain the stress is calculated using the equations given below. ε represents strain at ith iteration in the following equations.

$s = \mathrm{E}_m e_1 \qquad e < e_1 \quad , \mathrm{E}_m = Uncracked Young's\ Modulus$

$s = \mathrm{E}_m e_1 \qquad e_1 < e < e_2$

$s = \mathrm{E}_m e_1 + \mathrm{E}_{m2}(e - e_2) \qquad e_2 < e < e_3 \quad , \mathrm{E}_{m2} = Uncracked Young's\ Modulus$

$\mathrm{E}_{m2} = (ft - \mathrm{E}_m e_1)/(e_3 - e_2)$

$s = ft + w(i)(-ft + ft/2)/w1 \quad e > e_3 \ and \ w(i) < w1$

$w(i) = e_3(\lg age) + (e - e_3)\lg age \quad , \lg age = localization\ zone$

$s = ft + (w(i) - w1)(ft/2)/(w1 - wc) \quad w1 < w(i) < wc$

$s = 1\mathrm{e}\text{-}6 \quad w(i) > \mathrm{wc}$

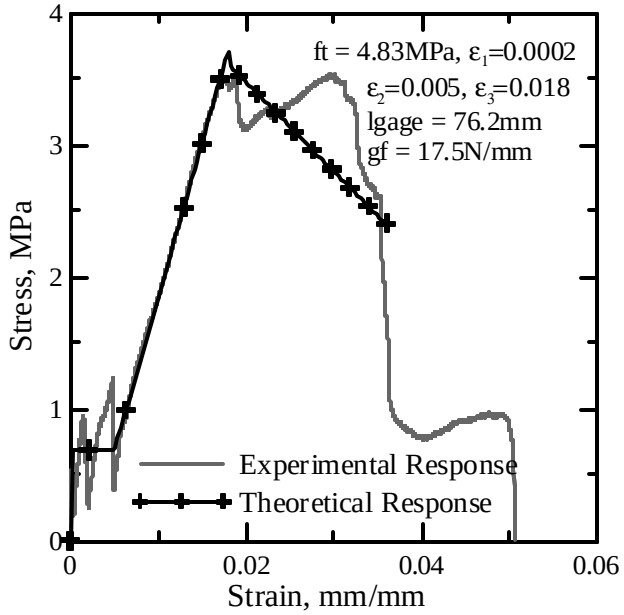

Figure 6.3 Comparison of Experimental and Theoretical Tensile response

Stress is calculated using the above equations and a stress-strain plot is obtained. Figure 6.3 shows a stress-strain plot obtained from the program compared with an experimental response. A parametric study was carried out to check the validity of the model.

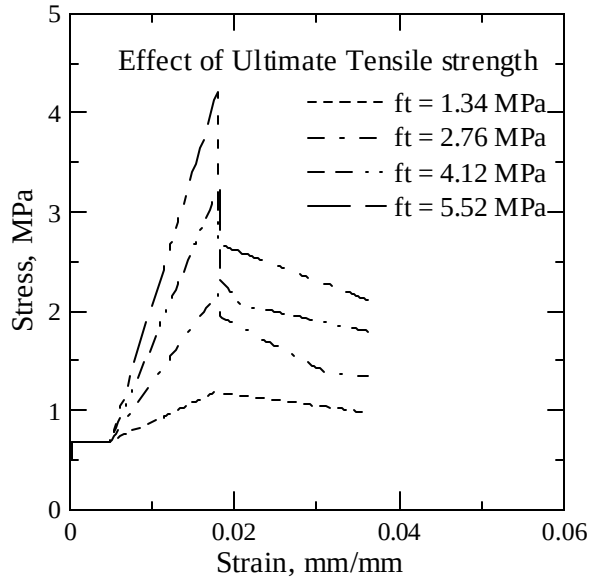

Figure 6.4 Parametric study to see the model response with varying ft

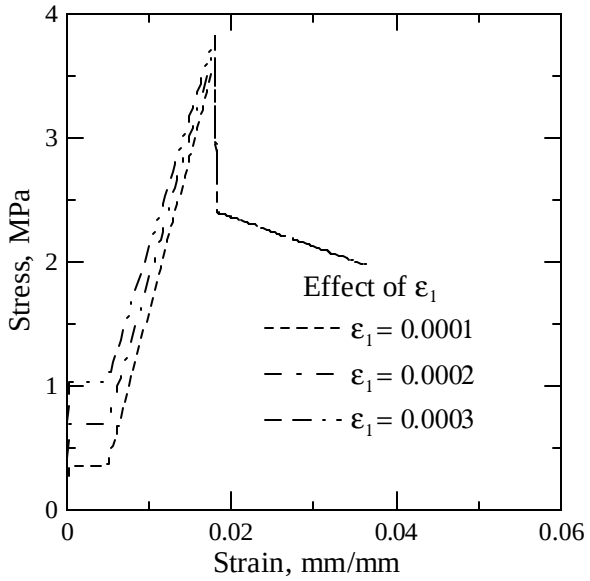

Figure 6.5 Parametric study to see the model response with varying ε_1

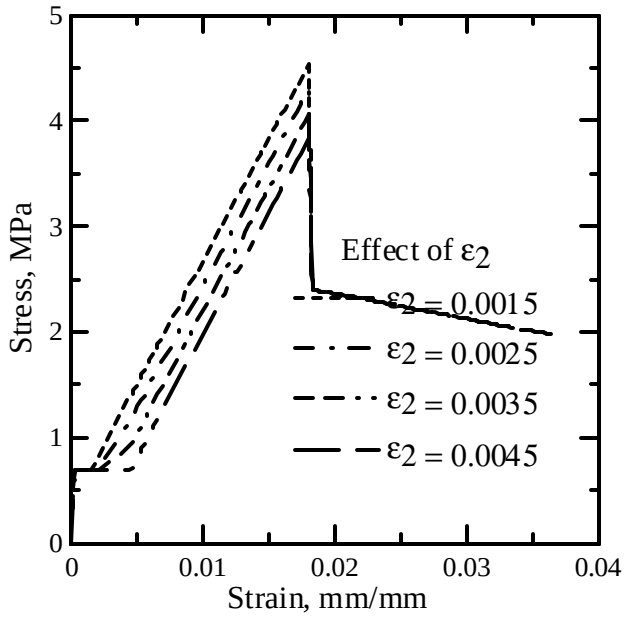

Figure 6.6 Parametric study to see the model response with varying ε_2

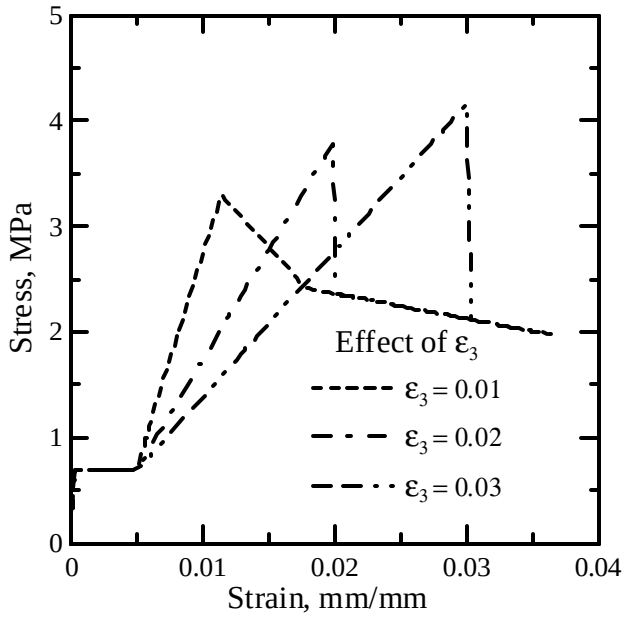

Figure 6.7 Parametric study to see the model response with varying ε_3

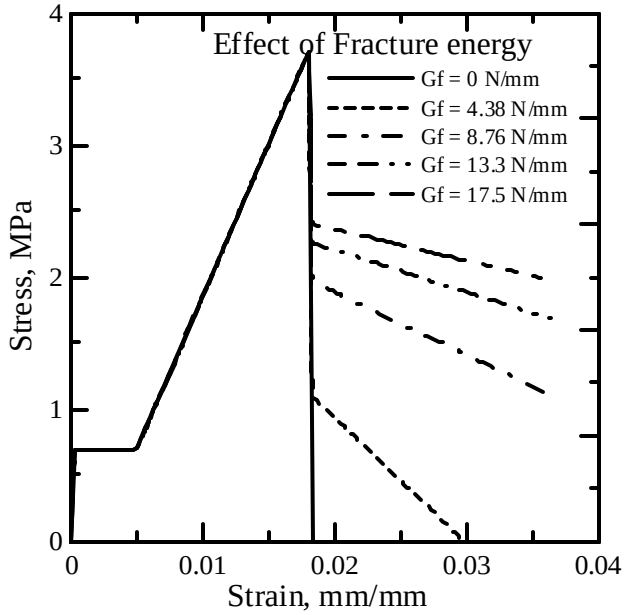

Figure 6.8 Parametric study to see the model response with varying Gf

6.3 Explanation of Flexure model

The model uses the above described parameters as an input and calculates the load-deflection response for a similar specimen. Additional information related to young's modulus of fabric and volume fraction of fabric was also provided as an input. The E value for Glass fabric is 72 GPa. This information was provided by Saint Gobain Technical fabrics. Additional information related to fabric is provided in chapter 2. The volume fraction for fabric was calculated to equal to 0.0288. The following steps briefly describe the steps followed for modeling the flexure response.

1. Input all the parameters
2. Impose curvature incrementally
3. Compute strain
4. Compute stress from calculated strain

5. Compute moment from calculated stress
6. Compute load deflection from moment curvature.

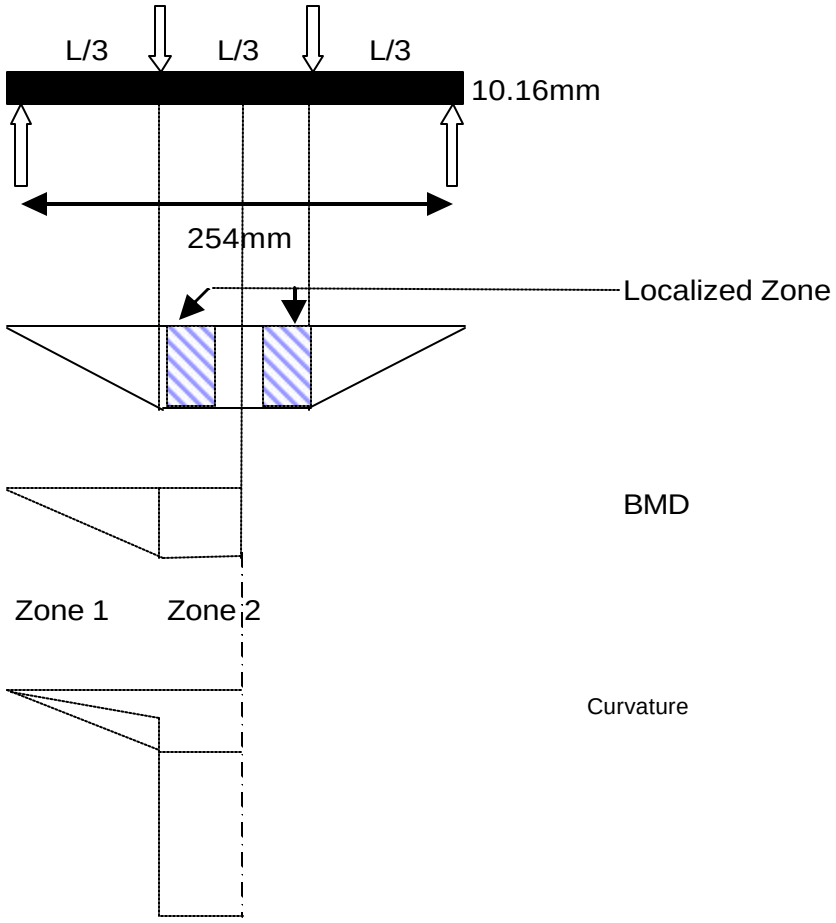

Figure 6.9 Geometry of the case studied

Figure 6.9 shows geometry of the case studied. The localized zone for the points under load has been shown. Initially the curvature coincides with the bending moment. After localization comes into picture, some points are under loading and some are under unloading. This is shown by the dotted lines in the curvature diagram above. The program has been modeled using 16 fabric layers. The thickness of fabric is very small as

compared to the overall specimen thickness. Therefore, 2 layers have properties of fabric or of composite and the rest of 14 layers have matrix properties. The calculation of E_m, w(i), w1 and wc is done using same formulas as given above but now they are calculated for matrix properties as well as composite properties. The matrix properties are such that ft value is equal to tensile strength of matrix, G_f is very small as matrix is very brittle and does not have significant post crack response, and strain values are very small and very near to each other because matrix alone does not undergo any elongation. A layered approach was used for modeling the flexural response.

Table 6.1

Matrix properties used in flexure model as an input

ft	G_f	ε_1	ε_2	ε_3	lgage
2.0685 MPa	0	0.00018	0.00019	0.00021	38.1

Incremental curvature is applied as a linear function of i^{th} iteration. For very iteration strain is calculated due to incremental curvature for top layer and bottom layer. The top layers are in compression and the bottom layers are in tension. From the calculated strain, stress is calculated using the same equations as explained in section 6.2 but is calculated separately for top and bottom layers. Moment is calculated from the stress distribution using trapezoidal numerical integration method. Load is calculated from the moment using P = 2*Moment / Shear span where the shear span is equal to Effective length/ 3 for a 4-point bending test. The failure check used is shear failure. The ultimate shear strength used is Tensile strength of matrix / 2. This is obtained from Von

Mises theory. Shear strength is calculated as $\tau = 3/2 * P / (Width*Thickness)$. When this value is equal to ultimate shear strength that means the specimen has failed in shear. The curvature is integrated to get the deflection values. For every iteration, the program loops through all the layers, updates the neutral axis and calculates stress-strain, moment-curvature and load-deflection values. Figure 6.10 shows layer details used to model the response and figure 6.11 shows the output from the program.

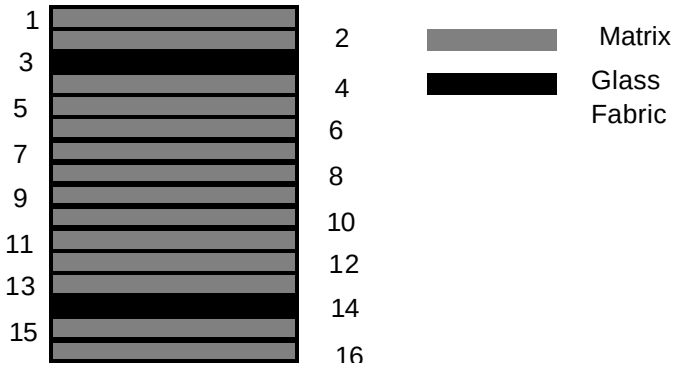

Figure 6.10 Details of layer properties used by the model

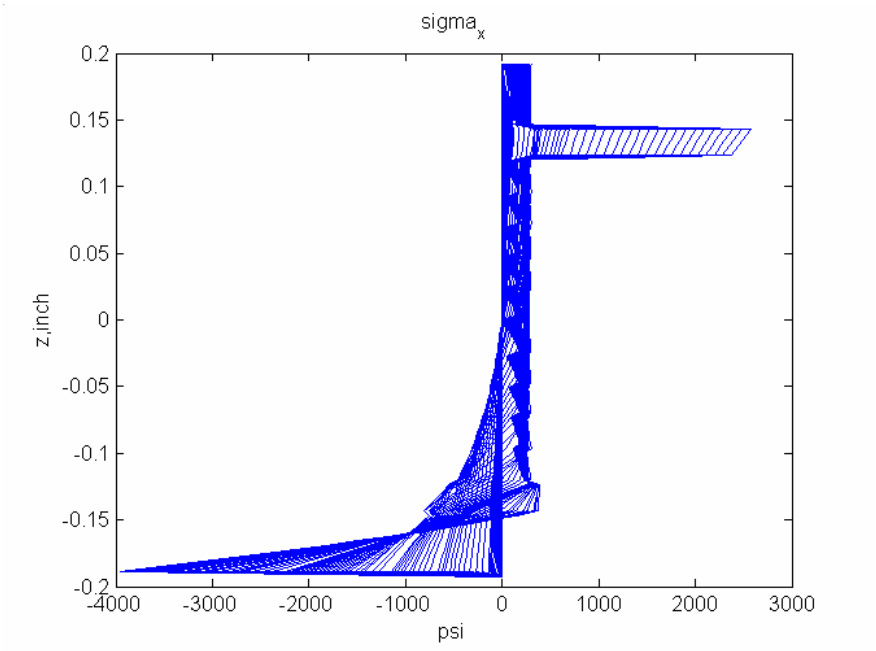

Figure 6.11 Output from the model showing stress distribution in x direction

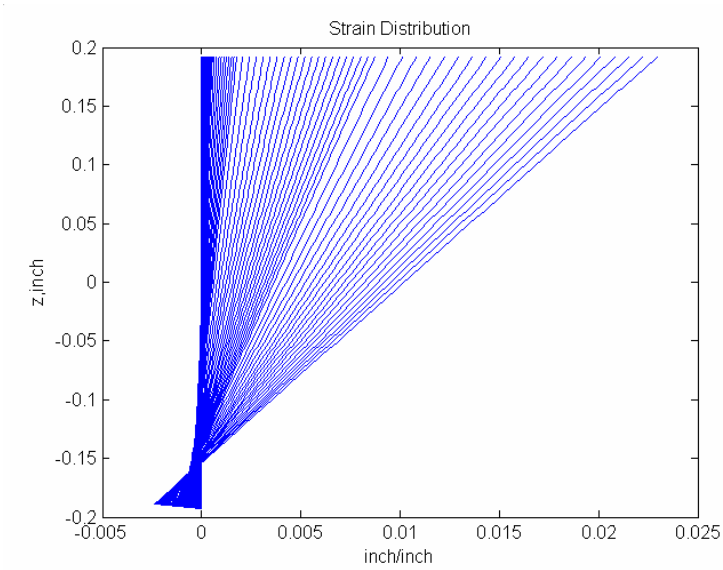

Figure 6.12 Output from the model showing stress distribution in x direction

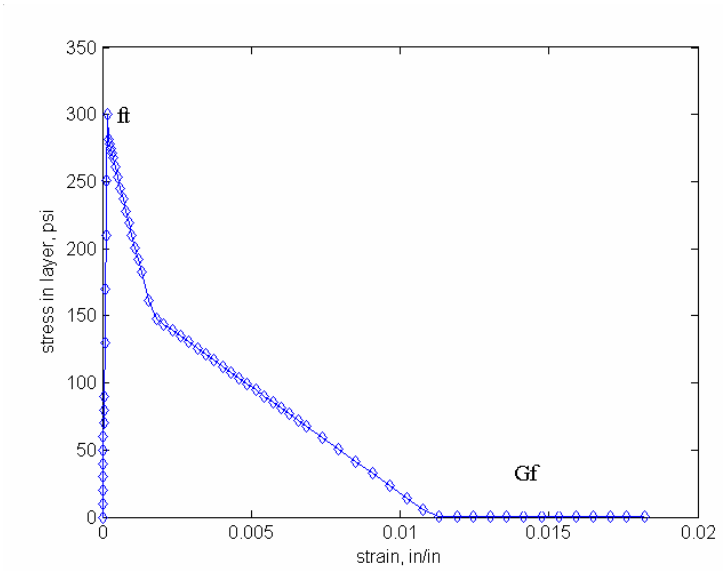

Figure 6.13 Output from the model showing stress distribution in layer 13 (matrix only)

The value of strains, fracture energy and tensile strength used for matrix are provided in table 6.1.

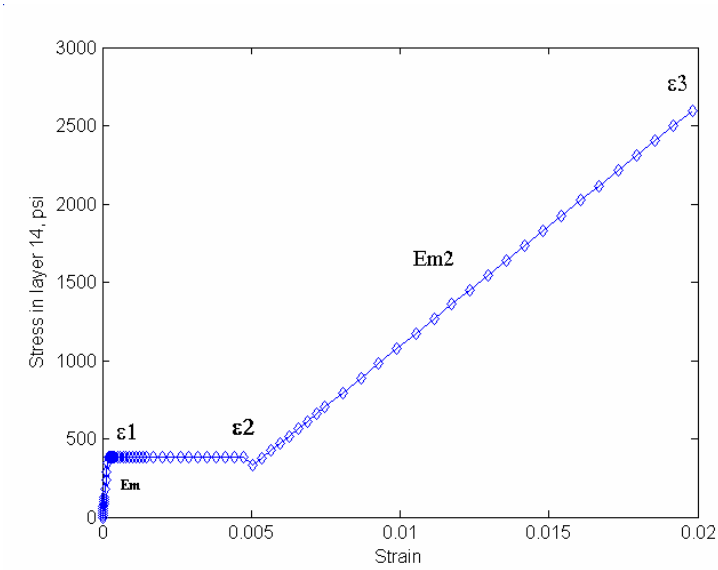

Figure 6.14 Stress distribution in a layer with glass fabric properties

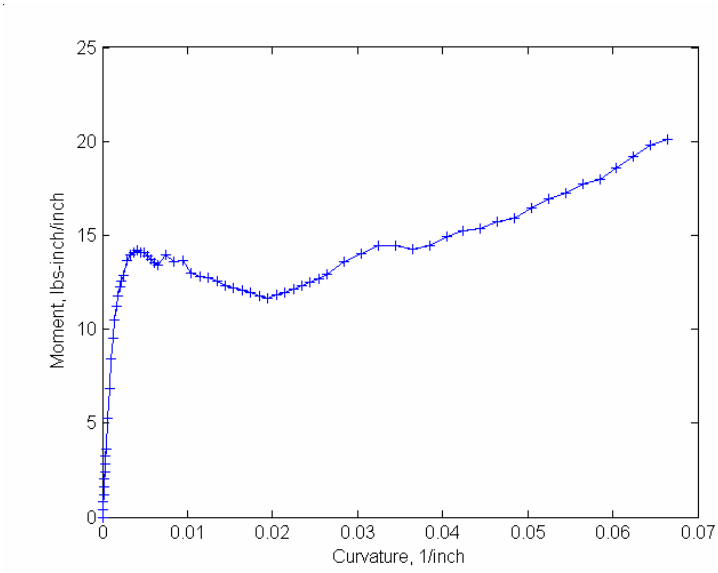

Figure 6.15 Moment curvature distribution

Figure 6.16 through 6.18 provide a comparison between an experimental flexural response and a simulated flexural response. The zone of maximum cracking is effective length / 3 for 4-point bending test specimens. The average crack spacing is around 38.1mm for the type of specimen shown in figure 6.16.

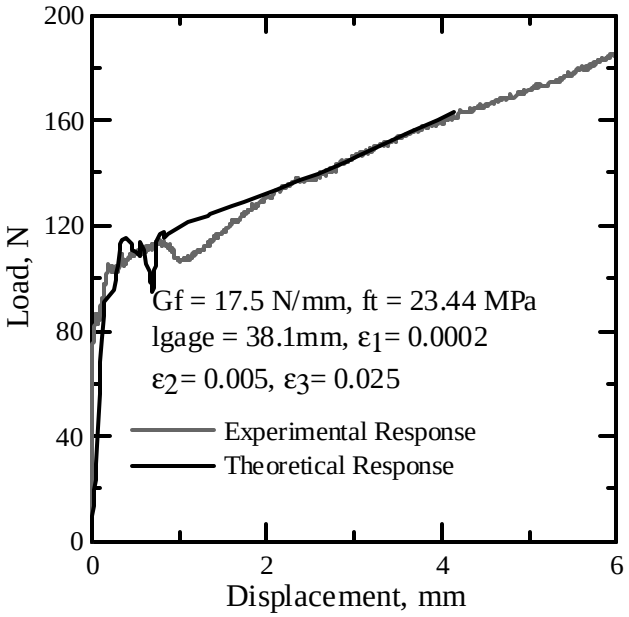

Figure 6.16 Comparison between experimental and theoretical flexural response

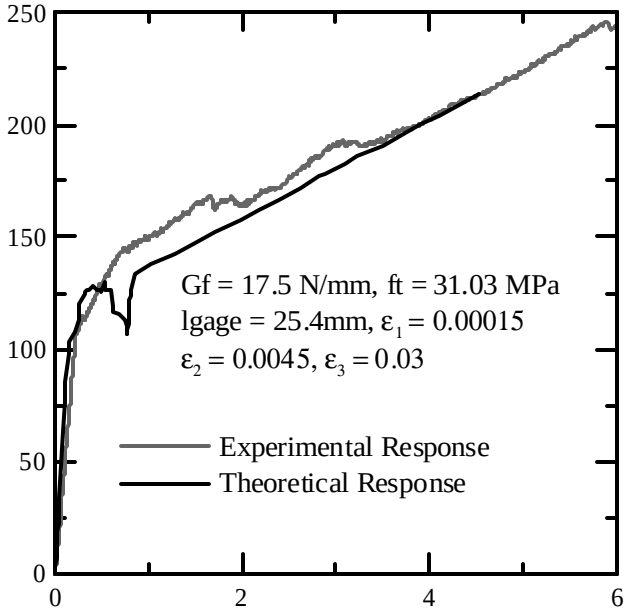

Figure 6.17 Comparison between experimental and theoretical flexural response

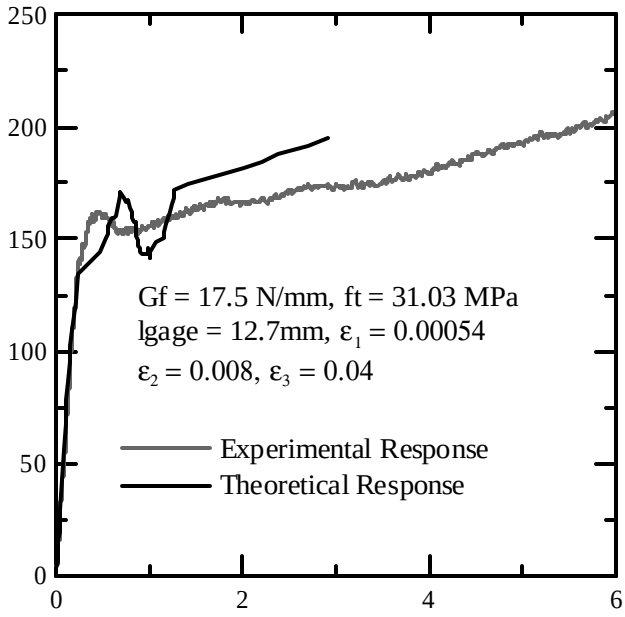

Figure 6.18 Comparison between experimental and theoretical flexural response

A parametric study was conducted on the model to see the effect of number of layers, change in ultimate tensile strength and change in strain values on the predicted load-deflection response.

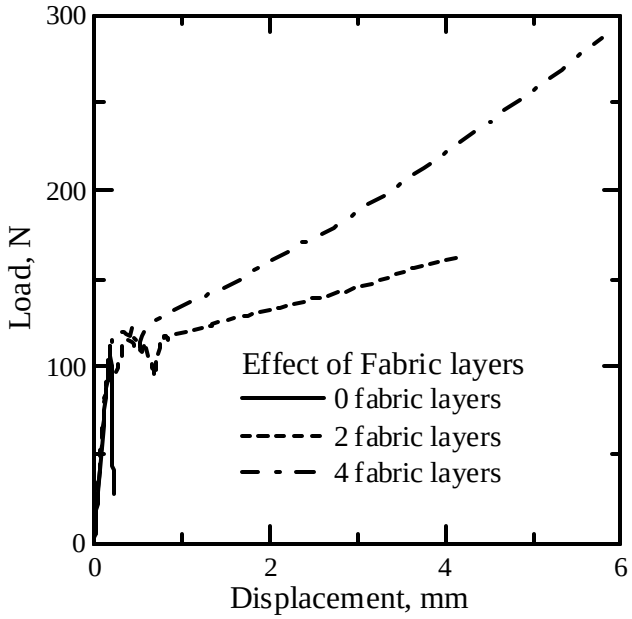

Figure 6.19 Parametric study to see the effect of number of fabric layers

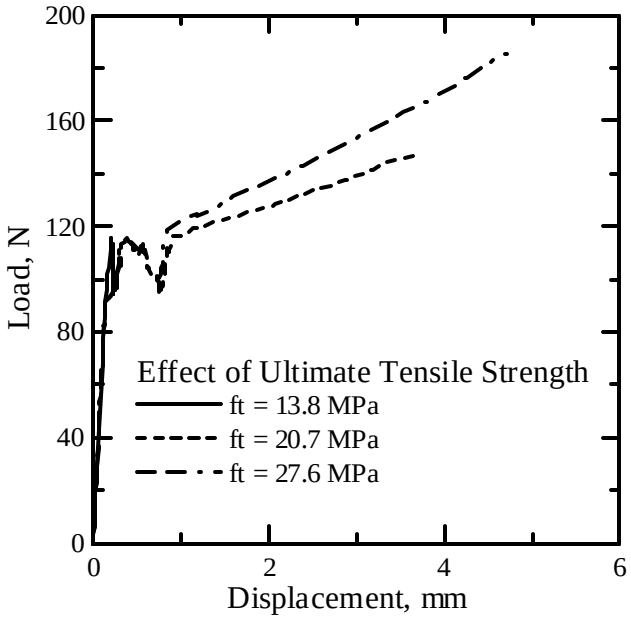

Figure 6.20 Parametric study to see the effect of change in Ultimate tensile strength

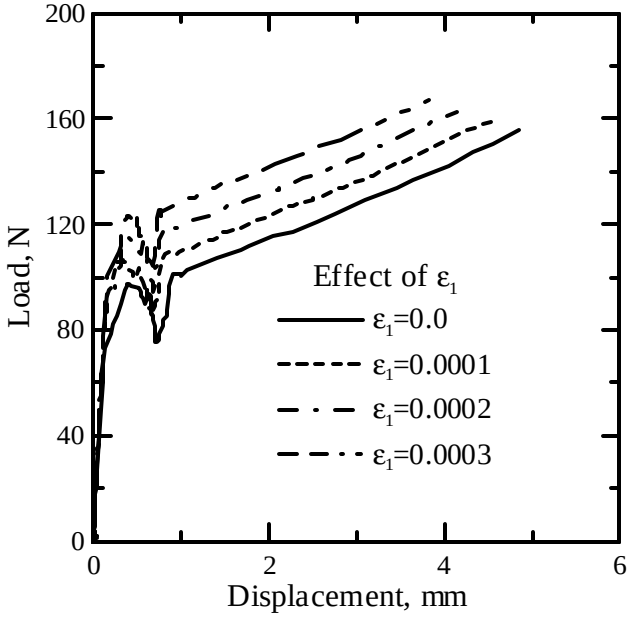

Figure 6.21 Parametric study to see the effect of change in matrix cracking strain

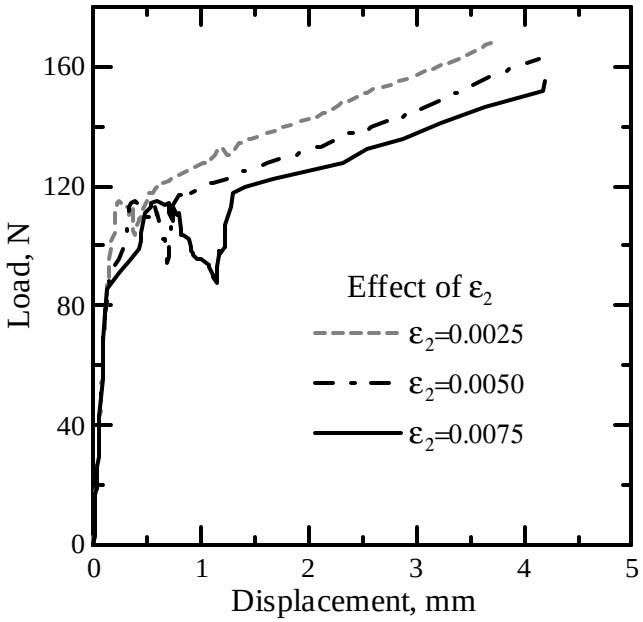

Figure 6.22 Parametric study to see the effect of change in end of matrix cracking strain

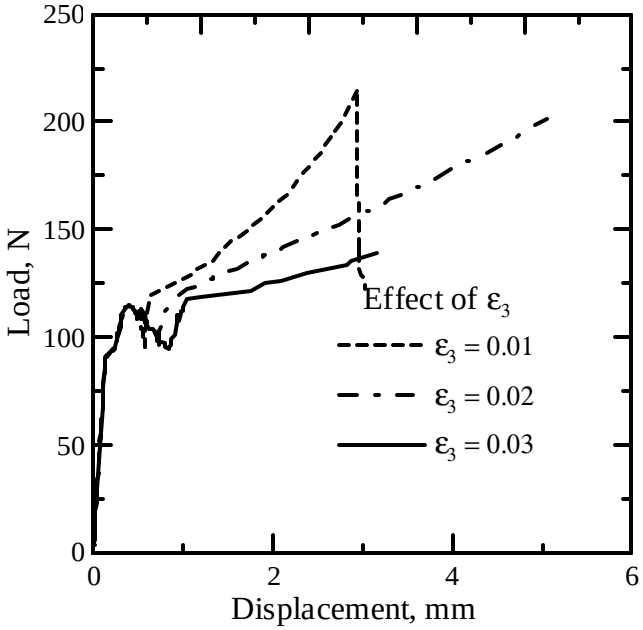

Figure 6.23 Parametric study to see the effect of change in ultimate strain

6.4 Comparison between Tensile and Flexural results

Keeping the above discussion in mind the difference in ultimate tensile strength value in tensile and flexural model can be explained. Flexural model also predicts a tensile response and generates a moment-curvature response from the calculated stress-strain values. Later, the moment-curvature values are used to generate a load-deflection response. For a tensile specimen shown in figure 6.3 the ultimate tensile strength is 4.83 MPa and for predicting flexural response for a similar specimen the ultimate tensile strength used is 23.44 MPa. This can be attributed to the fact that experimental tensile strength is an underestimate of actual strength. The other reason is that the tensile model represents ft as tensile strength of the composite whereas; the flexure model represents ft as the tensile strength of the fabric layer and there are 2 fabric layers out of 16 layers and all the strength is mainly due to these 2 layers. Therefore, a larger value is used to predict an accurate flexural response.

CHAPTER 7

CONCLUSIONS

Saint Gobain Technical Fabrics provided AR Glass fabric with a motive to use it as Seismic Reinforcing grid for retrofitting structures damaged by earthquakes. The fabric was used to manufacture cement composites and the specimens were studied for properties in tension, flexure and bond. In the second phase of the project the specimens were aged for two different ages and studied for the effect of ageing on tensile and flexural properties. Lastly the focus was on modeling the tensile and flexural response of the specimens.

Phase 1

Specimens were cast in structures laboratory at Arizona State University. Initially, the specimens were cast with fabric freely laid in the specimens. Specimens were cast with different number of fabric layers and tested under tension. Analysis showed that as the number of fabric layers increase from 1 layer to 2 layers to 3 layers the maximum stress carried by the specimens goes from 1.51MPa to 2.33MPa to 3.88MPa. Specimens were also cast with 2 layers of fabric but lesser thickness. A comparison between results showed that reducing the thickness by 28.6% can increase tensile strength by 57.4%. Secondly the manufacturing process was improved and a mold was developed that enabled the fabric to stay stretched and aligned while casting. The specimens were cast with 2 layers of fabric and took 48.9% higher tensile stress than the specimens with 2 layers and fabric freely laid. The mold also enabled the fabric to be oriented by a fixed angle and then cast. The specimens were cast using 25.4mm and 50.8mm orientation and

were tested in tension as well as flexure. The specimens with 25.4mm orientation could take 4.89MPa whereas; specimens oriented at 50.8mm could take 2.69MPa of tensile stress. In flexure, the specimens oriented at 25.4mm could take a maximum load of 455.26N and the specimens oriented at 50.8mm could take a maximum load of 411.68N. This study showed that small orientation gives a better bond and anchorage between the fabric and the matrix. Studying the above effects showed that specimens cast with lesser thickness, fabric aligned and stretched and small orientation give much better results. Using this Saint Gobain manufactured specimens with 2 layers of same fabric. Specimens were cast with 2 different fabric coatings and had machine and cross machine direction of fabric. These specimens were tested in tension and flexure. Cross machine direction specimens took a higher tensile stress of 6.01MPa as compared to 4.94MPa took by machine direction specimens for one fabric coating. Also, machine direction specimens could take a maximum flexural stress of 15.7MPa as opposed17.64MPa taken by cross machine direction specimens. For the other fabric coating, machine direction specimens took a tensile stress of 5.13MPa and cross machine direction specimens took a tensile stress of 4.92MPa. In flexure, machine direction specimens took a flexural stress of 16.79MPa whereas; cross machine direction specimens could take a flexural stress of 12.77MPa. It was due to the difference in fabric coating which affects the bond between the fabric and the matrix. Specimens were also cast using 2 layers of fabric and were cast directly on the masonry block. The mold developed enabled to keep the fabric stretched and aligned. These specimens were tested in tension to determine the ability of the masonry-composite unit as a laminate. The comparison of obtained load-displacement

plot showed that specimens took similar maximum tensile stress as tensile specimens and has higher displacement. These studies provide a clear understanding of how the specimens are going to behave in tension, flexure and bond depending on the fabric arrangement. Using this data the fabric will be used to repair damaged masonry structures in a cost effective manner.

Phase 2

In the second phase of the project the specimens were cast by Saint Gobain Technical Fabrics and were used to study ageing effect on tensile and flexural properties. The specimens were aged at 80^{o}C for 14 days and 28 days. A set of specimens of the same batch was tested un-aged to establish the properties of fresh specimens for comparison between un-aged and aged specimens. Un-aged machine direction specimens could take a maximum tensile stress of 5.03MPa and cross machine direction specimens could take a maximum tensile stress of 4.65MPa. Specimens aged for 14 days could take maximum tensile stress of 3.76MPa in machine direction 4.02MPa in cross machine direction. Specimens aged for 28 days could take maximum tensile stress of 3.87MPa in machine direction and 3.85MPa in cross machine direction. The effect of ageing decreased the tensile strength significantly in machine direction. This can be explained using the fabric geometry. The fabric geometry is such that it has bulge of filaments in the machine direction. When the specimen is aged, the products of hydration formed due to increased moisture and elevated temperature will accumulate in this region. This makes the fabric weak in machine direction as compared to cross machine direction. Similar effect is observed in flexural properties. Un-aged specimens could take a

maximum load of 422.6N in machine direction and 395.2N in cross machine direction. Specimens aged for 14 days could take a maximum load of 330.47N in machine direction and 377.56N in cross machine direction. Specimens aged for 28 days could take a maximum load of 304.02N in machine direction and 377.35N in cross machine direction. The ageing effect is studied to get a better understanding of composite's behavior with natural weathering and usage over the years.

Theoretical Modeling

A theoretical model was developed to simulate the experimental tensile response. The model gives a certain set of parameters including fracture energy, maximum tensile strength, strain at which specimen cracks and strain at maximum tensile stress. These parameters are used as input for flexural model and it generates a response similar to experimental flexure response for a specimen similar to one used by tension model. This program predicts the initial slope and the point at which slope changes very accurately. After the first crack it predicts the slope accurately but does not go till the maximum load. This is not done because after a certain deflection there is hinge formation in the specimen and the load is only taken by the fabric. It no more requires to be analyzed as a composite. Moreover, the program assumes only one crack whereas; in experiment there are 3-4 cracks in the specimen. Also, the experiment is deflection controlled and at no point deflection decrease as the test is in progress. But the model generates the load-deformation response from the moment curvature response. If the moment decreases and then increases the load goes back and forth. The program can be further modified to take care of these points.

Further work

The aged specimens can be studied under SEM to see the region of accumulation of products of hydration.

REFERENCES

Saadatmanesh, Hamid (1997). Extending service life of concrete and masonry structures with fiber composites. *Construction and Building Materials.* 11, 327-335.

Agarwal, B. D., & Broutman, L. J. (1990). *Analysis and performance of fiber composite.* New York: Wiley-Interscience Publication.

Mayrhofer, Chr. (2001). Reinforced masonry walls under blast loading. *International Journal of Mechanical Science.* 44, 1067-1080.

Greszczuk, L. B. (1969). Theoretical Studies of the Mechanics of the Fiber-Matrix Interface in Composites. *ASTM STP 452, American Society for Testing and Materials.* 42-58.

Albert, M. L., Elwi, A. E., Cheng, J. J. R. (2001). Strengthening of unreinforced masonry walls using FRPs. *Journal of Composites for Construction.* 5(2), 76-84.

Hull, D. (1981). *An introduction to composite materials.* New York: Cambridge University Press.

Jai, J., Springer, G. S., Kollar, L. P., Krawinkler, H. (2000). Reinforcing masonry walls with composite materials – Model. *Journal of Composite Materials.* 34(18), 1548-1581.

Jai, J., Springer, G. S., Kollar, L. P., Krawinkler, H. (2000). Reinforcing masonry walls with composite materials - Test results. *Journal of Composite Materials.* 34(16), 1369-1381.

Jones, R. M. (1999). *Mechanics of Composites Material* (2nd ed.). Philadelphia: Taylor & Francis.

Kelly, A., & Tyson, W. R. (1965). Fiber-Strengthened Materials. *High-Strength Materials; Proceedings of the Second Berkeley International Materials Conference: High-Strength Materials – Present Status and Anticipated Developments. Held at the University of California, Berkeley.* Ed. Victor F. Zackay. 578-602.

Galano, L., Gusella, V. (1998). Reinforcement of masonry walls subjected to seismic loading using steel X-bracing. *Journal of Structural Engineering-ASCE*. 124(8), 886-895.

Mobasher, B., Kingsbury, D., Montesinos, J., & Gorur, R. S. (2003). Mechanical Aspects of Crimped Glass Reinforced Plastic (GRP) Rods. *IEEE Transactions on Power Delivery*. 18, 852-8.

Peled, A., Benture, A., & Yankelevsky, D. (1994). Woven Fabric Reinforcement of Concrete Matrix. *Journal of Advanced Cement Based Materials.* 1, 216-23.

Saadatmanesh, H., Ehsani, M. R. (1998). *Fiber Composites in Infrastructure.* Tucson-University of Arizona.

Peled, A., & Mobasher, B. (2003). The Pultrusion Technology for the Production of Fabric-Cement Composites. *Brittle Matrix Composites 7 – Proceedings of the 7th International Symposium.* Ed. Brandt, A. M., V. C. Li, and I. H. Marshall. Cambridge: Woodhead Publ. Ltd.; Warsaw: ZTUREK Research-Scientific Institute. 505-14.

Mane, S. A., Desai T. K., Kingsbury, D., & Mobasher, B. (2002). Modeling of Restrained Shrinkage Cracking in Concrete Materials. *ACI Special Publications*. 219-242.

Talreja, R. (1986). Stiffness Properties of Composite Laminates with Matrix Cracking and Interior Delamination. *Engineering Fracture Mechanics.* 25, 751-62.

Gurney, C., & Hunt, J. (1967). Quasi-Static Crack Propagation. *Proceedings of the Royal Society of London Series A – Mathematical and Physical Sciences.* 299. 508-24

Mobasher, B. (2000). Micromechanical Modeling Of Angle Ply Cement Based Composites. *Proc., 6th Int. Sym. on Brittle Matrix Comp., (BMC6).* Warsaw, Poland

Haupt, G. J. (1997). *Study of Cement Based Composites Manufactured by Extrusion, Compression molding and Filament Winding.* MS Thesis. Tempe: Arizona State University.

Hetényi, M. (1983). *Beam on Elastic Foundation.* Ann Arbor: University of Michigan Press.

APPENDIX A

GRAPHS FOR ALL THE TESTED SAMPLES

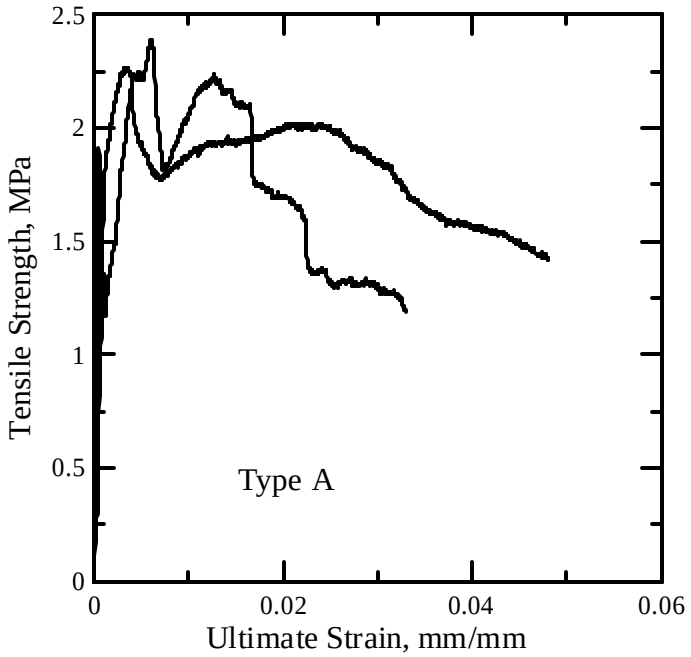

Figure A -1 Stress-strain plots for specimens cast with fabric freely laid

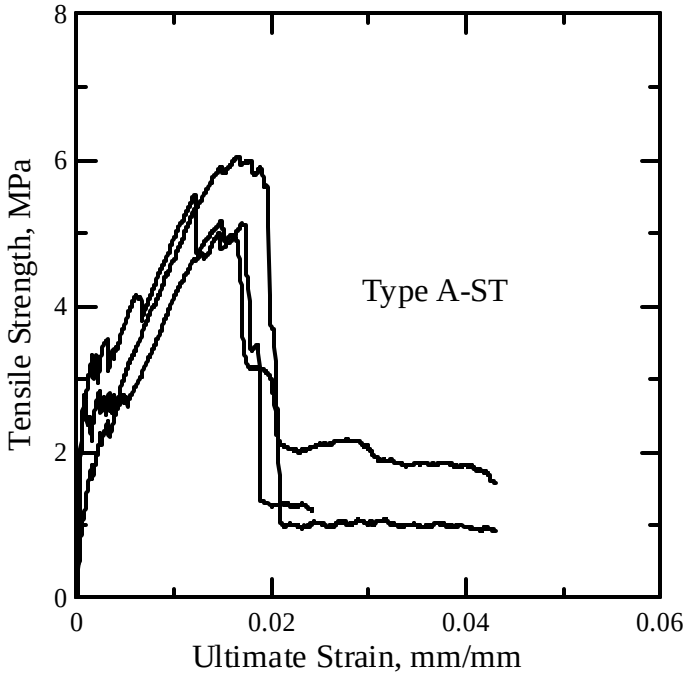

Figure A -2 Stress-strain plots for specimens cast with fabric freely laid and lesser specimen thickness

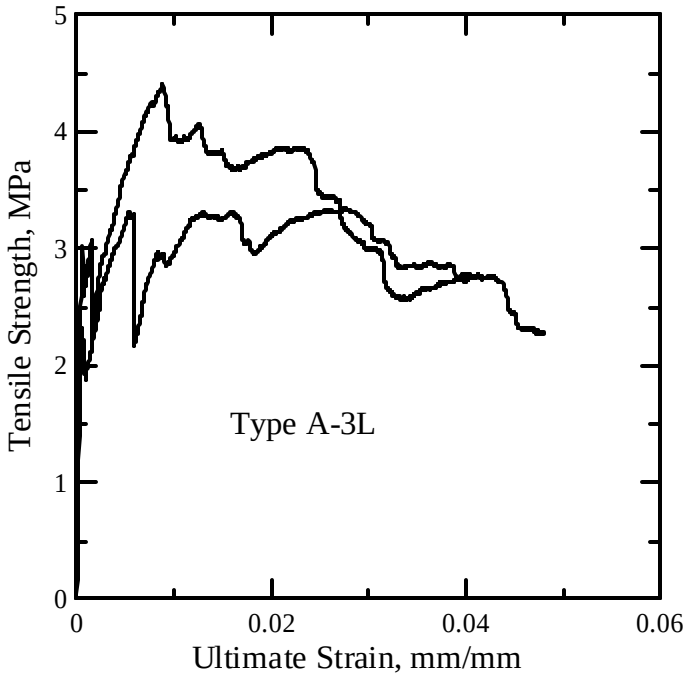

Figure A -3 Stress-strain plots for specimens cast with fabric freely laid and 3 layers of fabric

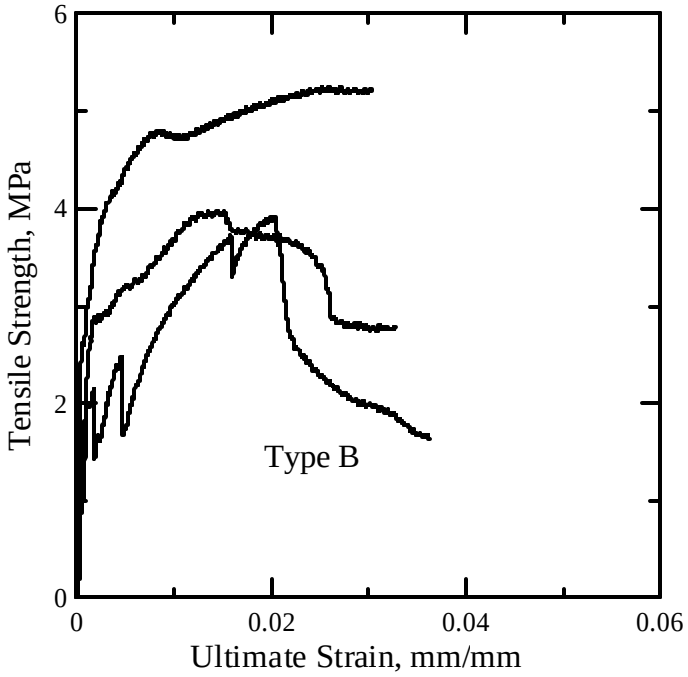

Figure A -4 Stress-strain plots for specimens cast with fabric freely stretched and aligned

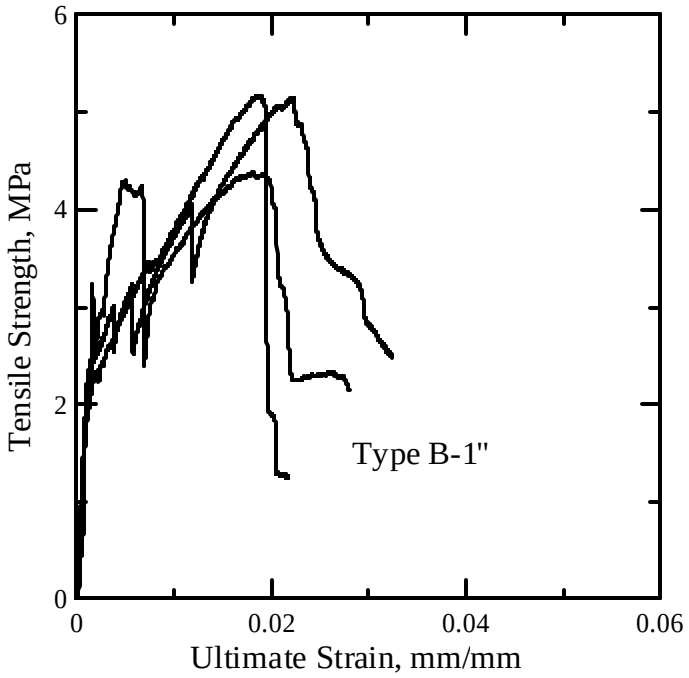

Figure A -5 Stress-strain plots for specimens cast with fabric freely stretched and aligned and fabric oriented at 25.4mm

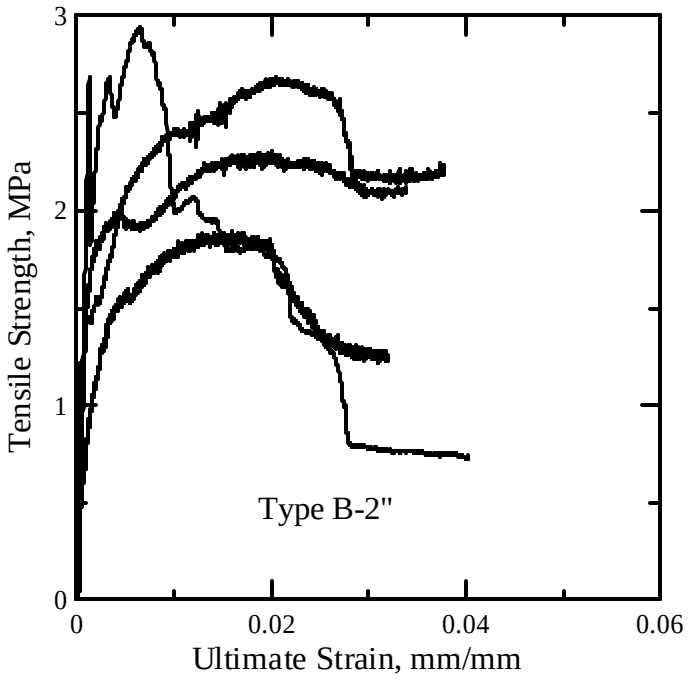

Figure A -6 Stress-strain plots for specimens cast with fabric freely stretched and aligned and fabric oriented at 50.8mm

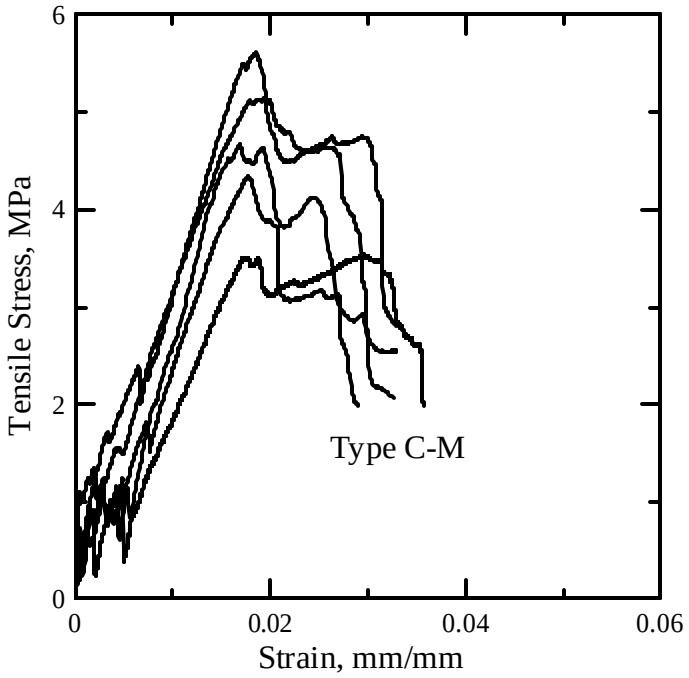

Figure A -7 Stress-strain plots for specimens cast by Saint Gobain Technical Fabrics with fabric in machine direction along the test direction

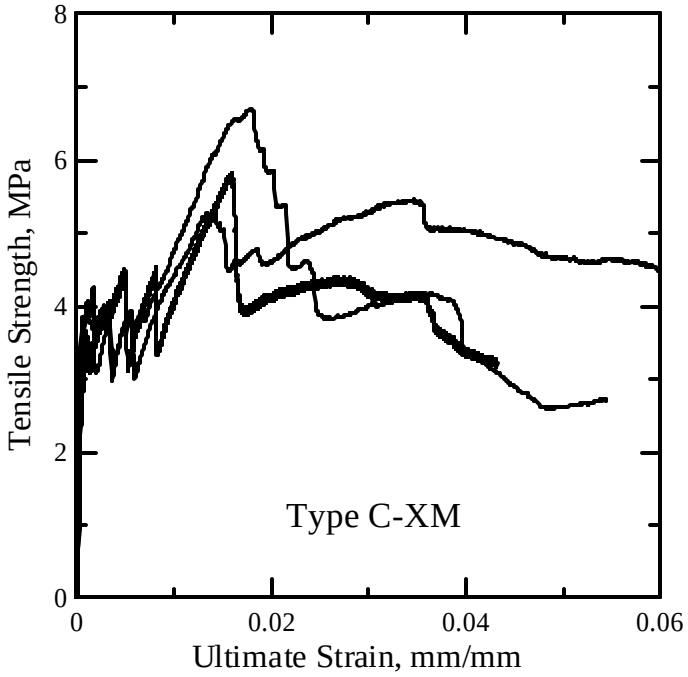

Figure A -8 Stress-strain plots for specimens cast by Saint Gobain Technical Fabrics with fabric in cross machine direction along the test direction

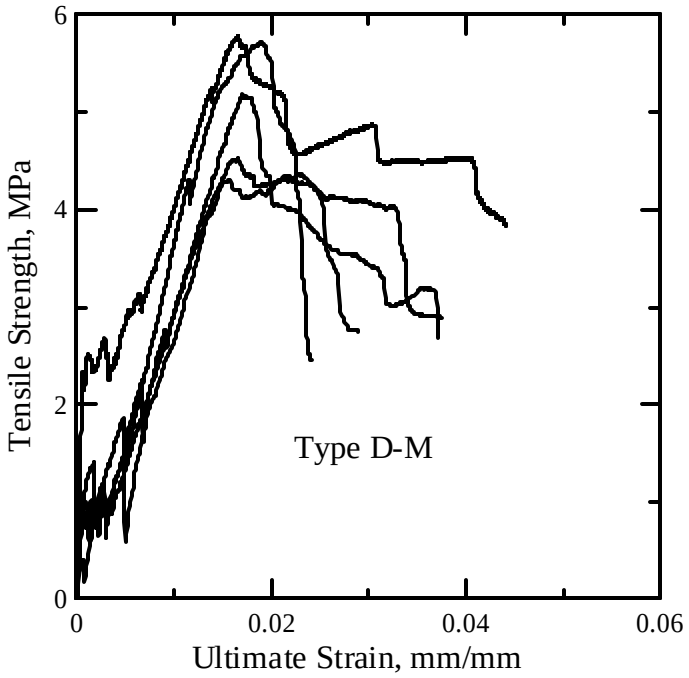

Figure A -9 Stress-strain plots for specimens cast by Saint Gobain Technical Fabrics with fabric in machine direction along the test direction

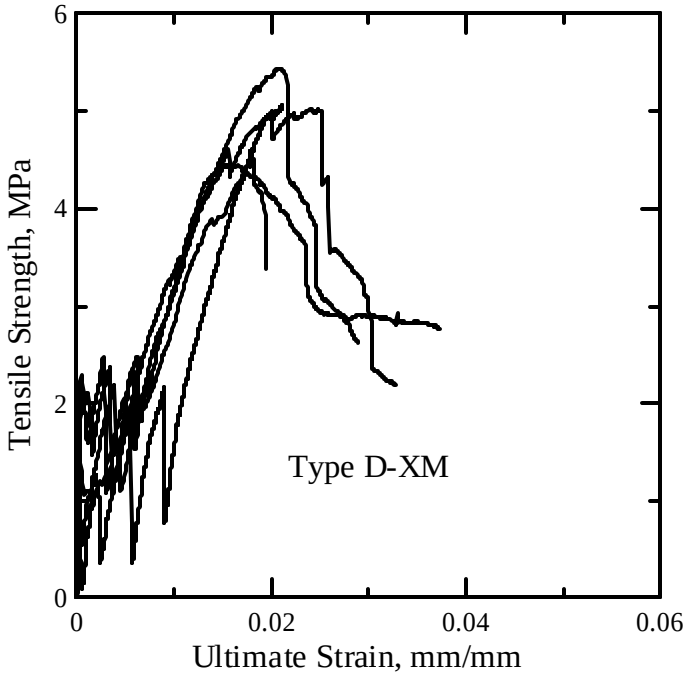

Figure A -10 Stress-strain plots for specimens cast by Saint Gobain Technical Fabrics with fabric in cross machine direction along the test direction

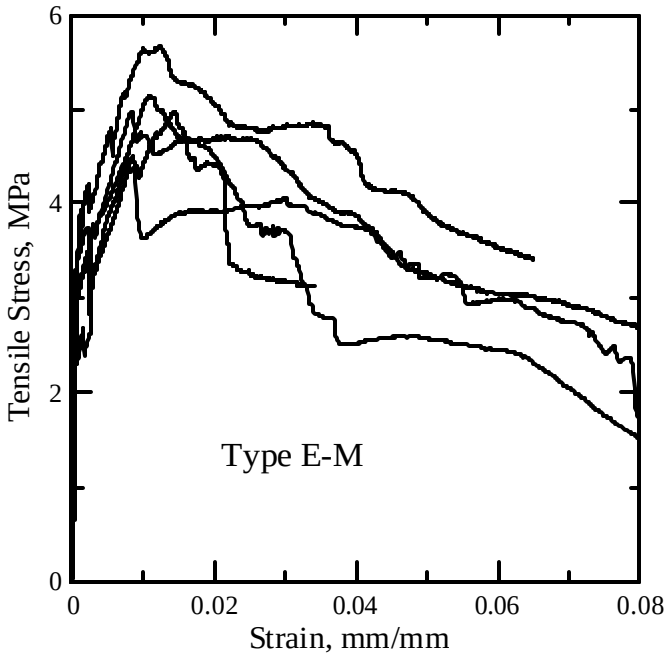

Figure A -11 Stress-strain plots for specimens cast by Saint Gobain Technical Fabrics with fabric in machine direction along the test direction, tested un-aged

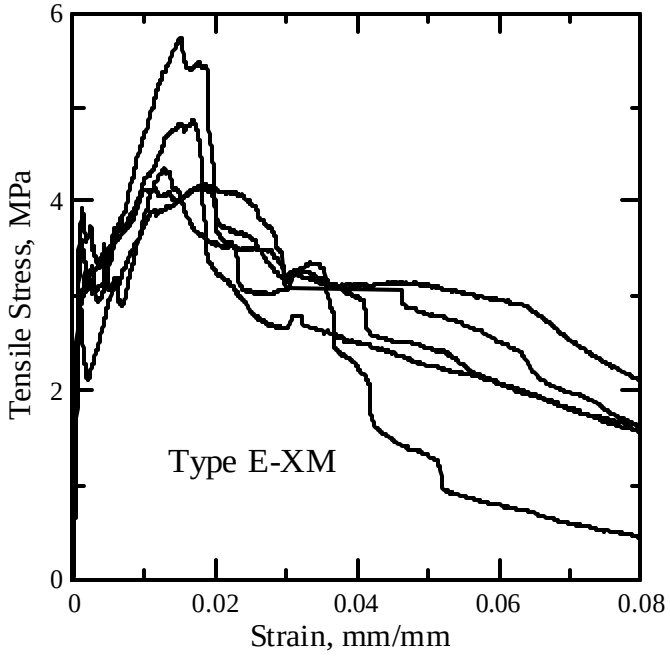

Figure A -12 Stress-strain plots for specimens cast by Saint Gobain Technical Fabrics with fabric in cross machine direction along the test direction, tested un-aged

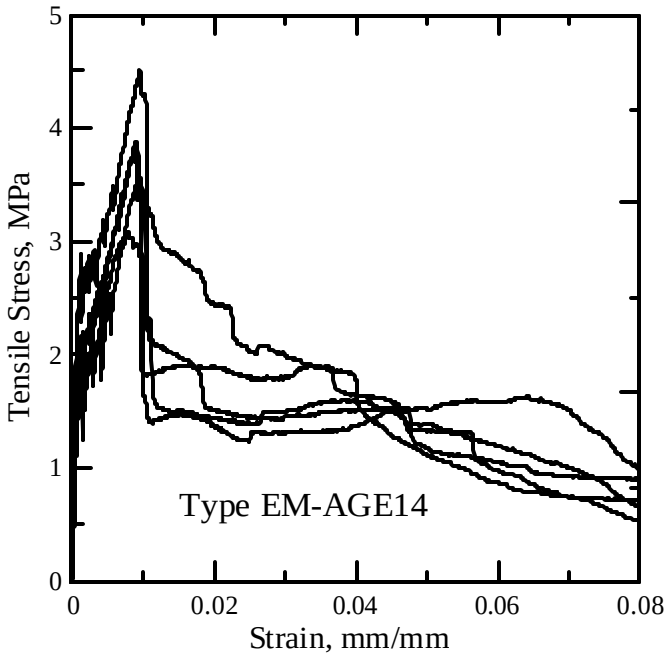

Figure A -13 Stress-strain plots for specimens cast by Saint Gobain Technical Fabrics with fabric in machine direction along the test direction, aged for 14 days

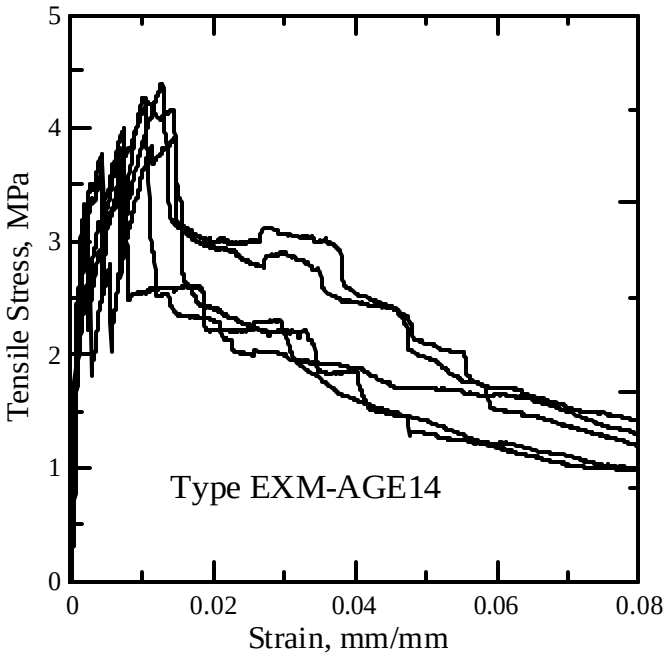

Figure A -14 Stress-strain plots for specimens cast by Saint Gobain Technical Fabrics with fabric in cross machine direction along the test direction, aged for 14 days

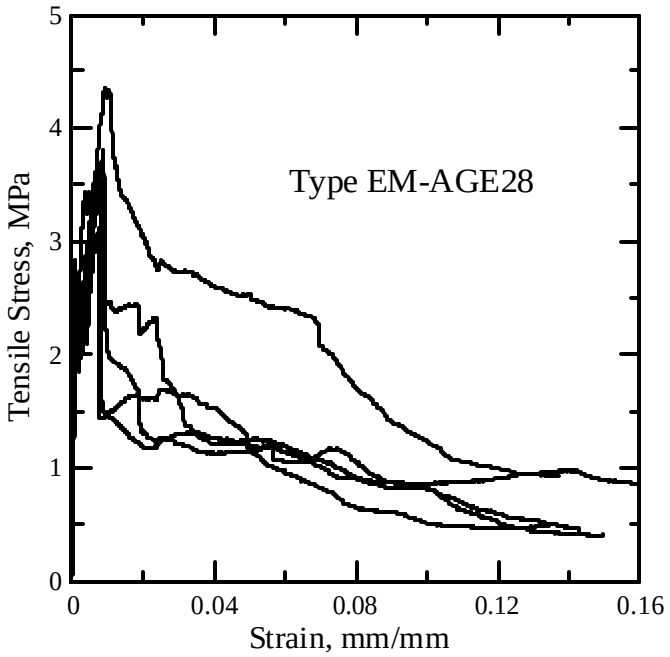

Figure A -15 Stress-strain plots for specimens cast by Saint Gobain Technical Fabrics with fabric in cross machine direction along the test direction, aged for 28 days

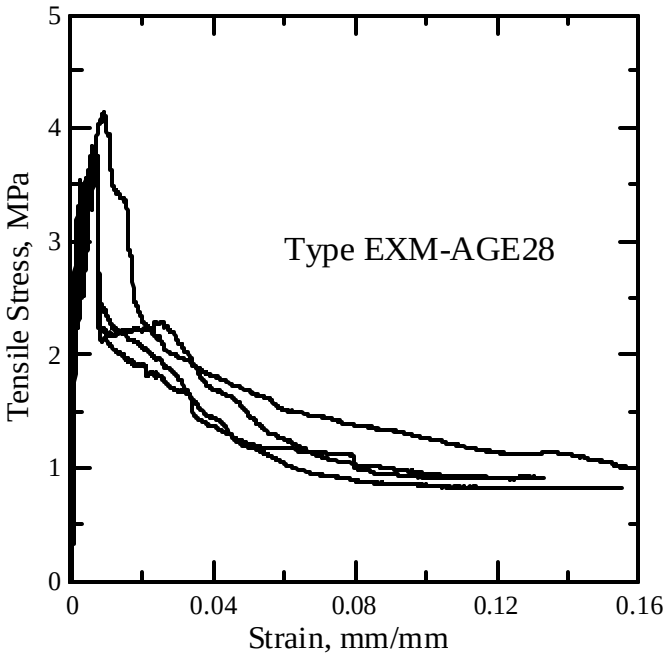

Figure A -16 Stress-strain plots for specimens cast by Saint Gobain Technical Fabrics with fabric in cross machine direction along the test direction, aged for 28 days

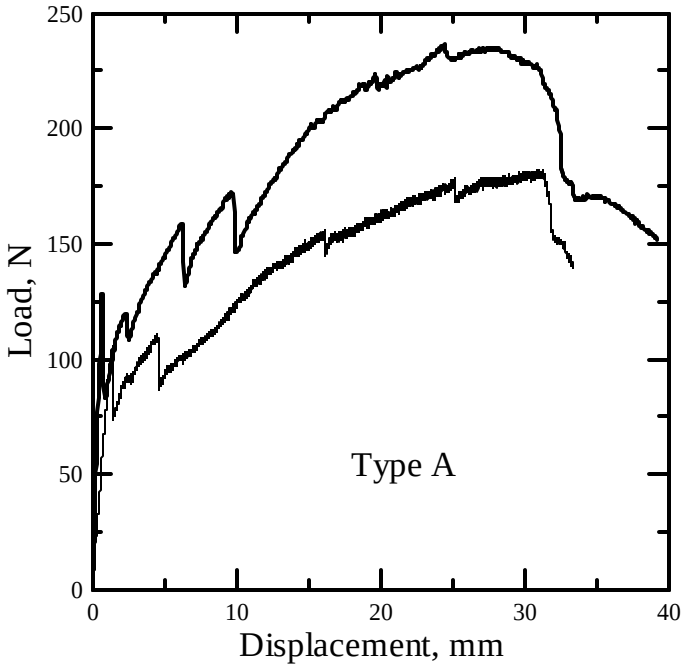

Figure A -17 Load vs. displacement plots for specimens cast with fabric freely laid

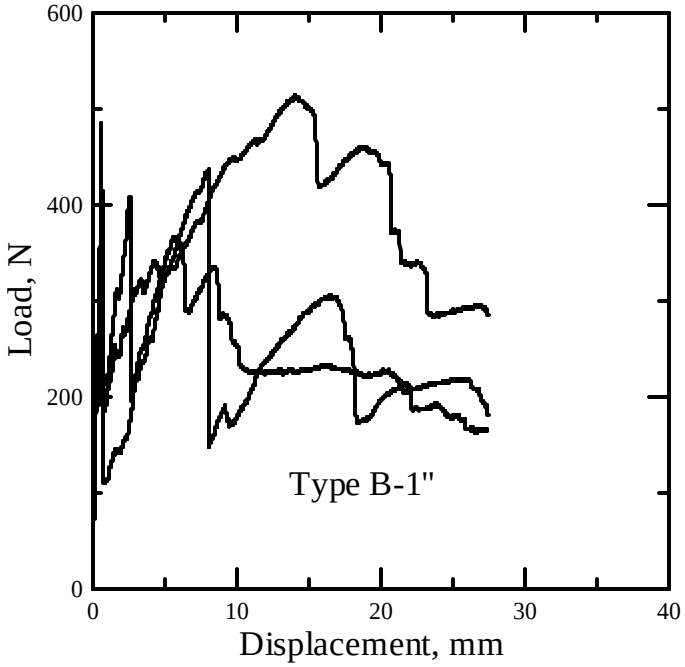

Figure A -18 Load vs. displacement plots for specimens cast with fabric aligned and stretched and oriented at 25.4mm

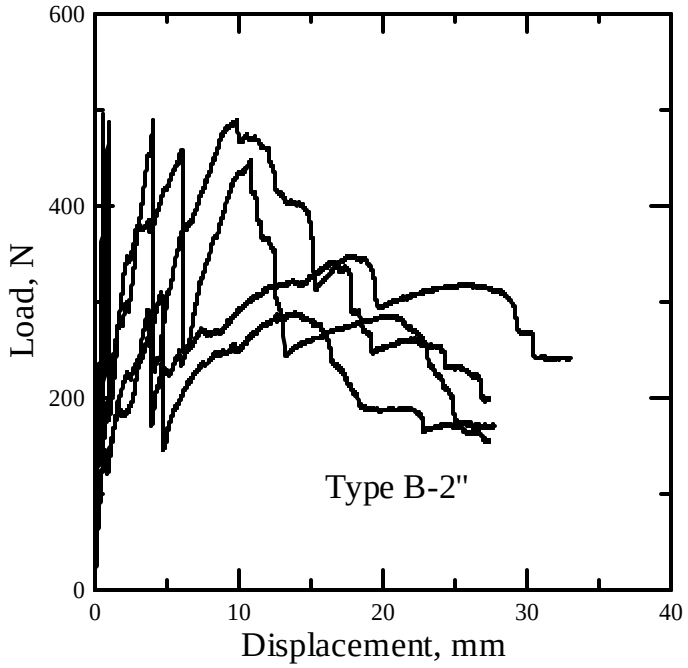

Figure A -19 Load vs. displacement plots for specimens cast with fabric aligned and stretched and oriented at 50.8mm

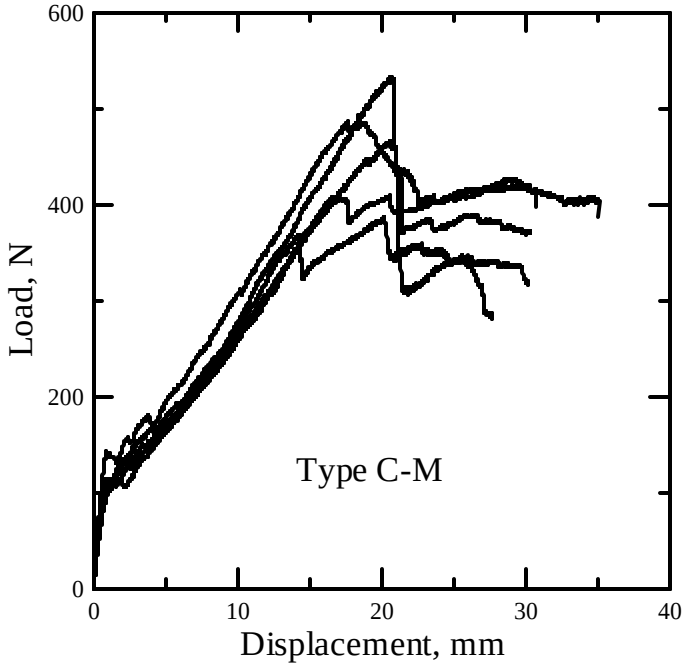

Figure A -20 Load vs. displacement plots for specimens cast by Saint Gobain Technical Fabrics and fabric in machine direction

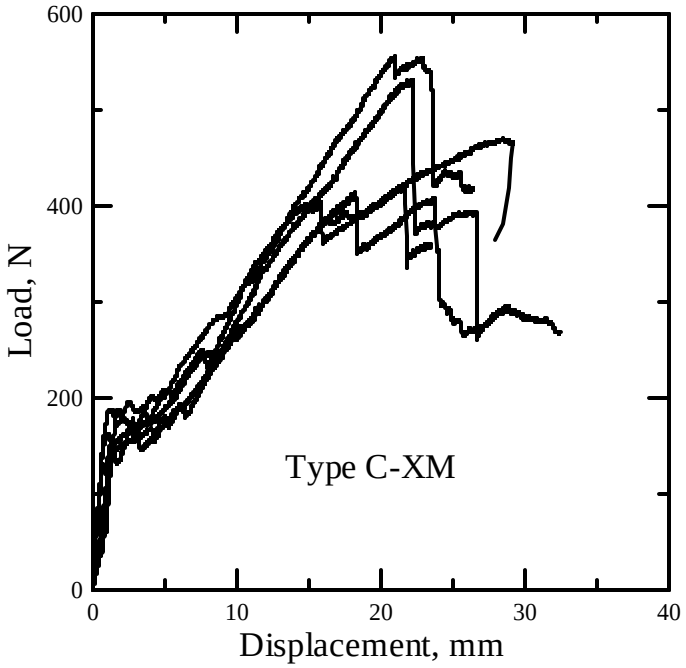

Figure A -21 Load vs. displacement plots for specimens cast by Saint Gobain Technical Fabrics and fabric in cross machine direction

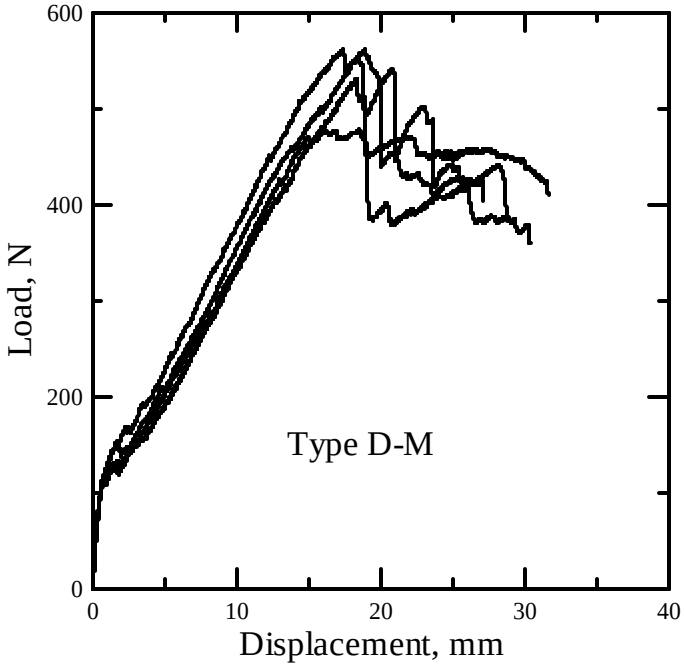

Figure A -22 Load vs. displacement plots for specimens cast by Saint Gobain Technical Fabrics and fabric in machine direction

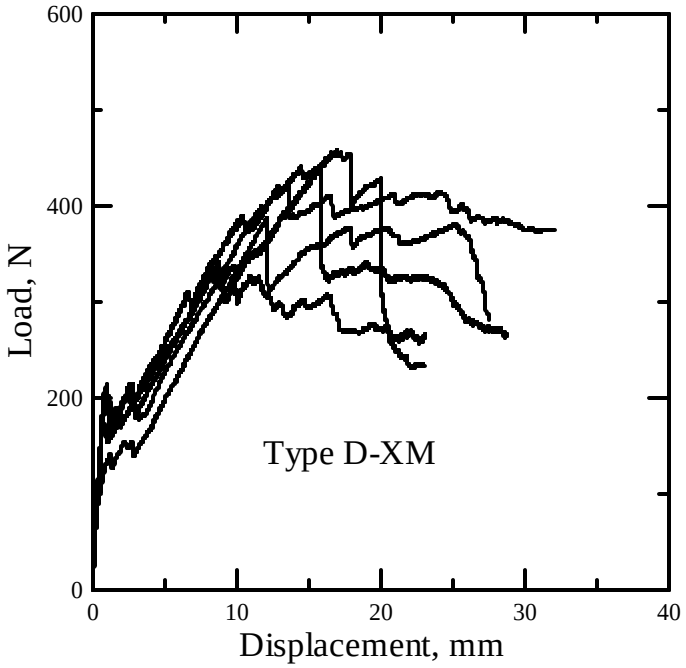

Figure A -23 Load vs. displacement plots for specimens cast by Saint Gobain Technical Fabrics and fabric in cross machine direction

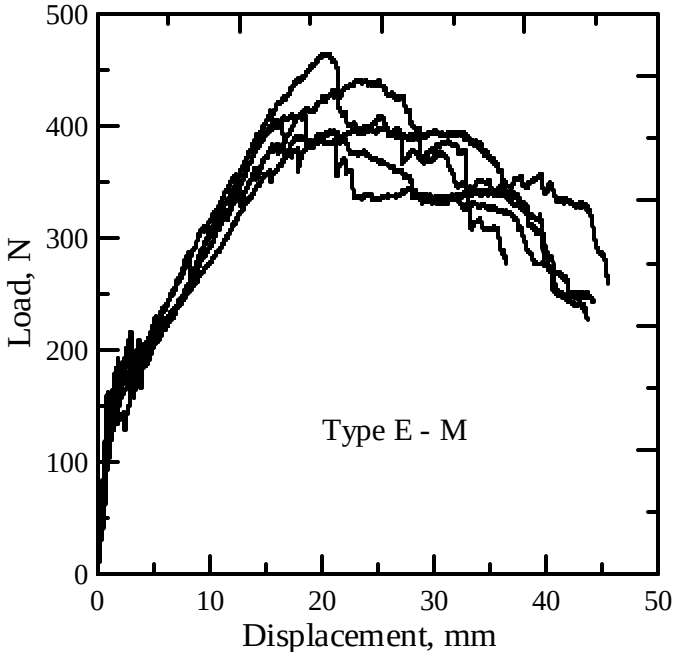

Figure A -24 Load vs. displacement plots for specimens cast by Saint Gobain Technical Fabrics and fabric in machine direction, tested un-aged

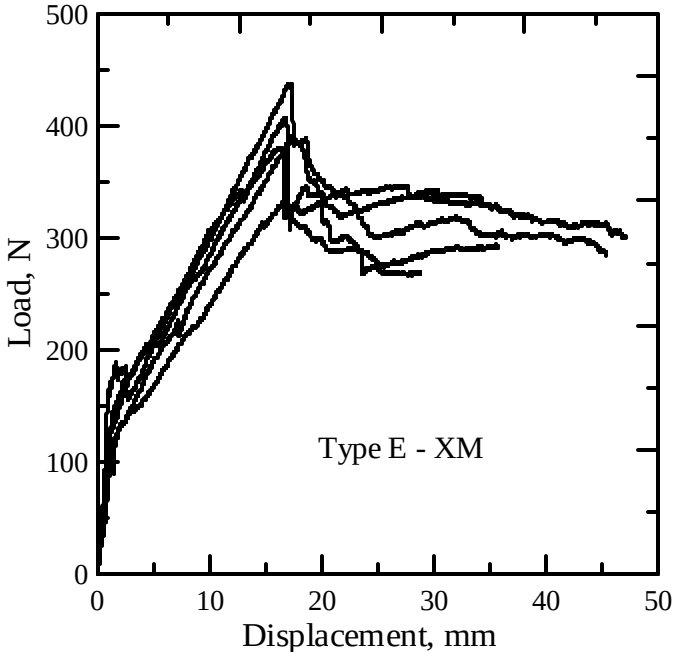

Figure A -25 Load vs. displacement plots for specimens cast by Saint Gobain Technical Fabrics and fabric in cross machine direction, tested un-aged

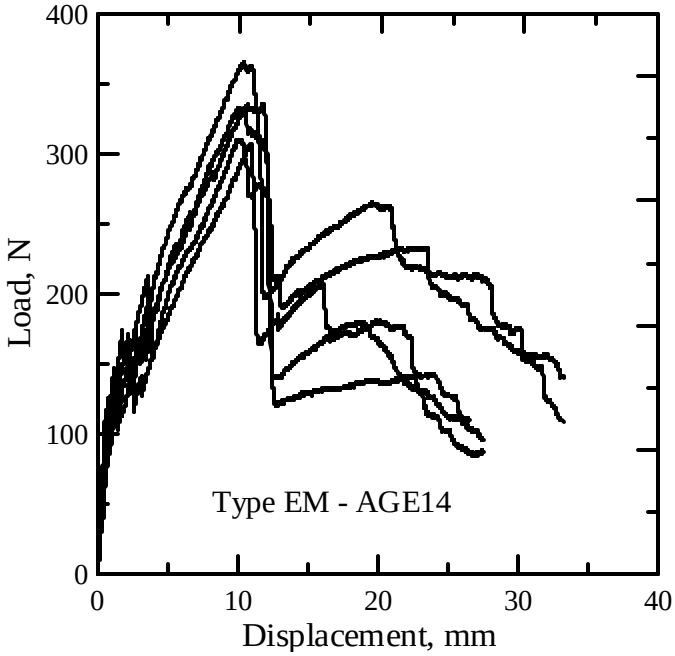

Figure A -26 Load vs. displacement plots for specimens cast by Saint Gobain Technical Fabrics and fabric in machine direction, aged for 14 days

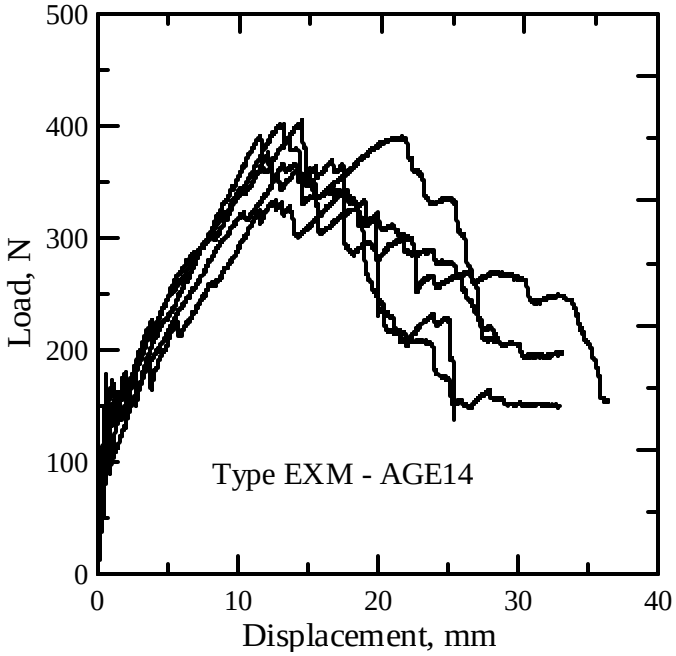

Figure A -27 Load vs. displacement plots for specimens cast by Saint Gobain Technical Fabrics and fabric in cross machine direction, aged for 14 days

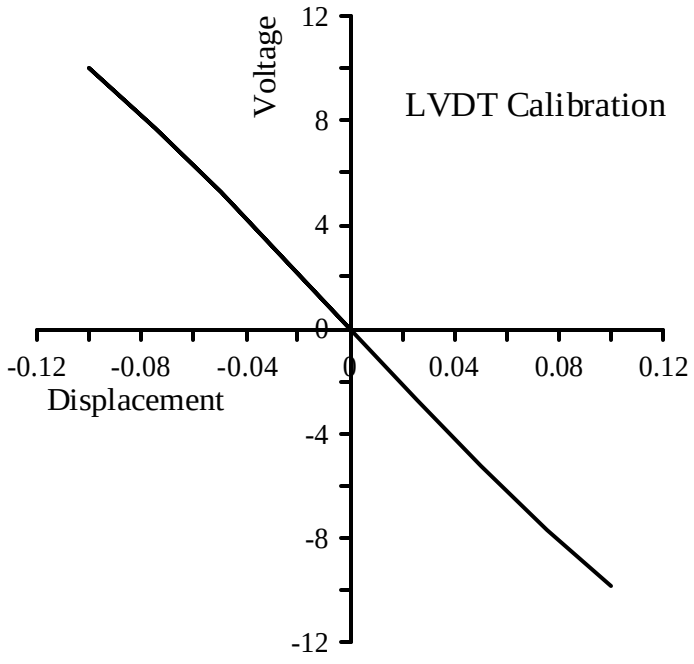

Figure A -28 Graph showing calibration of LVDT used in flexure tests

Figure A -29 Figure showing crack formation during flexure test and shows how the crack propagates along the fabric rather than going through and through the matrix and crack it

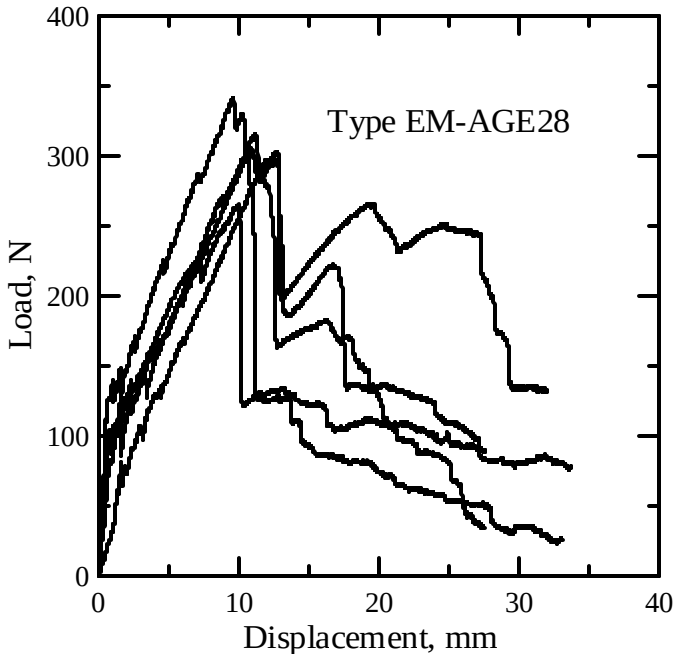

Figure A -30 Load vs. displacement plots for specimens cast by Saint Gobain Technical Fabrics and fabric in machine direction, aged for 28 days

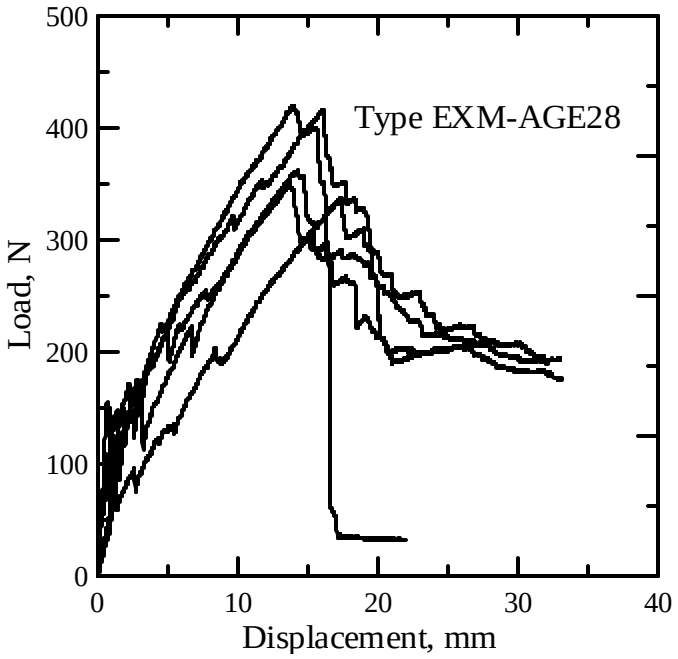

Figure A -31 Load vs. displacement plots for specimens cast by Saint Gobain Technical Fabrics and fabric in cross machine direction, aged for 28 days

Table B-1

Mechanical properties in Tension for all specimens of

Type A - fabric freely laid (11.35x67.26x234.19) mm

Type A-3L - specimens with 3 layers of fabric (11.3x68.28x234.19) mm

Type A-1L - specimens with one layer of fabric (11.32x68.26x234.19) mm

Type A-ST - specimens with lesser thickness (8.01x69.43x234.19) mm

Specimen Group	Young's Modulus, E, MPa	First Crack Stress, MPa	First Crack Strain, %	Maximum Load, KN	Maximum Stress, MPa	Strain at Ultimate Load, %	Toughness, MPa	Ave load, N /mm
Type A	6176.71	1.91	0.05	1.84	2.39	1.00	0.08	13.64
	3644.86	2.26	0.35	1.74	2.27	1.20	0.13	12.97
	4455.62	1.98	0.42	1.80	2.34	1.10	0.10	13.39
Avg.	4759.06	2.05	0.27	1.79	2.33	1.10	0.10	13.33
Std.Dev.	1292.91	0.19	0.19	0.05	0.06	0.10	0.03	0.34
Type A – 3L	5130.41	2.82	0.07	3.48	4.41	0.80	0.24	25.19
	10029.98	2.22	0.06	2.52	3.35	0.70	0.17	18.70
Avg.	7580.19	2.52	0.06	3.00	3.88	0.75	0.20	21.95
Std.Dev.	3464.51	0.42	0.00	0.68	0.75	0.07	0.04	4.59

Type A – 1L	2891.43	1.49	0.17	1.17	1.51	0.80	0.06	8.61
	3106.50	1.53	0.18	1.16	1.49	1.20	0.06	8.44
Avg.	2998.97	1.51	0.18	1.16	1.50	1.00	0.06	8.52
Std.Dev.	152.07	0.03	0.00	0.01	0.01	0.28	0.00	0.12
Type A – ST	7202.98	2.67	0.09	3.21	6.04	1.80	0.12	22.96
	2617.67	1.82	0.16	3.04	5.17	1.85	0.13	21.93
	3214.99	3.32	0.16	2.85	5.18	1.78	0.09	20.56
Avg.	4345.21	2.61	0.13	3.03	5.47	1.81	0.11	21.82
Std.Dev.	2492.85	0.75	0.04	0.18	0.50	0.04	0.02	1.20

Table B-2

Mechanical properties in Tension for all specimens of

Type B – Specimens cast using aligned and stretched fabric (11.9x67.72x213.69) mm

Type B – 1” - Specimens with fabric oriented at 25.4mm (11.64x68.79x234.95) mm

Type B – 2” – Specimens with fabric oriented at 50.8mm (11.43x67.65x225.70) mm

Specimen Group	Young's Modulus, E, MPa	First Crack Stress, MPa	First Crack Strain, %	Maximum Load, KN	Maximum Stress, MPa	Strain at Ultimate Load, %	Toughness, MPa	Ave load, N /mm
Type B	2920.65	2.14	0.18	3.26	3.92	1.80	0.09	24.10
	9421.26	2.53	0.05	4.16	5.25	2.00	0.14	30.74
	6503.77	2.85	0.18	3.16	3.98	2.10	0.11	23.30
Avg.	6281.89	2.51	0.14	3.53	4.39	1.97	0.11	26.05
Std.Dev.	3255.98	0.36	0.07	0.55	0.75	0.15	0.03	4.08
Type B – 1”	4091.02	2.43	0.14	4.14	5.17	2.18	0.08	30.11
	3983.31	3.01	0.37	4.12	5.14	2.30	0.12	29.94
	3893.04	3.12	0.14	3.26	4.07	2.20	0.16	23.70
Avg.	3989.12	2.85	0.22	3.84	4.80	2.23	0.12	27.92
Std.Dev.	99.12	0.37	0.14	0.50	0.63	0.07	0.04	3.65

Type B – 2”	3206.44	1.81	0.20	1.71	2.30	2.30	0.07	13.16
	3262.34	1.22	0.05	2.00	2.68	2.50	0.09	15.34
	1062.69	1.56	0.53	1.41	1.90	2.00	0.05	10.84
	3510.15	0.93	0.03	3.04	2.94	0.80	0.06	22.04
Avg.	2760.41	1.38	0.20	2.04	2.46	1.90	0.07	15.35
Std.Dev.	1139.48	0.39	0.23	0.71	0.46	0.76	0.02	4.83

Table B-3

Mechanical properties in Tension for all specimens of

Type C – M – specimens cast by Saint Gobain Technical fabrics with fabric in machine direction (9.91x63.08x205.64) mm

Type C – XM – specimens cast by Saint Gobain Technical fabrics, fabric in cross machine direction (9.31x63.15x200.19) mm

Specimen Group	Young's Modulus, E, MPa	First Crack Stress, MPa	First Crack Strain, %	Maximum Load, KN	Maximum Stress, MPa	Strain at Ultimate Load, %	Toughness, MPa	Ave load, N /mm
Type C- M	5842.1	1.21	0.48	2.13	3.53	2.969	0.10	16.97
	4368.17	1.54	0.43	3.49	5.60	1.868	0.15	27.26
	5916.8	1.07	0.29	2.70	4.32	1.783	0.08	21.48
	6001.5	1.70	0.31	3.22	5.16	1.971	0.15	25.69
	5865.40	1.21	0.29	2.94	4.67	1.712	0.12	23.34
Avg.	5537.98	1.38	0.33	3.08	4.94	1.83	0.13	24.44
Std.Dev.	781.89	0.29	0.07	0.34	0.56	0.11	0.03	2.55
Type C- XM	5397.86	3.57	0.16	3.56	5.86	1.63	0.27	28.29
	4781.16	3.89	0.17	3.19	5.48	3.49	0.43	25.08
	7887.09	3.82	0.17	3.84	6.69	1.80	0.27	30.51
	258.01	1.88	0.88	1.34	2.31	1.96	0.004	10.61
	1472.40	1.40	0.18	2.64	4.59	2.42	0.07	20.94
Avg.	6022.04	3.76	0.17	3.53	6.01	2.31	0.32	27.96
Std.Dev.	1644.35	0.17	0.01	0.32	0.62	1.03	0.09	2.73

Table B-4

Mechanical properties in Tension for all specimens of

Type D – M – specimens cast by Saint Gobain Technical fabrics with fabric in machine direction (9.6x62.82x209.49) mm

Type D–XM – specimens cast by Saint Gobain Technical fabrics, fabric in cross machine direction (10.03x62.57x192.96) mm

Specimen Group	Young's Modulus, E, MPa	First Crack Stress, MPa	First Crack Strain, %	Maximum Load, KN	Maximum Stress, MPa	Strain at Ultimate Load, %	Toughness, MPa	Ave load, N /mm
Type D- M	3712.30	1.19	0.28	2.73	4.54	1.67	0.17	21.72
	3809.30	1.01	0.28	3.34	5.74	1.91	0.14	26.59
	4661.71	1.41	0.18	3.23	5.18	1.72	0.14	25.65
	3861.7	1.13	0.27	2.63	4.39	2.35	0.12	20.99
	4344.89	1.41	0.21	3.09	5.13	1.87	0.16	24.60
Avg.	836.94	0.52	0.09	0.39	0.65	0.29	0.04	3.09
Std.Dev.	3712.30	1.19	0.28	2.73	4.54	1.67	0.17	21.72
Type D- XM	4412.89	1.06	0.03	3.18	5.09	2.16	0.22	25.40
	8381.32	2.27	0.06	2.74	4.44	1.57	0.18	21.83
	5118.63	1.10	0.04	3.23	5.04	2.43	0.17	25.85
	6101.45	2.12	0.12	3.54	5.46	2.10	0.12	28.29
	4786.97	1.40	0.04	2.76	4.54	1.82	0.03	22.15
Avg.	5760.25	1.59	0.06	3.09	4.92	2.02	0.14	24.70
Std.Dev.	1593.80	0.57	0.03	0.34	0.42	0.33	0.07	2.71

Table B-5

Mechanical properties in Flexure (3 Point Bending Test) for all specimens of

Type B – 1" - Specimens with fabric oriented at 25.4mm (11.64x73.2x254.00) mm

Type B – 2" – Specimens with fabric oriented at 50.8mm (11.43x68.78x225.70) mm

Specimen Group	Young's Modulus, E, MPa	First Crack Stress, MPa	First Crack Deflection, mm	Maximum Load, N	Flexural Strength, MPa	Deflection at Maximum Load, mm	Toughness, MPa.mm	Ave. Load, N/mm
Type B–1"	10276	6.5	0.61	366.75	6.9	5.73	6600.36	25.8
	13429	8.4	0.73	514.14	10.5	14.09	11061.64	36.2
	17883	10.5	0.70	484.89	10.5	1.45	7302.13	37.1
Avg.	13862.53	8.48	0.68	455.26	9.28	7.09	8321.38	33.02
Std.Dev.	3822.19	1.96	0.06	78.03	2.08	6.43	2398.94	6.27
Type B–2"	10704	10.5	0.65	495.29	10.6	0.77	10889.01	37.6
	10913	11.3	0.97	487.48	11.4	0.67	8574.89	37.4
	16440	7.3	0.66	322.93	7.4	0.57	6977.27	25.0
	12383	5.5	0.59	341.02	7.6	16.73	8081.62	26.4
Avg.	12609.87	8.65	0.72	411.68	9.25	4.68	8630.70	31.63
Std.Dev.	2660.27	2.71	0.18	92.39	2.05	8.03	1647.06	6.83

Table B-6

Mechanical properties in Flexure (4 Point Bending Test) for all specimens of

Type C – M – specimens cast by Saint Gobain Technical fabrics with fabric in machine direction (9.8x76.8x254) mm

Type C – XM – specimens cast by Saint Gobain Technical fabrics, fabric in cross machine direction (9.43x77.9x254) mm

Specimen Group	Young's Modulus, E, MPa	First Crack Stress, MPa	First Crack Deflection, mm	Maximum Load, N	Flexural Strength, MPa	Deflection at Maximum Load, mm	Toughness, MPa.mm	Ave. Load, N/mm
Type C - M	24174	3.8	1.1	465.5	17.0	20.1	7339.3	32.2
	23189	3.5	0.7	386.7	12.4	19.6	7326.9	26.6
	32604	3.7	0.8	419.7	15.0	29.0	6973.6	29.0
	20612	3.4	0.6	533.5	18.2	20.2	9934.9	36.6
	28111	4.7	0.9	485.7	16.0	17.5	8355.7	33.6
Avg.	25738	3.8	0.8	458.2	15.7	21.3	7986.1	31.6
Std.Dev.	4690.3	0.5	0.2	57.2	2.2	4.5	1205.4	3.9
Type C - XM	32752	6.5	1.1	421.2	14.7	21.5	8797.4	28.5
	32406	6.3	1.4	555.6	19.2	20.4	9747.5	37.7
	29151	5.4	1.3	413.5	14.3	18.0	8202.6	28.1
	30908	6.5	1.1	530.3	21.4	23.2	9695.5	36.1
	27059	5.2	0.7	469.8	18.6	28.2	6191.2	32.0
Avg.	30455	6.0	1.1	478.1	17.6	22.3	8526.8	32.5
Std.Dev.	2372.874	0.6	0.3	63.7	3.0	3.8	1456.8	4.4

Table B-7

Mechanical properties in Flexure (4 Point Bending Test) for all specimens of

Type D – M – specimens cast by Saint Gobain Technical fabrics with fabric in machine direction (10.2x77.6x254) mm

Type D – XM – specimens cast by Saint Gobain Technical fabrics, fabric in cross machine direction (10.19x78.2x254) mm

Specimen Group	Young's Modulus, E, MPa	First Crack Stress, MPa	First Crack Deflection, mm	Maximum Load, N	Flexural Strength, MPa	Deflection at Maximum Load, mm	Toughness, MPa.mm	Ave. Load, N/mm
Type D - M	16634	3.3	0.7	561.8	16.8	16.9	11147.7	38.2
	20944	3.5	0.7	561.6	17.4	18.3	9716.8	38.4
	20695	3.6	0.8	477.6	15.9	17.9	9442.8	32.7
	22127	3.5	0.8	531.3	17.0	17.9	7359.2	36.0
	29031	2.3	0.7	395.7	12.7	17.8	8040.7	26.8
Avg.	20099.8	3.5	0.7	533.1	16.8	17.8	9416.6	36.3
Std.Dev.	2393.6	0.2	0.1	39.6	0.6	0.6	1562.1	2.7
Type D-XM	31091	5.4	0.7	341.4	10.7	8.3	5485.5	22.9
	17381	5.7	0.9	440.9	13.6	15.2	8050.5	29.7
	25299	5.2	0.8	458.5	13.6	16.5	8605.8	31.0
	28898	6.4	0.8	416.9	13.2	14.1	10912.4	28.1
	27042	4.3	0.5	386.5	12.8	11.8	8024.1	26.5
Avg.	25942	5.4	0.7	408.8	12.8	13.2	8215.7	27.7
Std.Dev.	5247.8	0.8	0.1	46.4	1.2	3.3	1932.7	3.2

Table B – 8

Mechanical properties in Tension for all specimens of

Type E – M – specimens cast by Saint Gobain Technical fabrics with fabric in machine direction (10.53x63.65x201.52) mm

Type E–XM – specimens cast by Saint Gobain Technical fabrics, fabric in cross machine direction (10.19x63.39x201.47) mm

Type EM-AGE14 – specimens similar to Type E-M and aged for 14 days (9.6x62.82x209.49) mm

Type EXM-AGE14 – specimens similar to Type E-XM and aged for 14 days (10.03x62.57x192.96) mm

Type EM-AGE28 – specimens similar to Type E-M and aged for 28 days (9.82x63.52x211.28) mm

Type EXM-AGE28 – specimens similar to Type E-XM and aged for 28 days (9.19x63.14x213.79) mm

Specimen Group	Young's Modulus, E, MPa	First Crack Stress, MPa	First Crack Strain, %	Maximum Load, KN	Maximum Stress, MPa	Strain at Ultimate Load, %	Toughness, MPa	Ave load, N/mm
Type E- M	5381.99	3.40	0.21970	3.21	4.96	1.4380	0.03	25.27
	5212.96	3.91	0.10280	3.70	5.66	1.2350	0.17	29.06
	5805.27	3.58	0.25790	3.48	5.13	1.0690	0.14	27.34
	5959.54	2.87	0.12100	3.37	4.94	0.8437	0.14	26.52
	5217.36	3.29	0.10000	3.07	4.46	0.7699	0.12	24.08
Avg.	5515.42	3.41	0.16028	3.37	5.03	1.07112	0.12	26.45
Std.Dev.	346.19	0.38	0.07338	0.24	0.43	0.27564	0.05	1.91

Specimen Group	Young's Modulus, E, MPa	First Crack Stress, MPa	First Crack Strain, %	Maximum Load, KN	Maximum Stress, MPa	Strain at Ultimate Load, %	Toughness, MPa	Ave load, N/mm
Type E- XM	6169.97	3.31	0.1868	2.56	4.15	1.8170	0.22	20.22
	3567.26	2.86	0.0984	2.81	4.36	1.2790	0.18	22.19
	4099.79	3.07	0.1048	2.82	4.18	1.8090	0.17	22.24
	4679.57	3.59	0.1110	3.27	4.85	1.6800	0.12	25.75
	4560.78	3.93	0.1191	3.55	5.73	1.5010	0.03	27.95
Avg.	4615.47	3.35	0.1240	3.00	4.65	1.6172	0.14	23.67
Std.Dev.	973.17	0.42	0.0359	0.40	0.66	0.2283	0.07	3.12
Type EM-AGE14	4945.86	1.87	0.05833	2.35	3.86	0.8932	0.03	18.73
	2675.17	1.90	0.16220	2.11	3.50	0.9099	0.17	16.76
	3329.61	2.88	0.19110	2.61	4.49	0.9536	0.14	20.83
	5930.46	1.82	0.13000	1.92	3.08	0.7927	0.14	15.26
	5529.837	2.15	0.06387	2.30	3.84	0.8722	0.12	18.35
Avg.	4482.19	2.13	0.12	2.26	3.76	0.8843	0.12	17.99
Std.Dev.	1414.55	0.44	0.06	0.26	0.52	0.0593	0.05	2.10
Type EXM-AGE14	3791.18	3.08	0.1406	2.63	4.21	1.0690	0.22	21.00
	3321.21	3.31	0.1934	2.69	4.36	1.2480	0.18	21.45
	2883.24	2.76	0.2000	2.49	3.89	1.4170	0.17	19.94
	3562.89	3.19	0.2229	2.76	4.26	1.0990	0.12	22.03
	2569.57	2.61	0.1099	2.05	3.36	0.7193	0.03	16.40

Avg.	3225.62	2.99	0.1734	2.52	4.02	1.1105	0.14	20.16
Std.Dev.	497.59	0.29	0.0465	0.28	0.41	0.2587	0.07	2.24
Type EM-AGE28	4401.79	2.74	0.1065	2.60	4.03	0.8764	0.19	20.34
	4435.48	2.80	0.1161	2.53	3.85	0.7798	0.18	19.83
	5635.85	2.23	0.1065	2.23	3.34	0.7385	0.17	17.51
	4071.84	2.36	0.0720	2.14	3.76	0.7862	0.28	17.01
	5373.131	2.74	0.0758	2.54	4.37	0.9536	0.28	20.03
Avg.	4783.62	2.57	0.0954	2.41	3.87	0.8269	0.22	18.95
Std.Dev.	679.60	0.26	0.0201	0.21	0.38	0.09	0.06	1.56
Type EXM-AGE28	6859.21	2.61	0.0797	2.45	3.61	0.5975	0.17	19.36
	6918.61	3.15	0.1603	2.49	3.77	0.7382	0.20	19.66
	7094.08	2.67	0.1104	2.26	3.84	0.5688	0.20	17.88
	6969.57	2.98	0.0950	2.49	4.17	0.9340	0.28	19.69
Avg.	6960.37	2.85	0.1113	2.42	3.85	0.7096	0.21	19.15
Std.Dev.	99.90	0.25	0.0350	0.11	0.23	0.1669	0.05	0.86

Table B – 9

Mechanical properties in Flexure for all specimens of

Type E – M – specimens cast by Saint Gobain Technical fabrics with fabric in machine direction (9.83x76.31x254) mm

Type E–XM – specimens cast by Saint Gobain Technical fabrics, fabric in cross machine direction (9.43x75.79x254) mm

Type EM-AGE14 – specimens similar to Type E-M and aged for 14 days (9.41x75.98x254) mm

Type EXM-AGE14 – specimens similar to Type E-XM and aged for 14 days (9.59x76.22x254) mm

Type EM-AGE28 – specimens similar to Type E-M and aged for 28 days (8.88x77.34x254) mm

Type EXM-AGE28 – specimens similar to Type E-XM and aged for 28 days (9.33x78.31x254) mm

Specimen Group	Young's Modulus, E, MPa	First Crack Stress, MPa	First Crack Deflection, mm	Maximum Load, N	Flexural Strength, MPa	Deflection at Maximum Load, mm	Toughness, MPa.mm	Ave. Load, N/mm
Type E- M	23636.80	4.64	0.27	431.6	14.38	21.02	14594.86	29.66
	23130.82	4.50	0.27	411.3	13.77	17.16	12812.57	28.56
	24394.20	4.68	0.27	464.1	16.38	20.01	12738.63	32.30
	26022.18	5.72	0.32	405.02	14.32	16.15	13258.76	28.24
	24707.00	4.45	0.26	400.99	14.05	20.3	14012.27	27.77
Avg.	24378.20	4.80	0.28	422.60	14.58	18.93	13483.42	29.31
Std.Dev.	1108.68	0.52	0.03	26.01	1.03	2.14	801.59	1.81

Specimen Group	Young's Modulus, E, MPa	First Crack Stress, MPa	First Crack Deflection, mm	Maximum Load, N	Flexural Strength, MPa	Deflection at Maximum Load, mm	Toughness, MPa.mm	Ave. Load, N/mm
Type E- XM	19878.48	6.40	0.43	381.4	14.22	16.18	13362.22	26.58
	20813.34	5.49	0.39	437.3	16.40	16.95	14206.35	30.52
	20452.85	5.63	0.43	407.09	15.25	16.51	13245.6	28.36
	19415.70	5.27	0.35	358.4	13.75	16.24	7970.8	25.21
	21010.10	5.52	0.40	391.8	14.85	17.45	8877.3	27.27
Avg.	20314.09	5.66	0.40	395.20	14.89	16.67	13604.72	27.59
Std.Dev.	661.40	0.44	0.03	29.45	1.02	0.53	524.28	2.00
Type EM-AGE14	21474.30	4.26	0.32	310.9	12.49	10.04	4782.73	22.65
	17839.58	3.72	0.24	306.3	11.55	10.84	4602.86	21.22
	24702.82	4.43	0.34	334.3	12.35	10.6	4694.53	22.64
	25726.07	4.58	0.36	334.96	12.78	11.8	7133.7	23.42
	22950.18	4.51	0.30	365.9	13.14	10.42	7259.25	25.13
Avg.	22538.59	4.30	0.31	330.47	12.46	10.74	5694.61	23.01
Std.Dev.	3091.39	0.35	0.05	23.76	0.59	0.66	1373.20	1.42
Type EXM-AGE14	25838.89	5.45	0.36	404.1	14.73	14.64	12018.86	28.35
	23208.29	5.26	0.39	362.2	13.23	16.21	10043.23	25.04
	21275.47	4.99	0.36	390.8	14.63	11.53	8070.16	27.51
	23309.04	4.27	0.35	343.5	12.20	17.78	10527.47	23.62
	24757.31	6.34	0.24	387.2	13.72	13.54	9969.48	26.62

Avg.	23677.80	5.26	0.34	377.56	13.70	14.74	10125.84	26.23
Std.Dev.	1729.40	0.75	0.06	24.33	1.05	2.41	1414.38	1.90
Type EM-AGE28	15313.98	4.85	1.51	341.51	14.11	10.55	7728.05	23.08
	10829.77	4.06	2.26	315.87	13.08	12.61	4787.02	21.35
	7817.65	4.47	2.70	300.16	12.31	11.92	4342.13	20.50
	9369.63	3.25	2.75	297.49	12.33	13.87	5217.60	20.07
	11104.99	4.42	2.85	265.09	11.41	12.00	3482.60	18.91
Avg.	10887.20	4.21	2.41	304.02	12.65	12.19	5111.48	20.78
Std.Dev.	2800.55	0.61	0.56	27.92	1.01	1.21	1597.51	1.55
Type EXM-AGE28	7164.81	4.01	1.53	415.95	13.91	16.44	10033.12	27.83
	11762.69	5.01	2.35	419.36	13.54	15.70	4975.09	28.09
	6213.04	3.90	2.18	338.34	14.37	18.29	8520.77	23.67
	9583.73	4.82	3.08	362.40	14.43	16.45	8985.57	24.30
	12590.83	4.25	2.22	350.71	14.00	15.41	10380.06	23.52
Avg.	9463.02	4.40	2.27	377.35	14.05	16.46	8578.92	25.48
Std.Dev.	2780.76	0.49	0.55	37.78	0.37	1.12	2151.46	2.29